

Dove 321  
7-8-06

THE GEOLOGY AND GEOCHEMISTRY OF THE PROTEROZOIC  
METAVOLCANIC AND VOLCANICLASTIC ROCKS OF THE  
GREEN MOUNTAIN FORMATION  
SIERRA MADRE RANGE, WYOMING

By  
Craig Alan Shadel

Submitted in Partial Fulfillment  
of the Requirements for the Degree of  
Master of Science in Geology

New Mexico Institute of Mining and Technology

Socorro, New Mexico

October 1982

"Shaping your stone means quietly doing your job, as well as you can. Your identity will soon be lost to history but your stone, if well shaped and polished will fit into the structure we call civilization and hold its weight, as time sweeps past us and others build upon us. History is full of greed, horror, and the worst of mankind -- but humanness is built of well shaped loving lives. What we do matters and if there is beauty in the world it is because many quiet souls have shaped their stones well and the cathedral of life is beautiful after all."

Thomas R. McGetchen -- Geologist  
(1936-1979)

#### ABSTRACT

The Green Mountain Formation is an early Proterozoic supracrustal succession located in the Sierra Madre Range in southern Wyoming. The volcanic-volcaniclastic succession is situated on the south side of the Wyoming Shear Zone which marks the boundary between the Archean Wyoming province and a Proterozoic province. Rocks of the Green Mountain Formation are part of the southward younging Proterozoic province which extends throughout Colorado and the Southwest.

The Green Mountain Formation is intruded by an extensive granitic terrane, and has been metamorphosed to grades ranging between greenschist and amphibolite facies. Isoclinal folding with associated thrust faulting and/or transposition of bedding occurs throughout some exposures of the succession south of this study. These features are not easily recognized in the areas of this study, but cannot be eliminated. The GMF in the area of Fletcher Park has been metamorphosed to the greenschist facies, but relict textures and structures are well preserved. Mafic rocks of this section appear to represent matrix-supported agglomerates and/or pyroclastic deposits, lapilli tuffs and/or brecciated flows, coarse to fine-grained volcaniclastic sediments, and fine-grained ash and/or sills and dikes. Felsic rocks appear to represent ash-flow tuff, volcanic breccia, fine-grained to porphyritic dikes and flows(?), and fine-grained water-laid tuff and/or volcaniclastic

sediments. Cherty exhalite units are associated with the top of felsic volcanic sequences, and have been targets of recent mineral exploration. The GMF in the area of Green Mountain has been metamorphosed to the amphibolite facies, and relict features are not as well preserved as in the Fletcher Park section. Mafic rocks are comprised of fine to medium-grained amphibolite and amphibolite breccia, and coarse-grained amphibolite. Some relict features are similar to those in mafic rocks of the Fletcher Park section, and appear to represent agglomerates, breccias, and fine-grained volcanics or volcaniclastics. Coarse-grained amphibolites may represent diabase sills. Felsic rocks of the of the Green Mountain area are represented by microcline-quartz-oligoclase schist and oligoclase-microcline-quartz schists. Some of the felsic schists appear to contain relict phenocrysts and possible lithic fragments, and may represent ash flow tuffs or other pyroclastic deposits. Fine-grained felsic schists probably represent fine-grained pyroclastic deposits and/or volcaniclastic sediments.

The geochemical characteristics dominantly classify the rocks of the GMF as subalkaline basalt, dacite, and rhyolite. A bimodal distribution is observed in various geochemical plots with a compositional 'gap' in andesite fields. Geochemical characteristics of the basaltic rocks are most consistent with low-K tholeiites of the island arc tholeiite series. Dacitic and rhyolitic rocks also display

many similarities to felsic rocks of the same series, but there are too many characteristics similar to calc-alkaline rocks to be conclusive. Trace element discrimination diagrams consistently indicate that both the mafic and felsic formed at a convergent plate boundary, namely in an island arc environment.

The overall characteristics of the Green Mountain Formation and its spatial relationships to other Precambrian rocks on a regional scale appear to be most easily explained by an immature island arc system. Tholeiitic or mixed tholeiitic and calc-alkaline volcanics were probably deposited in a back arc basin or the arc-trench gap. The model proposed by Is and Houston (1979) involves a northward migrating island arc system along a southward dipping subduction zone. The arc was then accreted to the Archean continent and its associated continental marginal sediments along the Wyoming Shear Zone.

#### ACKNOWLEDGEMENTS

Financial support for this project was provided by Conoco, Inc., and I would like to thank Craig Nelson of Conoco for his suggestions and time spent in the field.

I would also like to thank Dr. Kent C. Condie who suggested this project and served as my thesis advisor, as well as Dr. James M. Robertson and Dr. Antonius J. Budding who provided their time to serve on my thesis committee. All provided many useful criticisms and suggestions.

A special thanks goes to Phillip Allen and K. Babett Faris for their help and patience with neutron activation and X-ray fluorescence analytical procedures.

Above all I thank my family for their unending support, encouragement, and confidence throughout all the ups and downs encountered during the preparation of this project.

## TABLE OF CONTENTS

|   |    |
|---|----|
| Abstract                                    |    |
| Acknowledgements                            |    |
| Introduction .....                          | 1  |
| Precambrian Rocks .....                     | 1  |
| Purpose .....                               | 3  |
| Location .....                              | 3  |
| Previous Work .....                         | 7  |
| Methods .....                               | 7  |
| General Geologic Setting .....              | 9  |
| Introduction .....                          | 9  |
| The Archean Wyoming Province .....          | 10 |
| Proterozoic Geology of the Northern         |    |
| Sierra Madre Range .....                    | 11 |
| Proterozoic Rocks North of the              |    |
| Wyoming Shear Zone .....                    | 11 |
| Proterozoic Rocks South of the              |    |
| Wyoming Shear Zone .....                    | 12 |
| Petrography of the Green Mountain Formation |    |
| and Associated Rocks .....                  | 17 |
| Introduction .....                          | 17 |
| Granodiorite .....                          | 20 |
| Fletcher Park Section .....                 | 21 |
| General Description .....                   | 21 |
| Metarhyolites .....                         | 24 |
| Exhalite .....                              | 28 |
| Metadacites .....                           | 29 |

|  |     |
|--|-----|
| Metabasalts .....  | 33  |
| Green Mountain Section .....                                       | 39  |
| General Description .....  | 39  |
| Amphibolites .....   | 40  |
| Feldspar-Quartz-Mica Schists .....                                 | 43  |
| Geochemistry .....   | 47  |
| Introduction .....   | 47  |
| Plutonic Rocks .....   | 49  |
| Granodiorite .....   | 49  |
| Diabase .....  | 53  |
| Geochemistry of the GMF Volcanic<br>and Volcaniclastic Rocks ..... | 58  |
| Introduction .....   | 58  |
| Alteration .....   | 59  |
| Classification .....   | 67  |
| Rare Earth Elements .....  | 76  |
| Tectonic Indicators .....  | 79  |
| Rare Earth Elements .....  | 95  |
| Structure and Metamorphism .....                                   | 96  |
| Structure .....  | 96  |
| Fletcher Park Section .....  | 97  |
| Green Mountain Section .....                                       | 99  |
| Metamorphism .....   | 101 |
| Fletcher Park .....  | 102 |
| Green Mountain .....   | 106 |
| Discussion of Tectonic Environment .....                           | 110 |
| Summary and Conclusions .....                                      | 115 |



Appendices

|   |     |
|---|-----|
| A. Photographic Plates .....  | 125 |
| B. Brief Petrologic Descriptions of the<br>Green Mountain Formation ..... | 131 |
| C. Geochemical Analyses and CIPW Norms .....                              | 138 |
| D. Sample Collection and Preparation .....                                | 148 |
| E. Neutron Activation Technique .....                                     | 152 |
| F. X-ray Fluorescence Technique .....                                     | 155 |
| Bibliography .....  | 159 |

## LIST OF FIGURES

|            |   |    |
|------------|---|----|
| Figure 1.  | Regional location map of exposed Precambrian rocks of Wyoming and vicinity .....                    | 4  |
| Figure 2.  | Precambrian geology of the northern Sierra Madre Range and Medicine Bow Mountains .....             | 5  |
| Figure 3.  | Proterozoic age provinces of the southwestern United States .....                                   | 13 |
| Figure 4.  | Geologic map of the Fletcher Park section .....   | 18 |
| Figure 5.  | Geologic map of the Green Mountain section ....   | 19 |
| Figure 6.  | Ab-An-Or classification of the Encampment River Granodiorite .....                                  | 50 |
| Figure 7.  | Na <sub>2</sub> O-CaO-K <sub>2</sub> O diagram of granodiorite samples ..                           | 51 |
| Figure 8.  | Comparison of the REE patterns of the granodiorite with the GMF metarhyolites and metadacites ..... | 54 |
| Figure 9.  | Jensen cation plot of the GMF samples .....   | 55 |
| Figure 10. | TiO <sub>2</sub> versus 100(Mg/Mg + Fe <sup>2+</sup> ) plot of the GMF mafics volcanics .....       | 57 |
| Figure 11. | Frequency distribution histograms of some major and trace elements of the GMF .....                 | 62 |
| Figure 12. | Sample plot of the metasomatism correction method of Beswick and Soucie .....                       | 63 |
| Figure 13. | Ab-An-Or diagram of the Green Mountain Formation .....  | 65 |
| Figure 14. | SiO <sub>2</sub> vs Nb/Y classification of the Green Mountain Formation .....                       | 68 |
| Figure 15. | Zr/TiO <sub>2</sub> vs Nb/Y classification of the Green Mountain Formation .....                    | 69 |
| Figure 16. | REE envelopes of the GMF mafic rocks .....  | 77 |
| Figure 17. | REE envelopes of the GMF felsic rocks .....   | 77 |
| Figure 18. | Zr-Ti-Y plot of the GMF mafic volcanics .....   | 81 |
| Figure 19. | SiO <sub>2</sub> versus Cr plot of the GMF mafic volcanics .....                                    | 82 |

|  |     |
|--|-----|
| Figure 20. Ti versus Zr plot of the GMF mafic volcanics .....  | 83  |
| Figure 21. MgO versus FeOT plot of the GMF rocks .....   | 87  |
| Figure 22. MgO versus FeO + Fe <sub>2</sub> O <sub>3</sub> plot of the GMF .....                       | 89  |
| Figure 23. Th-Hf-Ta plot of the GMF felsic rocks .....   | 90  |
| Figure 24. ACF plot of the mafic rocks of the Fletcher Park Section .....                              | 103 |
| Figure 25. AKF plot of the felsic rocks of the Fletcher Park Section, chlorite zone ...                | 103 |
| Figure 26. AKF plot of the felsic rocks of the Fletcher Park Section, biotite zone ....                | 105 |
| Figure 27. ACF plot of the Green Mountain amphibolites .   | 107 |
| Figure 28. AKF plot of the Green Mountain felsic schists .....   | 107 |
| Figure 29. Model for the formation of the Green Mountain Formation and regionally associated rocks ... | 112 |
| Figure 30. Diagrammatic stratigraphy of the Fletcher Park and Green Mountain Sections ..               | 116 |
| Figure 31. Sample locations of the Fletcher Park section .....   | 150 |
| Figure 32. Sample locations of the Green Mountain section .....  | 151 |
| Figure 33. Sample calibration curve for trace element analysis by X-ray fluorescence .....             | 158 |

LIST OF TABLES

|   |     |
|---|-----|
| Table 1. Comparison of the average granodiorite to the average metarhyolite and metadacite .....  | 52  |
| Table 2. Summary of the classification schemes of the GMF .....                                   | 72  |
| Table 3. Average composition of the major rock types of the GMF .....                             | 73  |
| Table 4. Distinguishing trace element ratios of the GMF .....                                     | 75  |
| Table 5. Comparison of the GMF metatholeiites to various basalt types .....                       | 85  |
| Table 6. Comparison of the GMF metadacites to dacites of other tectonic environments .....        | 91  |
| Table 7. Comparison of the GMF metarhyolites to rhyolites of other tectonic environments .....    | 92  |
| Table 8. Neutron activation instrumental parameters ....  | 153 |
| Table 9. Element concentrations for intralab standards used for neutron activation analysis ..... | 154 |
| Table 10. Parameters for XRF analysis .....   | 157 |

## INTRODUCTION

### PRECAMBRIAN ROCKS

Precambrian rocks in general have been studied in order to gather information about the early history of the Earth. The tectonic environments in which suites of Precambrian rock were formed have been the subject of many of these studies. Since the recognition of plate tectonics as an important process in operation on the earth today, one goal of the study of Precambrian rocks is to see if they can be explained by similar types of tectonic processes. The comparisons of ancient and modern rocks are based on observations such as petrotectonic assemblages, geochemical characteristics, and isotopic studies. More information on Precambrian rock suites is still necessary if the evaluation of early tectonic processes is to be successful.

The rocks of the Green Mountain Formation, which are the subject of this study, are located along the boundary between two major Precambrian crustal provinces exposed in southern Wyoming. Because this provincial boundary is a likely remnant site in which interactions of crustal segments occurred, information gathered there can be used for further interpretations of tectonic processes of the Precambrian. Most of the studies of the Precambrian have concentrated on rocks of Archean age (>2.5 b.y.), and their interpretations relative to modern tectonic environments are faced with many uncertainties. The amount of geologic time represented by the Proterozoic covers about 2.0 billion

years of the Earth's history. Studies of Proterozoic rock suites such as the Green Mountain Formation may provide some important links in the extrapolation of tectonic interpretations from modern to Archean times.

Alternatively, if studies reveal that tectonic processes have changed throughout geologic history, Proterozoic assemblages such as the Green Mountain Formation provide information which may document these changes. Until it can be shown consistently that Precambrian assemblages do not represent suites similar to those formed in modern tectonic regimes, their direct comparisons are justified.

## PURPOSE

The purpose of this project is best divided into three main phases. The first objective is to present a detailed description of those exposures of the Green Mountain Formation (GMF) in the areas of Fletcher Park (FP) and Green Mountain (GM). These areas appear to represent the best preserved sections in terms of both metamorphism and deformation. Second, the rocks of the GMF will be described both petrographically and geochemically in order to classify and characterize them. Finally, on the basis of the above observations, and comparison to features observed in Phanerozoic tectonic regimes, a possible tectonic environment for the Green Mountain Formation is discussed.

## LOCATION

The study area is located in the Sierra Madre Range, Carbon County, Wyoming (Figure 1). These mountains are a northern extension of the Colorado North Park Range as part of the Central Rocky Mountain region. The sections studied in detail occur in the vicinity of Green Mountain, section 2, T 13 N, R 85 W, and to the northwest of Fletcher Park, section 20, T 13 N, R 86 W. The areas lie approximately 13 and 24km southwest of Encampment, Wyoming, respectively (Figure 2).

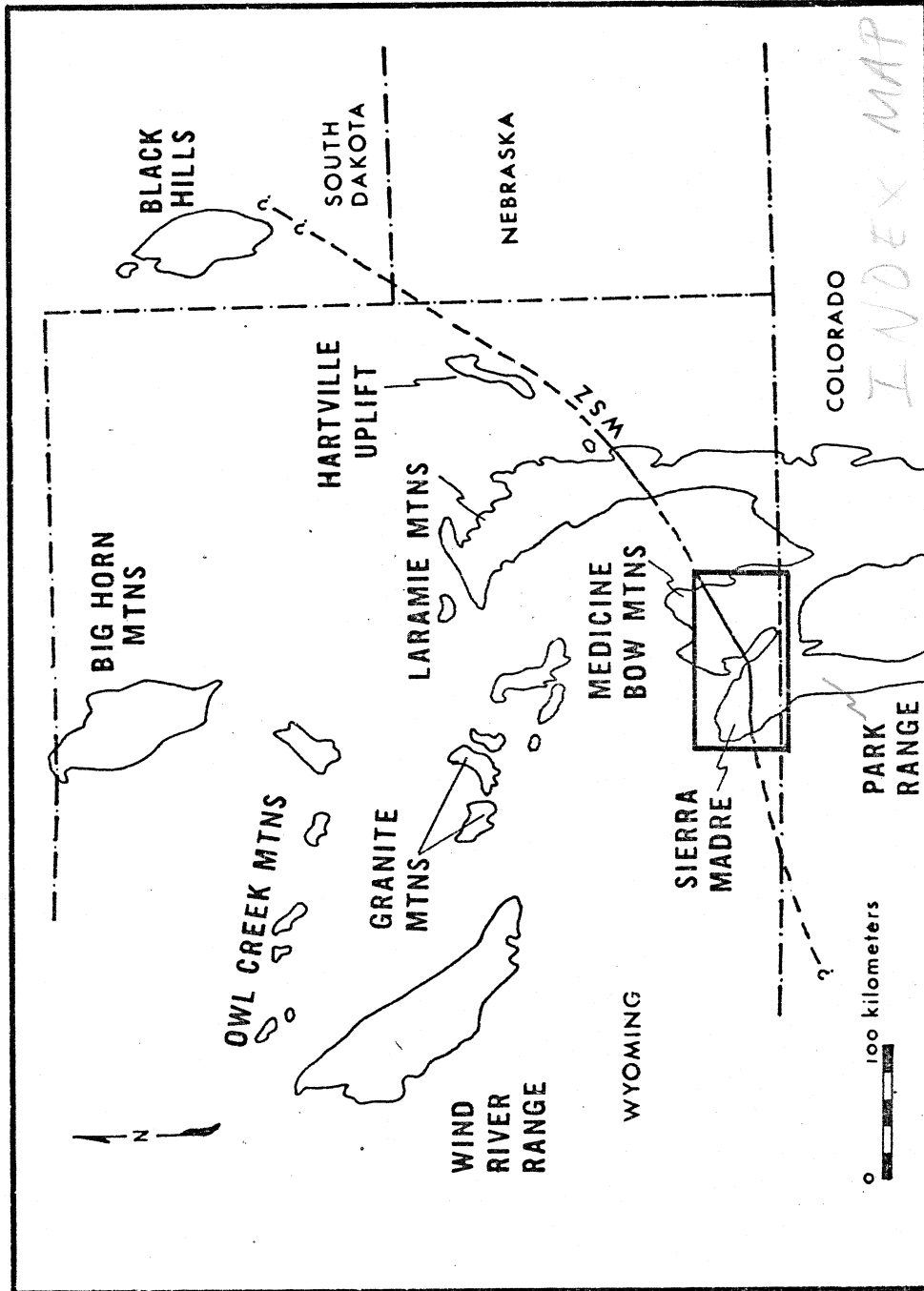


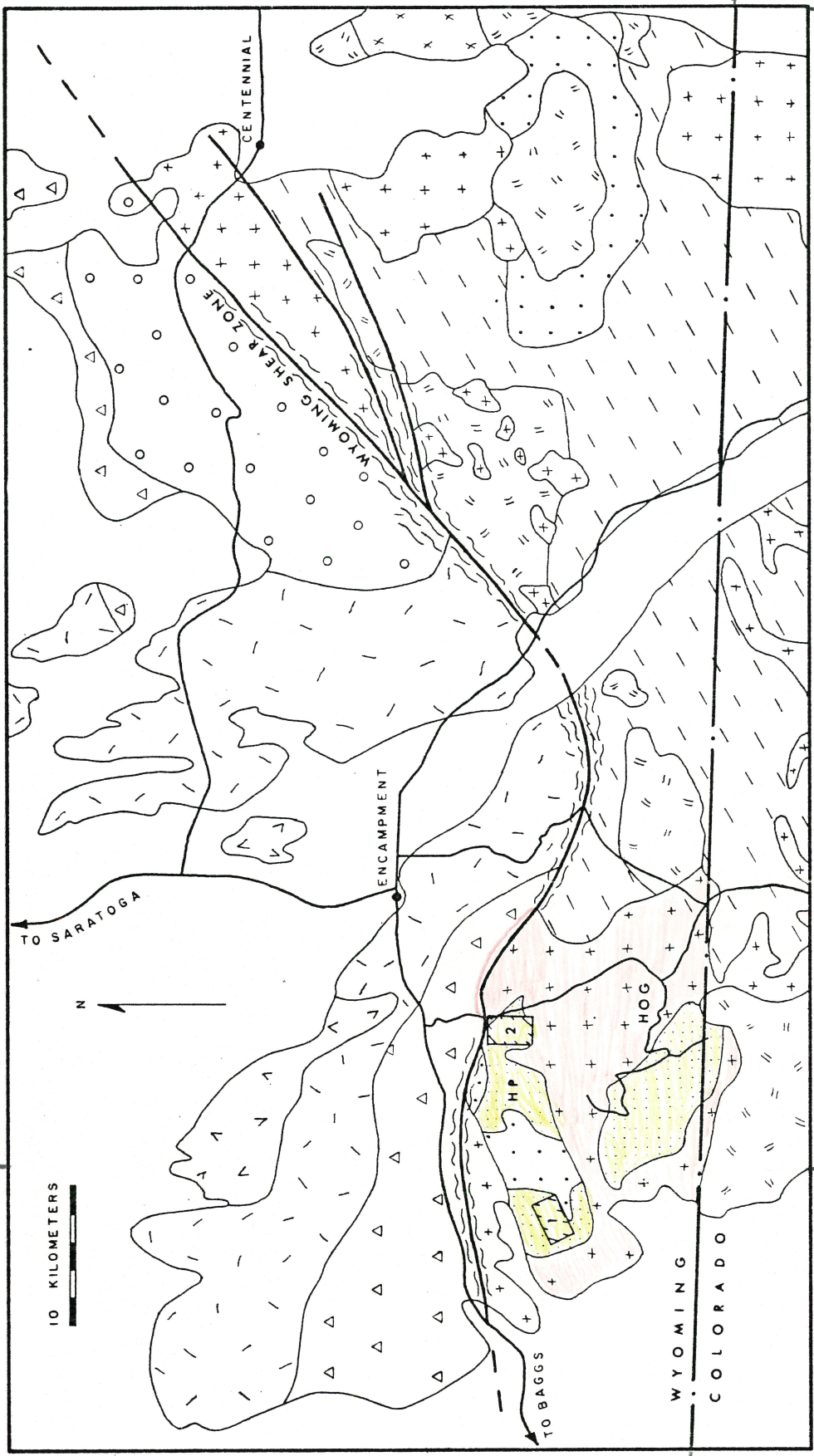
Figure 1. Regional location map of exposed Precambrian rocks of Wyoming and vicinity (after Hills and Houston, 1979). WSZ = Wyoming Shear Zone.



Lat & longitude

107°

106°



106

Figure 2. Precambrian geology of the northern Sierra Madre Range and Medicine Bow Mountains (modified after Hills and Houston, 1979). Explanation on next page.

41°

# EXPLANATION

## PROTEROZOIC

 GRANITIC ROCKS  
1400 my (INCL.  
SHERMAN GRANITE)

 GRANITIC ROCKS  
1635 TO 1730 my

 AMPHIBOLITE AND  
MINOR ULTRAMAFICS

 TONALITE AND  
GRANODIORITE

 LOWER PROTEROZOIC  
ROCKS UNDIVIDED

 GREEN MOUNTAIN  
FORMATION

 LIBBY CREEK GROUP

 DEEP LAKE GROUP

## ARCHEAN

 GRANITIC ROCKS

 FELDSPATHIC GNEISS  
AND MIGMATITE

 FAULT/SHEAR ZONE

 LITHOLOGIC CONTACT

 STUDY AREAS

HP = HUSTON PARK

HOG = HOG PARK

## PREVIOUS WORK

The first work in the Sierra Madre Mountains, by A.C. Spencer (1904) of the U.S.G.S., was an investigation of copper deposits of the Encampment District. This paper includes the first descriptions of units represented by the then unnamed Green Mountain Formation. In 1958, B.E. Ebbett of the Wyoming Geological Survey mapped an area of the northern part of the Sierra Madre range. Unpublished Masters theses by Merry (1963) and Lackey (1968) of the University of Wyoming contain mapping and petrographic descriptions of the Green Mountain Formation in the areas of Hog Park and Houston Park, respectively (Figure 2). The most recent work is a geological and geochemical study by A.F. Divis (1976) through the Colorado School of Mines. Although several papers have been written on the geology of the Sierra Madre, a lack of detailed work involving the Green Mountain Formation in specific is evident.

## METHODS

Two exposures of the Green Mountain Formation were examined, and for the purposes of this paper are referred to as the Green Mountain and Fletcher Park sections. The field relationships and physical characteristics of the lithologic units of the GMF are described. Samples of the lithologic units are used for thin section and geochemical study, and represent the compositional and textural varieties of the rock types present. Samples which contain a very heterogeneous mixtures of compositional rock types or are

obviously altered are not used for detailed geochemical study, but are used for general descriptive purposes. Out of the one hundred samples collected from the GMF, 49 are used for detailed thin section description, and 40 for geochemical studies. In addition, 11 samples collected by Craig Nelson of Conoco Inc. were analyzed.

The geochemical samples were analyzed for major and trace elements by instrumental neutron activation and X-ray fluorescence techniques. The results are plotted on various two- and three-component geochemical diagrams for purposes of classification, characterization, and interpretation of tectonic environment. Tectonic interpretations are based on physical characteristics and geochemical schemes constructed from observations in modern tectonic environments.

## GENERAL GEOLOGIC SETTING

## INTRODUCTION

The study areas for this project are located near the boundary between two major crustal provinces, the Archean Wyoming Province on the north and a Proterozoic province on the south. These provinces are separated by the Wyoming Shear Zone (WSZ) (Figure 2). This shear zone was originally defined by Houston and McCallum (1961) for a similar northeast trending feature in the Medicine Bow Mountains to the east. The Wyoming Shear Zone ranges from a few hundred meters of mylonite and phyllonite in the western Sierra Madres, to a zone of cataclastic augen gneiss and cataclastic migmatite over 7km wide in the east-central Medicine Bow Mountains (McCallum, 1964; Houston and others, 1968).

## THE ARCHEAN WYOMING PROVINCE

Rocks of the Archean Wyoming Province are exposed in the major mountain ranges of Wyoming and Montana, including the Sierra Madre and Medicine Bow Mountains where its southern boundary is defined. The Archean basement complex is composed of a granite-greenstone terrane ranging from upper greenschist to lower granulite facies of metamorphism. Amphibolite facies terranes are the most common, and are comprised of about 60% gneiss and migmatite, 30% granitic plutons and 10% greenstone belts (Condie, 1981). Diabase dikes are common, but are a minor rock type. The greenstone belts occur as amphibolite remnants within tonalitic to trondhjemitic gneiss. The main greenstone exposure is the South Pass belt (Condie, 1981).

The Archean rocks of the Sierra Madres and Medicine Bow Mountains consist of granitic gneiss, quartz-biotite gneiss, and migmatite, with less abundant amphibolite, and minor quartzite, marble, and ultramafics (Divis, 1979; Hills and Houston, 1979). The Archean terrane in the Sierra Madres is intruded by massive quartz monzonite and granite, often forming augen gneiss at the contacts. A U-Pb date from a zircon separate yields an age of  $2630 \pm 100$  m.y. for the Feldspathic Gneiss (Figure 2), and is interpreted to represent a minimum age due to a major metamorphic event (Divis, 1976). This age has also been recognized in several areas of southern Wyoming, including a similar gneiss in the Medicine Bow Range (Hills and others, 1968).

PROTEROZOIC GEOLOGY OF THE NORTHERN SIERRA MADRE RANGE  
PROTEROZOIC ROCKS NORTH OF THE WYOMING SHEAR ZONE

Proterozoic supracrustal rocks occur north of the Wyoming Shear Zone in the Sierra Madre Range. These rocks unconformably overly the Archean terrane (Graff, 1979; Figure 2). Sequences represented by the Phantom Lake suite and Deep Lake Group, are described by Graff (1979) as comprised of paraconglomerates, metavolcanics, quartzite, and stromatolitic limestone, unconformably overlain by uraniferous quartz-pebble conglomerate, phyllitic quartzite, metavolcanics, and metagraywacke. These units are also recognized in the Medicine Bow Mountains to the east, with the addition of a younger unconformable sequence known as the Libby Creek Group. This group consists of interbedded quartzite, quartz-pebble and paraconglomerate, phyllite, and stromatolitic carbonate.

The above sequences are interpreted as a marine transgressive-regressive assemblage plus fluvial sediments and minor volcanics deposited on the edge of the Archean craton (Graff, 1979). Overlying these sequences are fluvial and shallow-marine deposits, and glacial-marine and marine sediments which were deposited on a subsiding marine shelf (Graff, 1979; Karlstrom and Houston, 1979; and Lanthier, 1979). Mafic sills and dikes intrude all of the successions.

## PROTEROZOIC ROCKS SOUTH OF THE WYOMING SHEAR ZONE

The Proterozoic terrane south of the Wyoming Shear Zone in the Sierra Madre Range is part of a southward younging succession of age provinces. This Proterozoic basement complex extends throughout the Southwest. These provinces represent three main age ranges of 1750 to 1800 m.y. including the Sierra Madres, 1650 to 1720 m.y., and 1100 to 1200 m.y. as described by Condie (1982) (Figure 3).

The Proterozoic rocks of the Southwest are dominantly characterized by quartzite-shale-bimodal volcanic sequences (Condie and Budding, 1979; Condie, 1980). Calc-alkaline rocks have only been reported from the Yavapai series in Arizona, and have been suggested for the Green Mountain Formation of the Sierra Madre Range (Anderson and Blacet, 1972; Divis, 1976). A bimodal volcanic assemblage is observed throughout Colorado and northern New Mexico, with tholeiite and dacite to rhyolite end members dominating (Boardman, 1976; Condie and Budding, 1979; Condie, 1980; Condie and Nuter, 1981; Robertson, 1981). Field studies suggest that the bimodal volcanics and quartzite-shale assemblages are actually two separate groups (Condie, 1982). When these suites occur together, the quartzite-shale group overlies and is interbedded with the bimodal volcanics.

Proterozoic terranes of the Southwest have undergone at least two periods of deformation and metamorphism, usually to the amphibolite facies. The successions are intruded by granitic rocks of variable composition ranging from granite



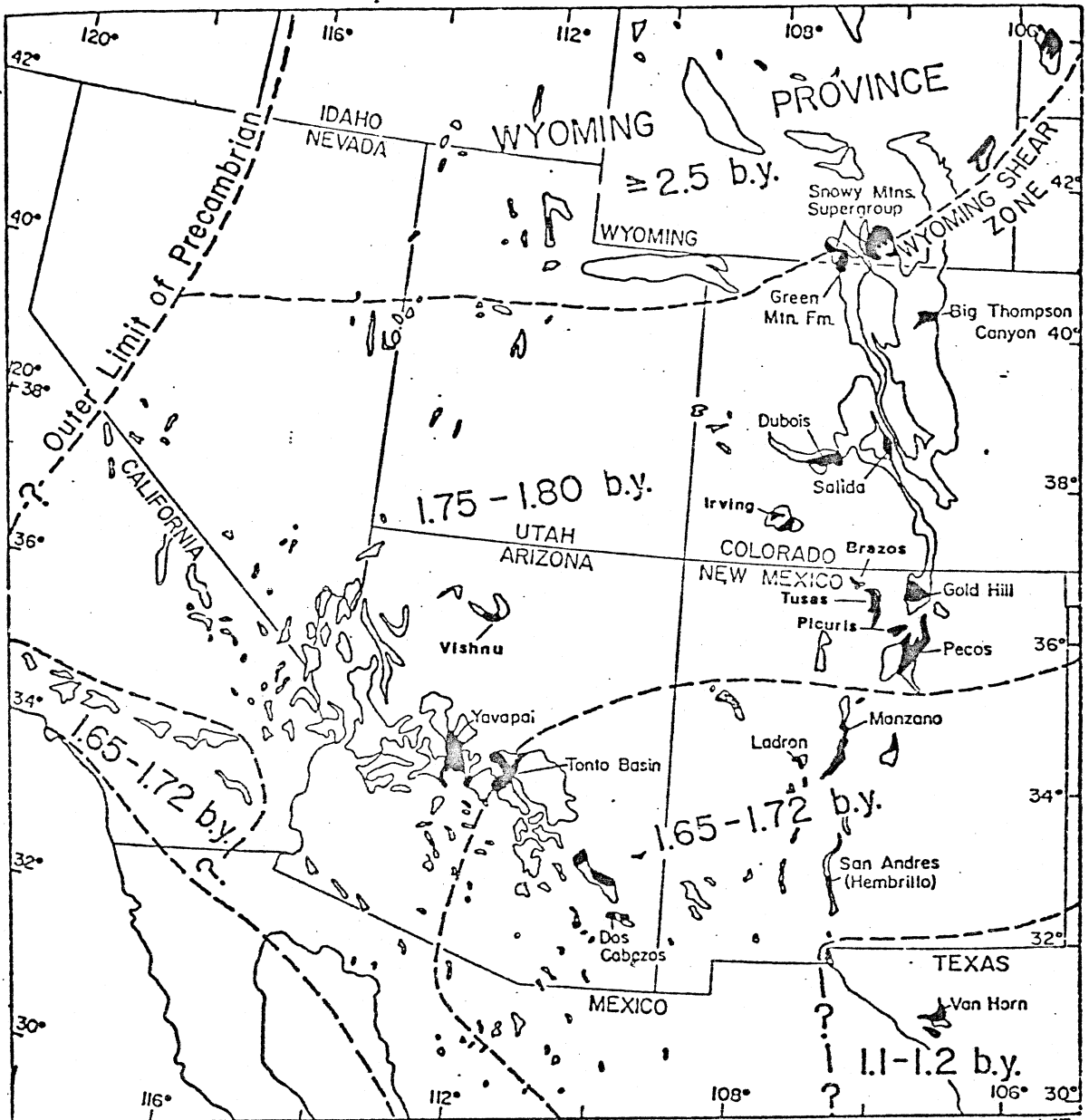


Figure 3. Proterozoic age provinces of the southwestern United States (after Condie, 1982).

to tonalite. These plutonic rocks range from syntectonic to post-tectonic in origin.

Isotopic studies of Sr87/Sr86 of the felsic volcanics and granitic rocks of the Southwest indicate the absence of Archean basement south of the Wyoming Shear Zone (Condie, 1982). This is an important constraint in the consideration of the tectonic models which have been proposed for the evolution of the Southwest, which include arc and continental rift types (Condie and Budding, 1979; Van Schmus and Bickford, 1981). No model as yet complies with all constraints and observed characteristics.

Proterozoic rocks south of the WSZ in the Sierra Madre consist of a supracrustal succession of metavolcanics and volcaniclastic sediments of the Green Mountain Formation and Big Creek Gneiss, both of which are intruded by granite and granodiorite (Figure 2). Phases of the intrusives are syntectonic to post-tectonic in origin, and comprise the major portion of the Proterozoic terrane. The supracrustal units are well to poorly foliated and fine- to coarse-grained. Parts of the Green Mountain Formation are the subject of this project.

Undifferentiated lower Proterozoic rocks occur in the southeastern part of the Sierra Madre Range where they are collectively referred to as the Big Creek Gneiss, and are comprised of banded hornblende and feldspathic gneiss (Figure 2). Phases of the BCG are layered hornblende gneiss, augen gneiss, pegmatitic gneiss, and calc-silicate

gneiss, which are locally migmatized (Divis, 1979). Further south in the Sierra Madres, the Big Creek Gneiss appears to extend into northern Colorado. Phases continue to represent about 50% each felsic gneiss and amphibolite (Snyder, 1980). The Big Creek Gneiss is suggested by Divis (1976) to be an equivalent to the Green Mountain Formation subjected to extreme metamorphism and metasomatism, but detailed trace element studies are needed to evaluate this interpretation.

Granitic rocks which dominate the terrane near the study area represent several compositional phases. The oldest unit is the Encampment River Granodiorite (ERGD), which only intrudes the Green Mountain Formation (Figure 2). The ERGD is medium-grained, moderately foliated, and ranges from granodiorite to granite in composition. The Sierra Madre Granite intrudes both the GMF and ERGD. It is comprised of fine to medium-grained to pegmatitic red granite, locally foliated at the contacts. The SMG is the most abundant rock of the granitic terrane. The youngest intrusive phase is minor in abundance and consists of light colored quartz monzonite. Plutons of this phase intrude most of the other plutonic rocks, and is most abundant in the Hog Park area.

South of the Hog Park area, near the Colorado-Wyoming border, is a large body of medium-grained gabbro (Figure 2). This gabbro is characterized by a hornblende-feldspar, +/- clinopyroxene, +/- biotite assemblage. The main gabbro body also contains minor amounts of olivine gabbro, peridotite,

and numerous basalt dikes (Snyder, 1980). The genetic relationship of the gabbro to the Green Mountain Formation and other rocks of the Sierra Madre Range has not been studied.

PETROGRAPHY OF THE  
GREEN MOUNTAIN FORMATION AND ASSOCIATED ROCKS

INTRODUCTION

The Fletcher Park area was described and sampled using mappable units recognized through work by Craig Nelson of Conoco, Inc. An introductory field tour, provided by C. Nelson, was helpful in establishing where the best outcrops occurred and served as beginning guidelines for subsequent work. The map compiled by C. Nelson (Figure 4) was provided for use after field work was completed, and includes modifications by work in this study. The Green Mountain area has not been previously mapped, and a detailed map was not compiled for this study. A generalized map based on the sampling traverses and correlations which were observed is provided (Figure 5).

The Fletcher Park section is described independently from the Green Mountain section for two reasons: (1) because the lower grade of metamorphism resulted in better preservation of original features, and (2) lack of stratigraphic control between the two areas. Because of the relatively low grade of metamorphism in the Fletcher Park section, and the preservation of primary textures, the rock names of the units are prefixed by 'meta-' followed by the name of the protolith (example metadacite). Metamorphic rock names are used for description of the Green Mountain section because of the higher metamorphic grade. Petrographic descriptions are summarized in Appendix A.

and TFR

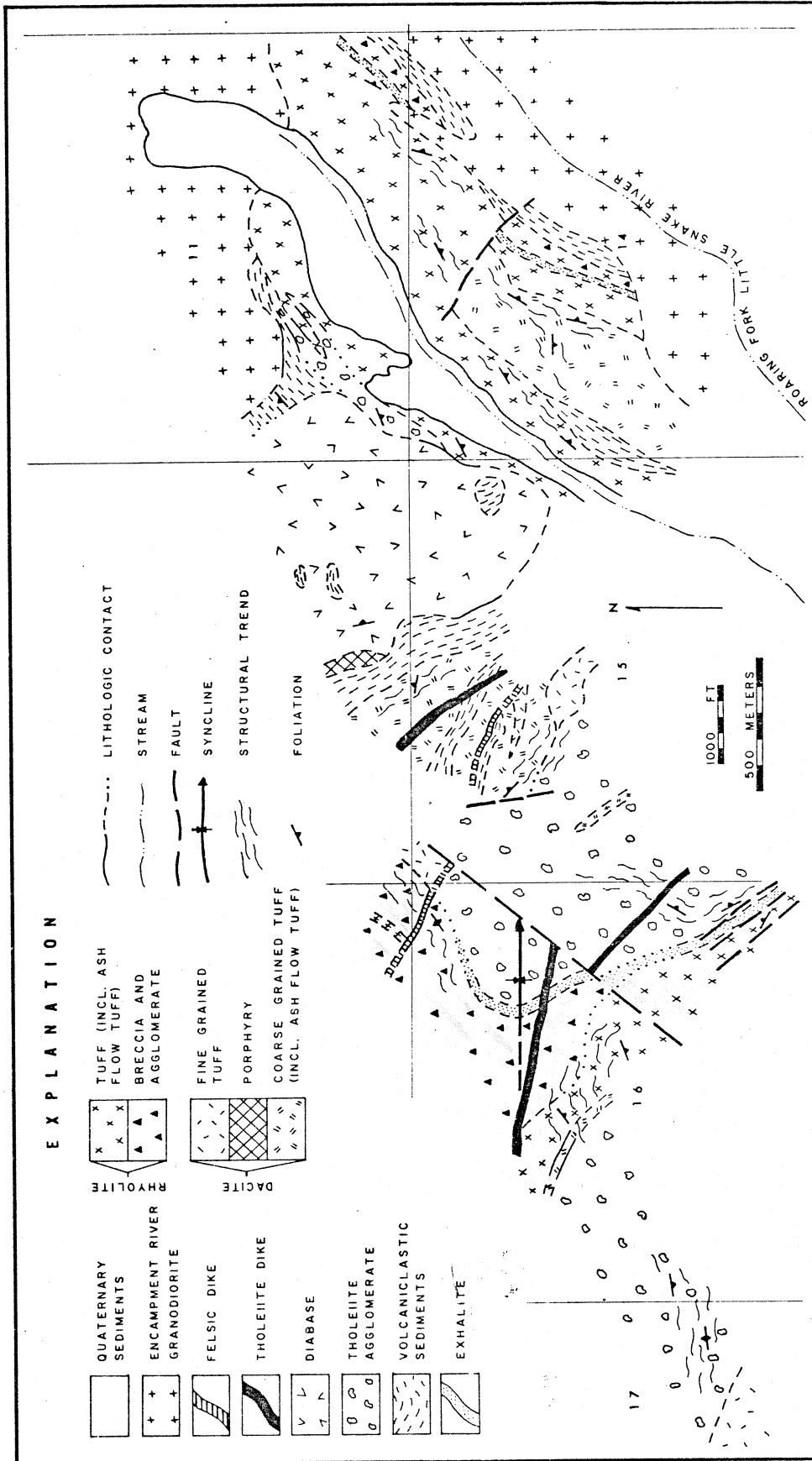


Figure 4. Geologic map of the Fletcher Park section (modified from map provided by C. Nelson of Conoco, Inc., and work in this study).

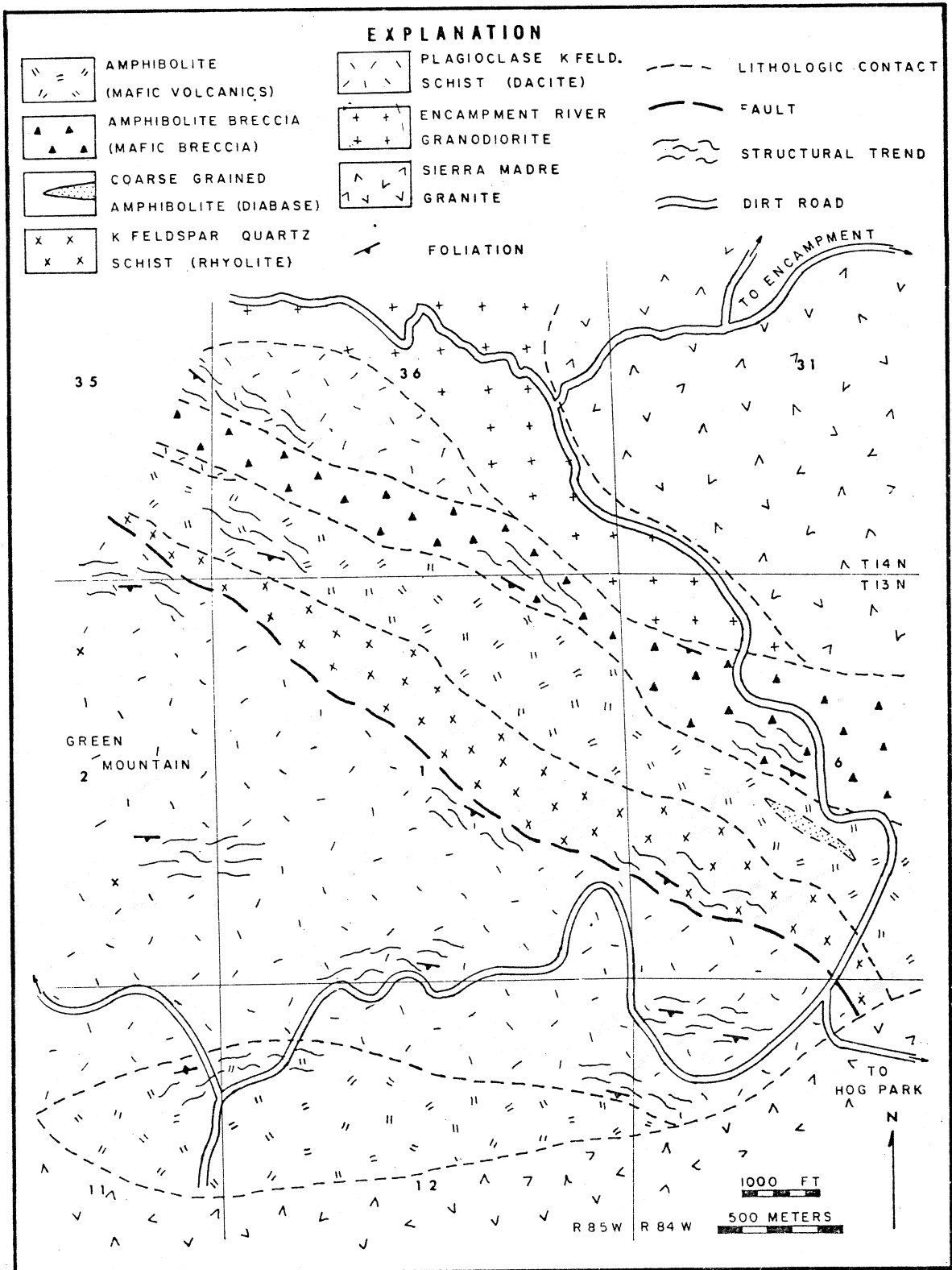


Figure 5. Geologic map of the Green Mountain section (this study).

## GRANODIORITE

The oldest intrusive phase of the granitic terrane which surrounds the Green Mountain Formation is the Encampment River Granodiorite. This was the only granitic phase which was sampled for description in this study. The overall abundance of the granodiorite is second to the Sierra Madre Granite, and only occurs between the Fletcher Park and Green Mountain study areas (Figure 2).

The Encampment River Granodiorite is a moderately to well-foliated, medium-grained rock. The unit ranges from pink to gray, weathering to darker shades of the same colors. Foliation is usually strongest near the contacts with the Green Mountain Formation. Mafic and felsic xenoliths most likely derived from the GMF are locally common. Small dikes associated with the main granodiorite body also intrude the GMF metavolcanic succession.

In thin section, the granodiorite generally has a hypidiomorphic-granular texture in less foliated samples. Where foliation is stronger, the texture appears to be gneissic in hand specimen, and a strong alignment of biotite in thin section is noticed. The mineral content is comprised of 1 to 3mm albite twinned oligoclase (An<sub>24</sub> to An<sub>27</sub>, 35 to 40%), quartz (15 to 20%), tartan twinned microcline (20 to 25%), 3 to 5% biotite, and 3 to 15% hornblende. Intergranular material comprised of the same minerals are less than 1mm. Accessory minerals include epidote, sericite, chlorite, zircon, and hematite.



## FLETCHER PARK SECTION

## GENERAL DESCRIPTION

The Fletcher Park sequence has an exposed stratigraphic thickness of approximately 3.3 kilometers, assuming isoclinal folding and transposition of bedding have not affected the area. This represents a minimum thickness since the base and top of the section are not exposed, but rather are in fault or intrusive contact with the surrounding granitic terrane. Although several faults are present throughout the section, most have very minor displacement and little affect on the area. In general, the FP section is comprised of metavolcanic and volcanoclastic units of basaltic, dacitic, and rhyolitic composition (Figure 4). Two volcanic cycles appear to be present, each represented by metabasalt overlain by metadacite and metarhyolite and terminating with cherty exhalite.

The felsic units of the FP section are rhyolitic to dacitic in composition, and have four textures which are observable in the field. These textures are: (1) porphyritic, (2) non-porphyritic, (3) fragmental, and (4) laminated. Porphyritic varieties contain feldspar +/- quartz phenocrysts, and commonly include several percent lithic fragments. Fragmental felsic units occur either as breccias with angular clasts ranging up to 10cm or more, or as finer-grained rocks with clasts less than 1cm supported by a fine-grained matrix. The non-porphyritic varieties are fine-grained and do not contain megascopic phenocrysts or

laminations. Laminated felsic units are similar to the non-porphyrific varieties, with the laminations providing the only distinguishing feature in the field.

Metadacites and metarhyolites of the GMF are usually distinguished petrographically, but due to very small grain size and degree of recrystallization, the laminated and non-porphyrific varieties may not display distinguishing features indicating their composition. Felsic rocks of possible rhyodacitic composition are recognized geochemically, but cannot be distinguished petrographically.

The felsic units mainly outcrop as cliffs and prominent ridges in the western, central, and eastern parts of the FP section, separated by thick mafic volcanic sequences. Individual felsic units are interbedded with adjacent felsic and mafic rocks, and a few thin rhyolitic to dacitic dikes (usually less than 1m thick) locally crosscut the section. Cherty exhalite units, which may contain intermixed carbonate, are associated with the tops of the felsic sequences. These units have been exploration targets for massive sulfide deposits.

The mafic units of the FP section are represented by basaltic metavolcanic and volcanoclastic rocks of various textural types, and a discordant intrusive body of diabase in the central part of the section (Figure 4). Metabasalts weather to a more subdued topography between the felsic dominated ridges. Textural varieties consist of matrix-supported agglomerates, lapilli tuff or brecciated

flows, fine-grained tuff, fine-grained dikes and sills, and coarse to very fine-grained volcanoclastic sediments.

The FP agglomerates occur as clast rich units supported by a fine-grained micaceous matrix. These units represent the most abundant mafic rock type of the FP section. Other fragmental mafic units contain abundant clasts less than 3cm which have a more angular character. Basaltic dikes and sills occur as thin units with very fine-grained textures. These units are distinguished in the field by their sharp contacts and cross-cutting relationships. Mafic volcanoclastic sediments occur as upward-fining sequences in the central part of the FP section, and as thin beds within the agglomerates. The Fletcher Park section is also intruded by a medium-grained diabase pluton occurring within the volcanoclastic part of the sequence (Figure 4).

## METARHYOLITES

The metarhyolites of the Fletcher Park section are located in the central and eastern part of the sequence, and are generally distinguished in the field by their light color. The colors which are most commonly observed are white, pale pink, or pale gray on the fresh surface, weathering to brown or reddish brown. Three of the four textural types are observed in the metarhyolites. The textures represented are porphyritic, fragmental, and laminated varieties. The porphyritic types occur throughout the FP section, while the fragmental types are most abundant in the central parts of the section and laminated types in the east. Sedimentary structures are commonly observed in the metarhyolites, namely low-angle cross-bedding, graded bedding, and possibly some cut-and-fill structures (Plate 1). These features either indicate that the units were deposited at least in part subaqueously, or were partially reworked by water after their deposition. The sedimentary features consistently indicate that the stratigraphic up direction is to the east in all parts of the section.

Porphyritic metarhyolites have characteristics of ash-flow tuffs, and are common in both of the felsic parts of the FP section (Plates 2 and 3). These units show various features such as broken phenocrysts of feldspar and quartz, flattened pumice fragments, and a cryptocrystalline matrix which may display a slight laminated appearance at the microscopic level. Because of the cryptocrystalline texture

of the matrix, only stained potassium feldspar and micas are identified. Phenocrysts of oligoclase (An<sub>10</sub> to An<sub>20</sub>), quartz, and sometimes potassium feldspar are abundant. These grains range from 2 to 3mm and modally comprise between 3 and 15%. Pumice fragments range up to 10% and have a cryptocrystalline appearance. The elongated to flattened pumice fragments are often molded around other grains. The laminations, which are sometimes observed in the porphyritic metarhyolites, may represent relict banding produced during the deposition of ash flows. Accessory minerals which may be observed include zircon, epidote, hematite, sericite (may be an abundant alteration product ranging up to 20%), chlorite, and biotite, all usually less than 5%.

The laminated metarhyolites are generally fine-grained and have a homogeneous character. Phenocrysts are often apparent on the weathered surface, only comprising a few percent of the grains. The laminated metarhyolites only occur in the eastern part of the Fletcher Park section, and conformably overly and interfinger with the porphyritic felsic metavolcanics. The laminated varieties are very fine-grained with an average grain size size of less than 0.5mm. The mineral content is comprised of modally indistinguishable quartz, feldspar, epidote, and mica. Staining for potassium feldspar is poor due to the small grain size, but this mineral appears to comprise between 25 and 35%. Quartz grains are usually clear in appearance, and

apparently comprise between 30 and 40%. One sample (GM-023) contains about 0.5% subhedral plagioclase grains ranging up to 2mm. Although sericitized, obscure albite twinning indicates a composition of An<sub>14</sub>. Sericite and chlorite are also present, each comprising between 10 and 15%. Epidote is also present, and comprises between 10 and 15%. The laminated metarhyolites are well foliated, with foliation defined by micaceous minerals and stretched patches of coarse and fine-grained material. The laminations are also defined either by the coarse and fine-grained layers or variations in mica content, and may be a result of deposition or metamorphic differentiation. The laminated metarhyolites may represent several possible rock types such as air-fall tuff, water-laid tuff, or tuffaceous sediment.

Fragmental metarhyolites occur as clast-supported breccias (Plate 4). The exposures contain angular to subangular rock fragments which range up to approximately 20cm in length. The matrix around the fragments is fine-grained and apparently silicified. Most of the clasts are felsic in composition, with minor occurrences of mafic and cherty types. The felsic clasts are similar to some of the rock types observed in the section, with the addition of abundant flow banded varieties. A thin section of a flow-banded clast (GM-006) from the metarhyolite breccia was studied, and is representative of the most common felsic clast type. This sample is comprised of a laminated matrix of interlayered granoblastic quartz-rich and

indistinguishable cryptocrystalline material. Relict phenocrysts of plagioclase (An8) are albite twinned, and comprise about 5% of the rock. Although most of the minerals are too fine-grained to identify, the sample is probably a mixture of quartz, feldspar, and sericite. Accessory minerals are epidote and iron oxides. The banding, which is also apparent megascopically, and a relict vitrophyric texture suggest that the fragment may be from a rhyolite flow or dome. The breccia accumulation with associated interfingering tuffs and exhalite may indicate proximity to a dome type structure. Possibilities include debris along the dome flanks or an explosion breccia near a volcanic vent.

## EXHALITE

Siliceous caps are associated with the top of the felsic volcanic sequences (Figure 4). These deposits were probably produced by exhalation of fluids during hydrothermal processes. The exhalite units are laterally continuous and have silicified the underlying volcanic unit. The deposits consist of microcrystalline chert which is locally hematitic. Milky white carbonate of unknown composition may be intermixed with the chert, giving the outcrop a pockety weathered surface. Colors of the chert are generally medium gray to reddish brown. Contact metamorphism has produced local garnet, and coarsely crystalline epidote, actinolite, and quartz. This feature is especially notable near the contact of the granodiorite in the eastern part of the Fletcher Park section. These cherty horizons have been recent exploration targets for massive sulfide deposits. Local minor occurrences of disseminated sulfides are present, but the economic potential of the exhalites were not a primary subject of this study. No thin sections of the exhalite were examined.



## METADACITES

Metadacites are found throughout the FP section, with the major units occurring in the western half of the area (Figure 4). The units are conformably interbedded with the adjacent rocks, although some thin intrusive dikes occur locally in the section. Metadacites are usually distinguished from the metarhyolites by their darker gray to greenish gray color, and weather dark brown, reddish brown, or dark gray. Three textural types are observed in the metadacites. These textures are porphyritic, non-porphyritic, and fragmental. Sedimentary structures are common in some of the fine-grained metadacites, and display the same eastward younging stratigraphic indications as the metarhyolites.

Porphyritic metadacites contain abundant phenocrysts of plagioclase (often greater than 5%) contained within a fine-grained groundmass. The porphyritic varieties form massive, weakly foliated outcrops, with bedding only apparent where sedimentary structures are observed. Plagioclase phenocrysts are apparent on the weathered surface as milky white laths ranging up to 4mm. Lithic fragments may also be observed, and comprise up to a few percent of the rock. In thin section, a pyroclastic texture is apparent, evidenced by broken phenocrysts, pumice fragments, and a fine-grained groundmass. The plagioclase (An<sub>26</sub> to An<sub>33</sub>) phenocrysts contain exsolved patches of microcline, and modally comprise between 5 and 20%. Quartz

phenocrysts are uncommon. Microcline displays tartan twinning, and is usually only recognized as patches of exsolution within plagioclase phenocrysts. Biotite and chlorite, comprising between 7 and 24%, occur as 1mm plates defining a moderate foliation. Lithic fragments commonly comprise up to several percent of the porphyritic metadacites, usually as subangular grains ranging up to 4mm. The fragments are composed of cryptocrystalline vesicular(?) pumice, microporphyritic volcanics, and minute, cryptocrystalline grains of various shapes possibility representing glass shards. The groundmass is a fine crystalline mixture of feldspar, quartz, chlorite, and sericite, probably representing devitrified glass. Accessory minerals which may be observed include epidote, zircon, apatite, and hematite.

One porphyritic metadacite in the central part of the FP section does not display a pyroclastic texture. It is characterized by 10% plagioclase phenocrysts of An<sub>32</sub>. The phenocrysts are euhedral to subhedral, and show very little sign of breakage. The groundmass is comprised of plagioclase microlites (An<sub>26</sub>, 20%), and a mixture of fine-grained chlorite, albite, quartz, sericite, and epidote. Although the sample is altered, and mineral identification is difficult, the unit appears to display a relict porphyritic hyalopilitic texture. The above characteristics suggest that the unit may be a dacite lava flow(s). This unit possibility represents the only felsic

flow observed in the Fletcher Park section, with the exception of the flow-banded fragments within the rhyolite breccia previously described.

Outcrops of fragmental metadacites are located in the central part of the Fletcher Park section, and are interbedded with volcanoclastic deposits. Contacts with the adjacent volcanoclastics are gradational. The fragmental metadacites are represented by moderately foliated units with abundant lithic fragments ranging up to 3cm in length. The surrounding matrix is fine-grained and chloritic. The fragments are subangular to subrounded and white to pale green. A variety of volcanic lithologies are represented by the lithic fragments, dominantly cryptocrystalline clasts which appear to be pumice, and fine-grained microphyritic volcanics. The fragments are supported by a microcrystalline matrix comprised of quartz, albite, sericite, chlorite, and epidote. Biotite plates ranging up to 0.5mm commonly occur around the fragments and define foliation in the matrix. The fragmental metadacites appear to represent lapilli tuffs which may have been deposited subaqueously as evidenced by their gradation into fine-grained volcanoclastics.

The non-porphyrific metadacites are mainly found in the central and western parts of the Fletcher Park section, and are interbedded with the mafic agglomerates and fragmental metadacites. Contacts range from sharp and conformable to gradational with the adjacent units. These non-porphyrific

units are dark gray to greenish gray on the fresh and weathered surface. Foliation is weak to moderately developed, and sedimentary structures are absent. In thin section, the non-porphyrific metadacites are too fine-grained for accurate mineral description. The microcrystalline material has an average grain size of less than 0.05mm. Although definitive optical properties can not be observed, the rock appears to contain a mixture of feldspar, sericite, chlorite, quartz, and epidote. Only quartz, biotite, and epidote are positively identified through the few coarse grains available. Overall, the matrix has a stretched, patchy appearance, in which patches are defined by changes in grain size or higher sericite content. These patches are discontinuous and range up to several millimeters in length. The patches may represent either relict laminations, or may be a feature produced by metamorphism. Overall, the above observed features suggest that the non-porphyrific metavolcanics may be deposits of metadacite ash.

## METABASALTS

Matrix-supported agglomerates are the most abundant rock type of basaltic composition in the FP section. These units are massive in outcrop with the coarse fragmental texture very distinctive (Plate 5). A lack of sorting or stratification characterizes the agglomerates. The weathered surface is medium green, with the clasts weathering to a lighter green than the matrix. The clasts, supported by a medium-grained micaceous matrix, have shapes ranging from rounded to angular (mainly subrounded), and range up to boulder size (>25cm). On the fresh surface, the matrix is distinguished from the clasts with difficulty. This relative indistinguishability reflects their similarity in composition. The clasts mainly display a fine-grained, often porphyritic texture. Felsic rock types are also present as clasts, but are minor in occurrence. One outcrop, at the base of the central mafic metavolcaniclastic sequence of Fletcher Park, contains channel-shaped accumulations of well rounded clasts (Plate 6). The clasts within the channels are similar in composition to the clasts of the mafic agglomerate, and appear to be poorly imbricated. This outcrop appears to be a volcaniclastic conglomerate derived from rocks similar to the agglomerates. The overall characteristics of the matrix-supported agglomerate suggests a possible mudflow or pyroclastic deposit. The degree of rounding of the clasts may be favorable for a mudflow origin.

In thin section, the matrix of the agglomerate is fine-grained and displays an average grain size less than 0.1mm. Actinolite (15 to 20%) occurs as anhedral, irregularly shaped grains ranging up to 0.5mm, and grain aggregates ranging up to 1mm. Biotite (10%) occurs as plates ranging up to 0.2mm, often as aggregates ranging up to 0.5mm. The rest of the matrix is comprised of fine crystalline epidote, chlorite, and feldspar. Some larger grains of the matrix were identified as albite. Several percent lithic fragments ranging up to 2mm are also present. A thin section was also made of one the clasts most common to the agglomerate. The clast is porphyritic, containing phenocrysts of plagioclase and actinolite-chlorite-epidote pseudomorphs after pyroxene ranging up to 5mm. The phenocrysts comprise a total of 20 to 25% of the clast. The groundmass is a fine crystalline mixture of epidote, chlorite, actinolite, and feldspar, and has an average grain size less than 0.1mm.

Another type of basaltic unit is comprised of approximately 40% breccia fragments ranging up to 3cm, averaging less than 1cm, and a fine-grained micaceous matrix. The fragments are irregularly shaped and stretched parallel to the moderately developed foliation. Individual units are less than 10m thick and medium green. The fragmental character of the breccia is evident on both the weathered and fresh surfaces.

Thin sections of the breccia reveal a matrix comprised

of approximately 35% plagioclase (An28) microlites ranging up to 0.2mm within a fine-grained epidote, chlorite, actinolite, and albite matrix. The microlites are random to subparallel in orientation and usually deformed. The rock fragments have several appearances, but are dominantly very fine-grained varieties comprised of actinolite, chlorite, epidote, and feldspar, and microporphyritic varieties containing between 25 and 30% randomly oriented plagioclase (An30) microlites within a microcrystalline groundmass. These mafic breccias may represent either lapilli tuff deposits, or possibly thin, brecciated basaltic flows. The presence of plagioclase microphenocrysts in the matrix probably favors the latter interpretation.

Metabasalt dikes and sills are a minor rock type, and intrude both the mafic and felsic parts of the Fletcher Park section. The thickness of the dikes and sills are generally less than 1m. Colors of these intrusives range from dark green to nearly black on both the fresh and weathered surfaces. In contrast to the gradational contacts exhibited by the fine-grained volcaniclastic rocks, contacts of the dikes and sills are sharp with the adjacent units. These intrusives are very fine-grained in hand specimen, and display a cryptocrystalline texture in thin section. A relict holohyaline texture is suggested, now devitrified to a probable mixture of actinolite, chlorite, epidote, and feldspar.

Mafic volcaniclastics are an important rock type.

These deposits occur as minor units within the mafic agglomerates, and as upward-fining sequences in the central part of the Fletcher Park section. Textures of the volcanoclastics range between pebbly, coarse-grained volcanic sandstones to very fine-grained volcanic siltstones. Contacts are gradational with adjacent volcanoclastic units as well as with the agglomerates. Colors are dark to light green on the fresh surface, and gray green or reddish brown on the weathered surface. Volcanoclastic units within the agglomerates are less than 1m thick, and the upward-fining sequences comprise a total thickness of approximately 70m.

Thin sections of the sandy volcanoclastic units have an average grain size of 0.3mm. The grains are subrounded to subangular in character and include a few percent fine-grained lithic fragments. The mineral content consists of 20 to 25% actinolite, 30% albite, 25% epidote, 15% chlorite, 3% biotite, and 2% magnetite and hematite. Actinolite and epidote range up to 0.5mm, with epidote often in aggregates ranging up to 3mm. The rest of the minerals are less than 0.1mm, with chlorite and biotite defining a moderate foliation. A clastic texture is apparent in both thin section and outcrop. Coarse-grained pebbly units exhibit the same mineral content as the sandy units. Coarse grains of actinolite are common, and display crystal forms which indicate that they are pyroxene pseudomorphs. The coarse-grained lithic fragments are microporphyritic and



similar in appearance to the clasts of the agglomerates. The silty volcanoclastic units have a cryptocrystalline texture, and appear to be composed of a mineral assemblage similar to the coarse-grained deposits. The volcanoclastic sediments are derived from mafic volcanic material. The thin, fine-grained volcanoclastics within the agglomerates may be accumulations of finer-grained minerals which settled out of suspension after subsqueous deposition of a mudflow. The upward-fining graded sequences may have been produced by turbidity currents.

The large mafic intrusive located in the central part of the FP section has a medium to dark green color on the fresh and weathered surfaces. The intrusive is medium-grained with a nearly equigranular texture, locally fine-grained. Milky white to pale green feldspar grains stand out as small laths against the darker green color of the rest of the rock. Outcrops are subdued, and have sharp, usually fine-grained contacts with adjacent units of the volcanic section. Xenoliths of the adjacent volcanics and volcanoclastics have been incorporated within the intrusion, and may occur as large isolated blocks ranging up to 20m or more.

In thin section, it is apparent that the mafic intrusive is quite altered, but primary petrographic features are still present. Saussuritized laths of plagioclase ranging up to 5mm are euhedral to subhedral. Albite twinning is generally not preserved, but the

plagioclase is calcic in composition and comprises about 45% of the rock. Actinolite is also abundant (45%), occurring as 2 to 3mm subhedral to anhedral grains. The relationship between the grains of actinolite and plagioclase resembles a relict subophitic texture, with the actinolite probably as pseudomorphs after pyroxene. Biotite and quartz comprise a few percent each as grains ranging up to 0.5mm. Biotite occurs mainly as patches within actinolite grains. Epidote occurs as irregular grains and aggregates ranging up to 1.5mm, and as very fine grains within actinolite and plagioclase. The above features indicate that the intrusive is a medium-grained diabase.

## GREEN MOUNTAIN SECTION

## GENERAL DESCRIPTION

The Green Mountain area lies approximately 9km to the east of the Fletcher Park section (Figure 2), and is the location of a metavolcanic sequence first described by Spencer (1904). This section is metamorphosed to a higher grade than the Fletcher Park section, resulting in poorer preservation of relict features. Although a few relict features are observed, such as phenocrysts, the metamorphic character is dominant, and the use of metamorphic terms to describe the rocks is more appropriate.

The GM section, in general, is comprised of amphibolite, amphibolite breccia and agglomerate, and various feldspar-quartz-mica schists (Figure 5). Compositional layering generally strikes east west and dips steeply to the south. Foliation throughout the GM section parallels the compositional layering. The section is in intrusive contact with the surrounding granitic terrane. The amphibolites are exposed in the northern and southern parts of the GM section, and the central part of the area is dominated by feldspar-quartz-mica schists. Rock units are best exposed in the southern third of the section. Units occurring on northern slope of Green Mountain are poorly exposed due heavy tree and ground cover. The exposed thickness is approximately 2.2km. This probably not a true thickness since both faulting and transposition of bedding appear to have affected the section.

## AMPHIBOLITES

Amphibolites of the GM section have two main textural appearances in terms of grain size. Textures are either fine to medium-grained (<5mm) or coarse-grained (>5mm). Most units appear to be laterally continuous, with amphibolite units usually traceable from one ridge to the next along strike. This traceability aids in locating the outcrop along the poorly exposed northern end of Green Mountain. Some variation in texture occurs along strike, probably representing different horizons within the amphibolites. Alternatively, these textural variations could represent lateral changes within the same horizon. The amphibolite exposure in the northern part of the section thickens to the east, while the southern amphibolite exposure has a uniform thickness.

Fine to medium-grained amphibolites occur in the northern and southern parts of the GM section (Figure 5). A banded appearance is observed in these amphibolites, defined by variation in the amphibole content. Colors of the amphibolites range from medium to dark green, greenish gray, to black on the fresh surface, and reddish brown or black on the weathered surface. Foliation is defined by the alignment of hornblende crystals. Hornblende together with white to gray plagioclase are the only minerals recognized readily in hand specimen. All fine to medium-grained amphibolites are conformable with adjacent compositional layers, and do not display cross-cutting relationships.

In thin section, medium green to brownish or bluish green pleochroic hornblende needles range up to 1mm in fine-grained amphibolites, and up to 5mm in medium-grained amphibolites. This mineral modally comprises between 35 and 70%. Granoblastic grains of plagioclase (An17 to An42) comprise between 20 and 35%; albite twinning is uncommon. Epidote and clinozoisite comprise between 1% and 20%, and are the only other minerals which may be abundant. The fine and medium-grained amphibolites display a nematoblastic texture. Accessory minerals may include quartz, biotite, hematite, magnetite, sericite, calcite, chlorite, and apatite.

Fragmental amphibolites also occur in the northern and southern parts of the GM section, and are interlayered with the fine to medium-grained amphibolites. Subangular to subrounded fragments ranging up to 3cm are apparent megascopically in the units of amphibolite breccia. Most of these units usually have a thickness less than 1m. In the northern amphibolite part of the Green Mountain section there are fragmental amphibolites with a different appearance. These units are strikingly similar to the metabasalt agglomerates observed in the Fletcher Park section. Clasts within this type of fragmental amphibolite are generally subrounded, and range up to 20cm or more. The clasts are supported by a fine-grained, well foliated matrix. Clasts of felsic composition are also present, but are minor in occurrence.

The agglomeratic unit of Green Mountain was not examined in thin section, but samples from the fragmental units containing the smaller clast size are described. Pleochroic hornblende displays the same character as in the fine-grained amphibolites, producing a nematoblastic texture. The hornblende is more abundant in the rock fragments in comparison to the matrix, and modally comprises between 40 and 65%. Granoblastic plagioclase ranges between 20 and 35%, and ranges in composition between An17 and An21. Epidote comprises between 1 and 20%. Accessory minerals which may be observed include quartz, hematite, calcite, and sphene.

Coarse-grained amphibolites are also present in the Green Mountain section, but form such a minor proportion of the total amphibolite section that only a field description is given. These amphibolites also appear concordant with compositional layering, but are laterally discontinuous. Hornblende laths ranging up to 1cm are subparallel in orientation, and comprise between 60 and 80% of the rock. Fine-grained milky white plagioclase ranges between 20 and 40%. Epidote is the only other mineral recognized, but is only minor in occurrence. The coarse-grained texture and concordant, but laterally discontinuous outcrop pattern suggests that these units may be diabase sills.

## FELDSPAR-QUARTZ-MICA SCHISTS

Felsic schists dominate the central part of the Green Mountain section, with a minor occurrence along the northern margin of the area (Figure 5). Geochemical characteristics indicate rhyolitic to dacitic compositions. The chemical differences are reflected in thin section by either microcline (rhyolitic) or oligoclase (dacitic) comprising the dominant feldspar. Textures vary from poor to moderately foliated and medium to coarse-grained. Plagioclase porphyroblasts may be evident on the weathered surface, and may be relict phenocrysts. A minor unit in the northern part of the Green Mountain section has a fragmental character similar to the felsic breccia of Fletcher Park.

Schists of rhyolitic composition are restricted to the northern part of the felsic section, and are represented by microcline-quartz-oligoclase-biotite assemblages. Although exposures are sparse, the rhyolitic part of the section has a total thickness of approximately 400m. Rhyolitic schists are light brownish gray to medium gray to pink, and weather to medium or dark brown, dark gray, or reddish brown. Foliation is weak to moderate and defined by the alignment of biotite grains and streaks. Phenocrysts, when present, are usually only apparent on the weathered surface as large milky white grains. Cross-bedding appears to be present locally, but can not be identified with confidence as an actual feature. The presence of possible relict phenocrysts suggest a volcanic crystal tuff origin, while units lacking

phenocrysts may be layered tuffs or volcanoclastic sediments.

In thin section, rhyolitic schists typically have a granoblastic texture of tartan twinned microcline (20 to 50%), quartz (22 to 40%), and oligoclase (An12 to An21, 10 to 21%) which is rarely albite twinned. Biotite has a subparallel to parallel alignment defining foliation, and modally comprises between 7 and 10%. Muscovite is sometimes present as coarse grains ranging up to 2mm, and is probably of secondary origin. Porphyroblasts of perthitic plagioclase are common, and may appear in thin section when not apparent in the hand specimen. These grains are 2 to 3mm in length and generally anhedral. The porphyroblasts, ranging in composition between An26 and An30, contain exsolved patches of microcline and often display a mortar texture. Quartz may occur in elongate aggregates ranging up to a few millimeters, and may represent recrystallized quartz phenocrysts. Accessory minerals which may be present include zircon, garnet, sericite, chlorite, epidote and/or clinozoisite, and calcite.

Schists of dacitic composition are the dominant felsic rock type of the Green Mountain section. These rocks are best exposed in the southern part of the area along the road on the main east trending ridge (Figure 5). Bold outcrops of dacitic schist are medium or dark gray to reddish gray, and moderately to strongly foliated. The dacitic schists weather to dark grays with 2 to 4mm feldspar porphyroblasts



a commonly observed feature. Some dacitic units also display ovate patches ranging up to 1cm which are composed of feldspar and quartz. These features may represent relict lithic fragments. The section of dacitic schists appears to thin to the east due to a northwest trending fault (Figure 5). The dacitic schists of the central part of the section probably represent porphyritic and fragmental pyroclastic deposits and volcaniclastic sediments.

In thin section, the dacitic schists typically have a granoblastic texture comprised of an oligoclase-microcline-quartz-biotite assemblage. Overall, the dacitic schists contain albite twinned and untwinned oligoclase (An16 to An26; 30 to 47%), tartan twinned microcline (16 to 25%), and quartz (20 to 28%). The average grain size is about 0.2mm. Biotite grains (8 to 16%) define the foliation and range up to 0.5mm. Accessories which may be observed include epidote/clinozoisite, zircon, hematite, sericite, garnet, muscovite, and calcite. Feldspar porphyroblasts may comprise up to 5%, and range in composition between An15 and An28. These porphyroblasts may represent relict phenocrysts preserved from an original volcanic protolith. The porphyroblasts are usually absent in the finer-grained dacitic schists.

Felsic breccia is present in the GM section as a minor rock type. Although no thin sections samples were taken, the similarity of the breccia to units in the Fletcher Park section warrants a description of their general

characteristics. A small outcrop of the breccia is located in the northern part of the felsic schist section, but no contact relationships are observed. The clasts are representative of various lithologies, but are dominantly fine to medium-grained feldspar-quartz-mica schists and minor amphibolite. The clasts range up to 20cm or more, and are angular to subrounded.

## GEOCHEMISTRY

## INTRODUCTION

The geochemical characteristics of the major lithologies of the Green Mountain Formation are determined as one of the objectives of this study. Some analyses of associated plutonic rocks are also included. The analyses were carried out by instrumental neutron activation and X-ray fluorescence techniques, with procedures, errors, and specific details described in Appendices E and F. The geochemical characteristics of the Green Mountain Formation are used for purposes of classification (assigning rock names), to evaluate possible geochemical trends of the volcanic suite as a whole, and for interpretation of tectonic environment. Forty samples are selected to represent the Green Mountain Formation. The samples are chosen to represent the least altered or weathered units, while maintaining a representative suite of the rock types present.

This section also evaluates the problem of alteration of the rocks of the GMF. In general, most major and trace elements may be severely affected by alteration. This places limitations on the reliability of the interpretations of geochemical parameters. Final interpretations, if possible, are primarily based on certain immobile trace elements discussed below. Classification and interpretations are based on geochemical schemes which are defined from modern rock suites and tectonic environments,

with the assumption that Precambrian tectonic processes were similar to modern processes and produced similar geochemical trends.

Before the geochemical data were plotted, major and minor element analyses were recalculated to 100% after subtracting volatiles (loss on ignition). Eleven major and minor elements and 22 trace elements were determined, and the results are listed in Appendix C.

## PLUTONIC ROCKS

The larger plutonic bodies in the metavolcanic and granitic terranes are considered separately from other dikes and sills. Although there are several intrusive bodies within the Precambrian terrane of the Sierra Madres, the only two studied are the diabase intrusive of the Fletcher Park section and the Encampment River Granodiorite. These were chosen because they are spatially the most closely associated intrusives to the Green Mountain Formation. The diabase directly intrudes the volcanic section of Fletcher Park, and the granodiorite occurs between areas of the Green Mountain Formation within the granitic terrane.

## GRANODIORITE

The Encampment River granodiorite is the oldest intrusive body of the granitic terrane which surrounds the Green Mountain Formation. Analyses of the unit are given in Appendix B. Small dikes associated with the granodiorite can also be found within the volcanic sequence of the GMF. Geochemical data from the granodiorite are plotted on the Ab-An-Or and Na<sub>2</sub>O-CaO-K<sub>2</sub>O diagrams (Figures 6 and 7). Most points indicate that the intrusive is indeed of granodiorite composition, although variation in the Ab-An-Or plot is evident. The chemical classification is consistent with the mineral assemblages observed in thin section (Appendix B).

The close association of the granodiorite with the GMF metavolcanics prompts their comparison. Table 1 compares the major and trace element composition of the granodiorite

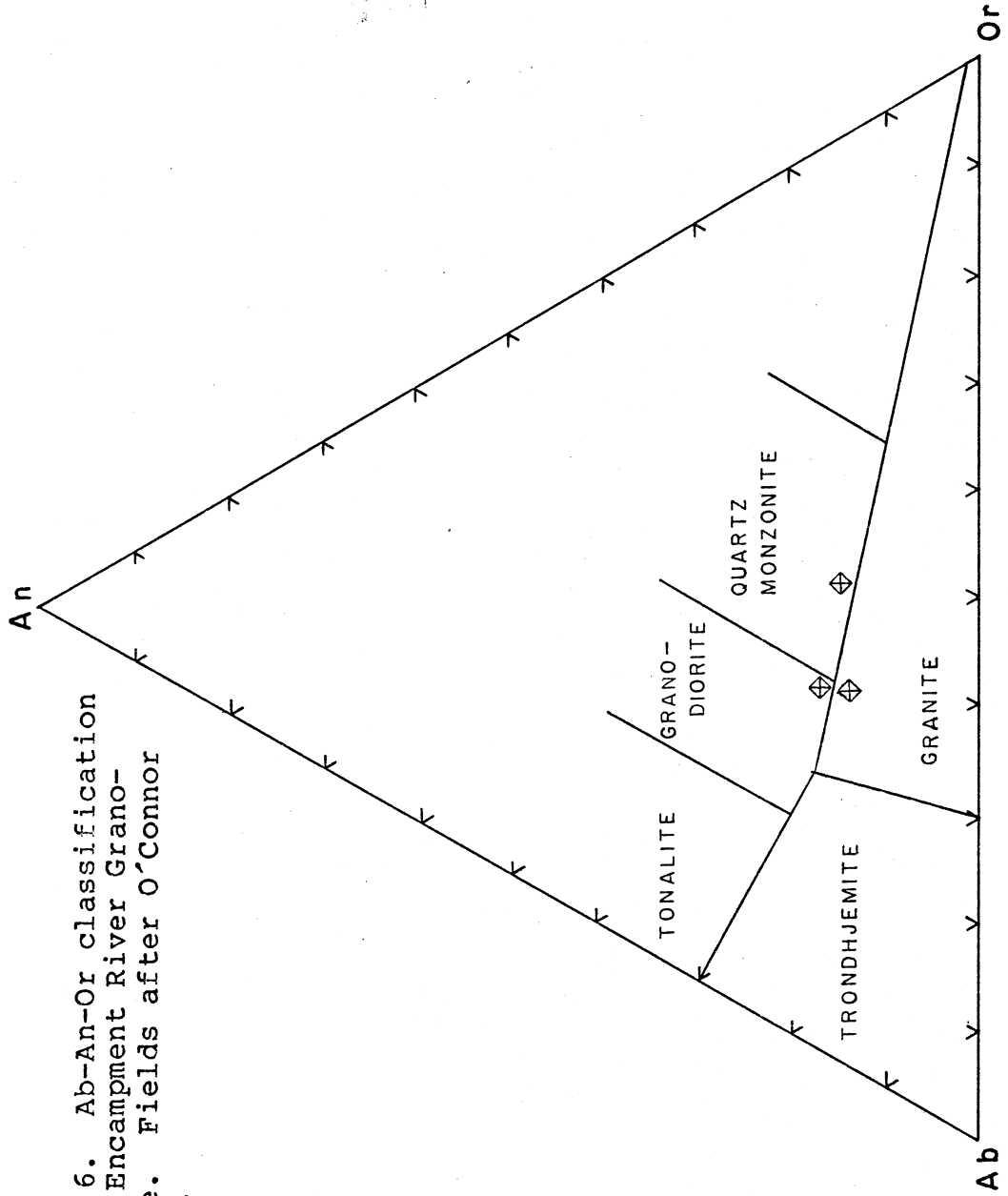


Figure 6. Ab-An-Or classification of the Encampment River Granodiorite. Fields after O'Connor (1965).

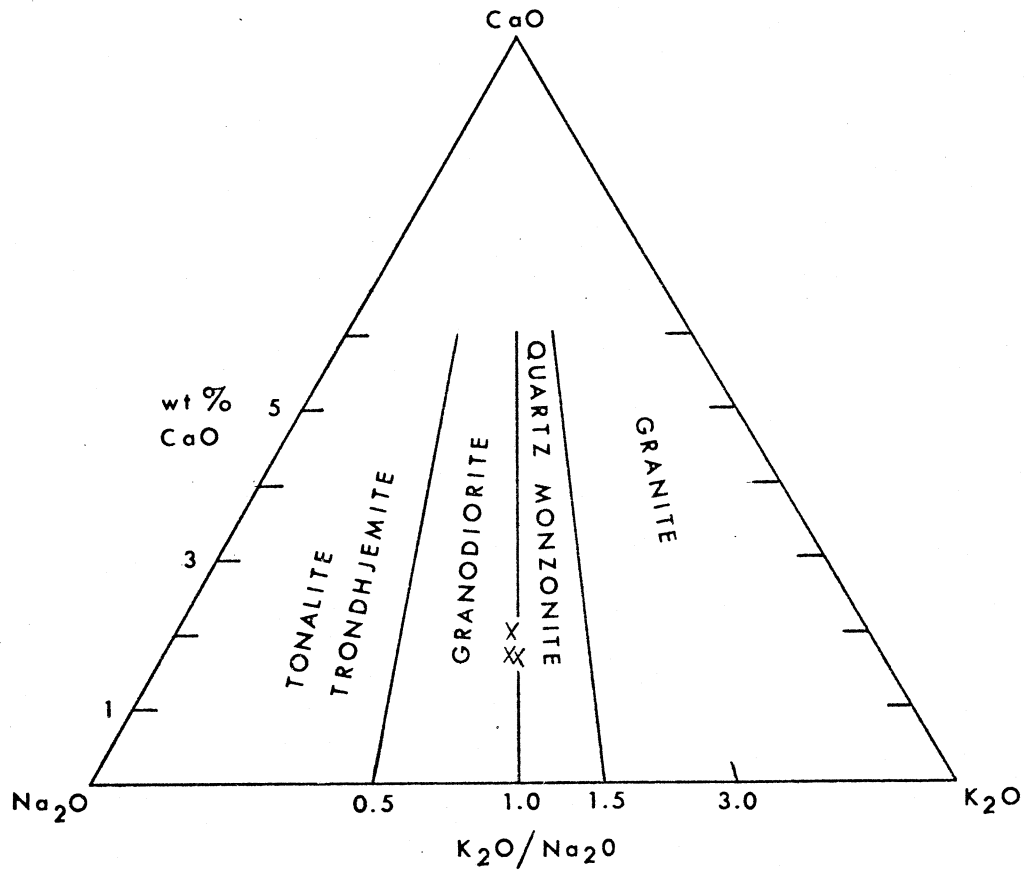


Figure 7. Na<sub>2</sub>O-CaO-K<sub>2</sub>O plot of the Encampment River Granodiorite.

TABLE 1

COMPARISON OF AVERAGE GRANODIORITE TO THE  
THE AVERAGE GMF RHYOLITE AND DACITE

|                                  | RHYOLITE | GRANODIORITE | DACITE |
|----------------------------------|----------|--------------|--------|
| SiO <sub>2</sub>                 | 73.38    | 72.72        | 66.12  |
| TiO <sub>2</sub>                 | 0.25     | 0.32         | 0.62   |
| Al <sub>2</sub> O <sub>3</sub>   | 13.30    | 14.17        | 15.88  |
| Fe <sub>2</sub> O <sub>3</sub> T | 2.24     | 2.92         | 5.33   |
| MgO                              | 0.54     | 0.71         | 1.24   |
| CaO                              | 1.44     | 1.84         | 2.62   |
| Na <sub>2</sub> O                | 3.72     | 3.70         | 4.63   |
| K <sub>2</sub> O                 | 3.96     | 3.59         | 2.88   |
| MnO                              | 0.06     | 0.04         | 0.14   |
| P <sub>2</sub> O <sub>5</sub>    | 0.03     | 0.06         | 0.20   |
| Rb                               | 75       | 55           | 73     |
| Sr                               | 169      | 284          | 341    |
| Cs                               | 0.9      | 1.2          | 1.5    |
| Ba                               | 1156     | 1166         | 1186   |
| Y                                | 40       | 27           | 33     |
| Zr                               | 220      | 165          | 148    |
| Hf                               | 5.4      | 4.6          | 3.3    |
| Nb                               | 13       | 12           | 9.2    |
| Ta                               | 0.8      | 1.0          | 0.7    |
| Sc                               | 8.5      | 7.2          | 14     |
| Cr                               | --       | --           | --     |
| Ni                               | 3.9      | 3.7          | 5.7    |
| Co                               | 1.8      | 3.0          | 5.9    |
| U                                | 3.1      | 2.8          | 2.6    |
| Th                               | 8.5      | 9.7          | 6.5    |
| La                               | 49       | 31           | 34     |
| Yb                               | 3.6      | 3.2          | 2.5    |

Total iron as Fe<sub>2</sub>O<sub>3</sub>

Oxides in weight percent

Trace elements in ppm

-- = not detected



with the GMF metarhyolite and metadacite. The trace element abundances of the granodiorite are similar, and usually have intermediate values between the metarhyolite and metadacite. The chondrite normalized rare earth patterns of the granodiorite are similar to the patterns of the metadacites in terms of LREE enrichment, HREE concentration, and moderate negative Eu anomalies (Figure 8). These similarities suggest that the granodiorite may represent the same magmatic source as the felsic metavolcanics of the GMF.

#### DIABASE

The diabase which intrudes the metavolcanic section of the Fletcher Park area was only analyzed for major and minor elements (Appendix C). The diabase plots with the GMF metabasalts on the Jensen Cation Plot (Figure 9), and the  $TiO_2$  versus  $100 \times Mg/(Mg/Fe^{2+})$  diagram (Figure 10). Trace element data are not available for comparison, but the diabase probably represents an intrusive equivalent to the mafic volcanics from a similar magmatic source. If the diabase is an intrusive member directly related to the volcanic section, the same problems of alteration of the volcanic rocks discussed below are also applicable.

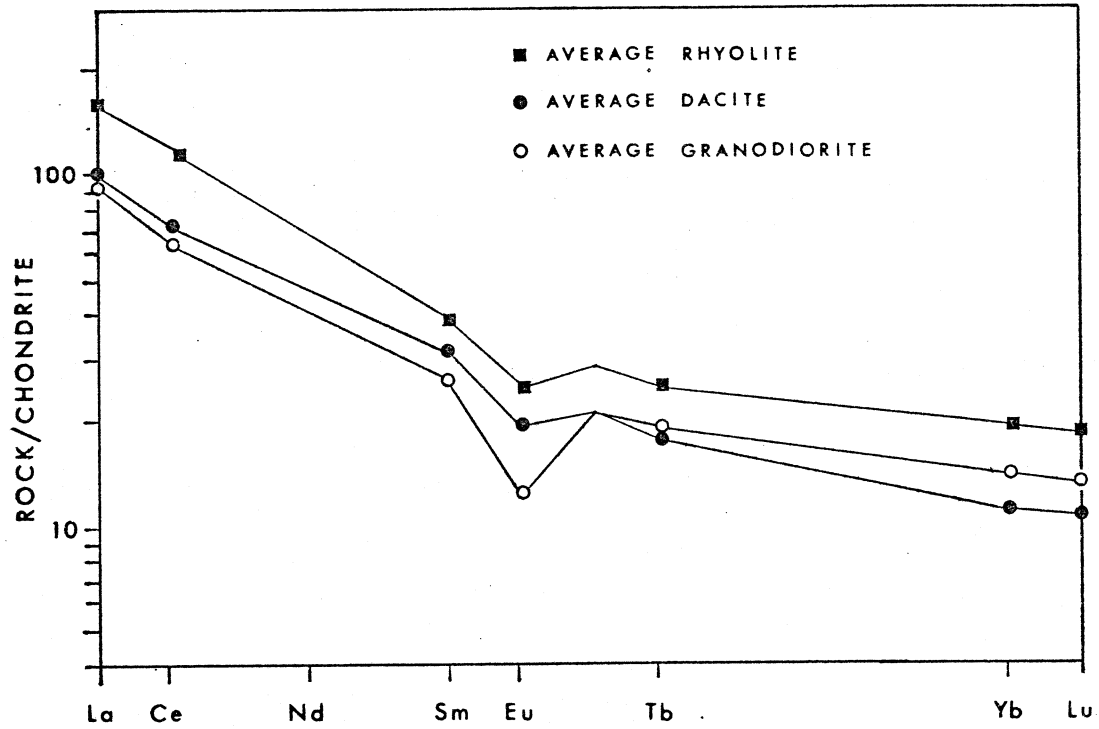


Figure 8. Comparison of the REE patterns of the granodiorite to the GMF felsic rocks.

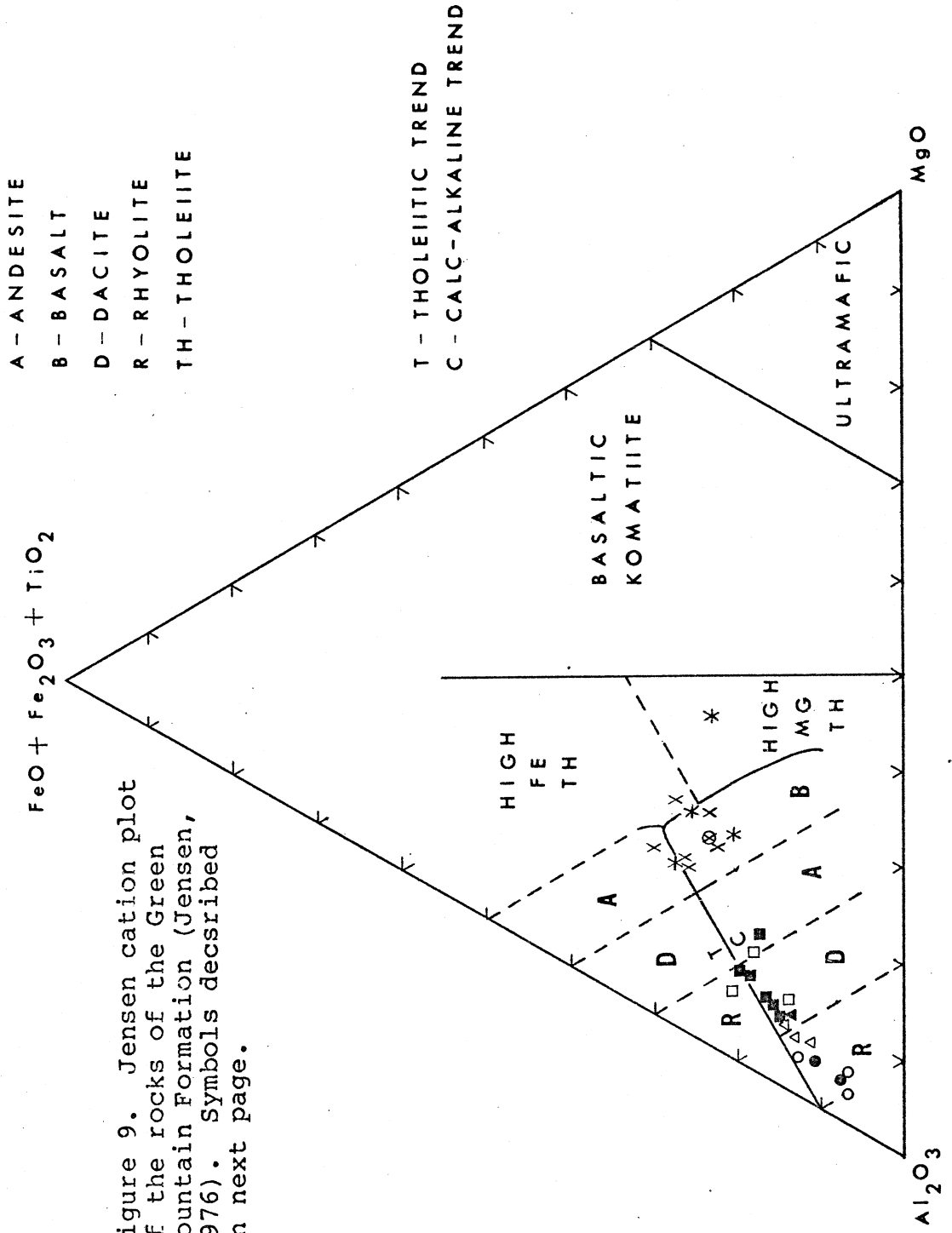


Figure 9. Jensen cation plot of the rocks of the Green Mountain Formation (Jensen, 1976). Symbols described on next page.

EXPLANATION OF SYMBOLS FOR  
GEOCHEMICAL DIAGRAMS

FLETCHER PARK

GREEN MOUNTAIN



RHYOLITE



RHYODACITE(?)



DACITE



THOLEIITE



---

---

GRANODIORITE



DIABASE



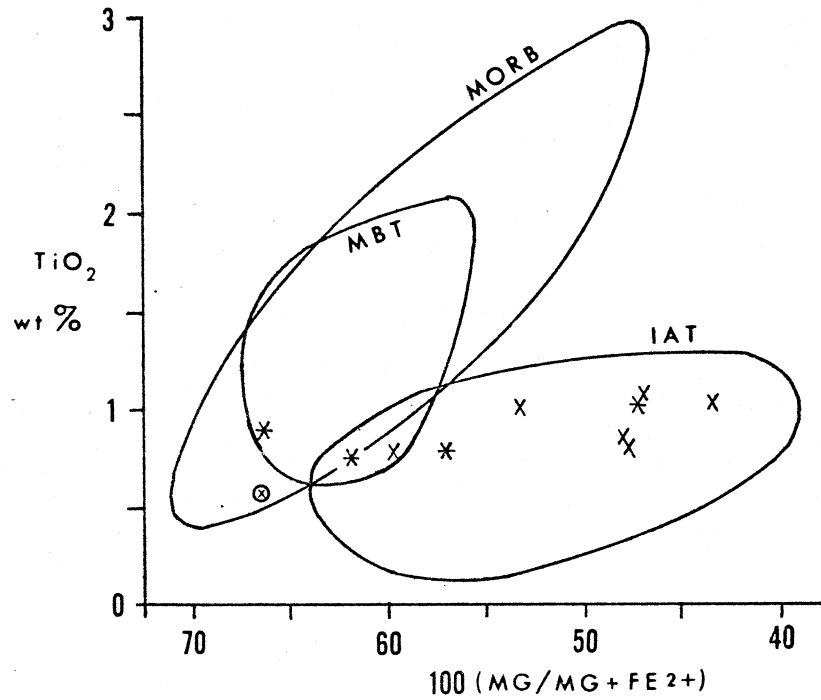


Figure 10.  $\text{TiO}_2$  vs  $100 (\text{Mg}/\text{Mg} + \text{Fe}^{2+})$  plot of the GMF mafic volcanics and diabase. MBT= marginal basin tholeiite, IAT= island arc tholeiite, MORB= mid-ocean ridge basalt. Symbols explained on page 56.

GEOCHEMISTRY OF THE GMF VOLCANIC AND VOLCANICLASTIC ROCKS  
INTRODUCTION

One of the basic purposes of determining the geochemical characteristics of rock samples is to classify them according to accepted schemes, and to characterize them for comparative purposes. This section discusses classifications schemes for assigning specific rock names, and possible criteria to distinguish the compositional members of the Green Mountain Formation. Because of the chemical similarities of the volcaniclastic rocks and the associated volcanic rocks, both groups are included in the same classification schemes. All classification schemes used in this study are derived from trace and major element characteristics of modern or Phanerozoic rock types. Specific classification schemes used in this study are the  $\text{SiO}_2$  vs Nb/Y and Zr/TiO<sub>2</sub> vs Nb/Y diagrams of Winchester and Floyd (1977), and the Jensen Cation Plot (Jensen, 1976). These diagrams were chosen for two reasons, (1) they represent both trace element and/or major element classifications, (2) the trace elements used are considered to be relatively immobile during alteration, and (3) to test the agreement between trace and major element schemes.

## ALTERATION

Before any study involving geochemistry can be successfully evaluated, the problem of alteration must be considered. Alteration of volcanics, volcanoclastic rocks, and associated intrusive rocks, can occur at any time during their geologic history. Changes in composition can occur during diagenesis, metamorphism, metasomatism, or sea-floor alteration, to name a few possible processes. The problem of alteration can be especially complicated for Precambrian rocks, because the original mineral content and physical characteristics may not be preserved.

Studies of younger volcanic suites show that the processes of alteration can significantly effect original major and trace element concentrations (Christensen and others, 1973; Hart and others, 1974; Hajash, 1975; Ludden and Thompson, 1978 and 1979). The effects of alteration in older rocks have also been evaluated, and show a variety of results (Condie and others, 1977; Hynes, 1980; MacGeehan and MacLean, 1980). Beswick and Soucie (1978) propose a graphical method to correct for alteration which is applied in this study. This method, in addition to observable physical and chemical characteristics, is used to screen the samples for alteration. High loss on ignition (>2.5%), extensive sericitization or other types of alteration, feldspathoids in normative calculations, and unusual chemical analyses are used to identify significantly altered samples. Only a few samples displayed one or more of these

features, and were rejected as 'significantly altered'.

Many studies evaluate the mobility of major and trace elements (Glikson, 1972; Hajash, 1975; Condie and others, 1977; Humphris and Thompson, 1978; Ludden and Thompson, 1979; MacGeehan and MacLean, 1980; Staudigel and others, 1981). The studies on alteration show various results which are sometimes contradictory. A summary of the effects of alteration includes light rare earth element enrichment of basalts during spilitization; the production of false calc-alkaline trends from original bimodal, iron enrichment trends; large ion lithophile element mobility during sea-floor weathering; and a flattening of bimodal frequency distribution curves of mobile elements. In fact, alteration studies show that most major and trace elements may be mobile under certain specific conditions. These same studies, however, show that some trace elements are relatively immobile during most alteration processes. These elements include Ti, Zr, Nb, Hf, Sc, and REE, and are considered to be the most reliable for the characterization of old and/or altered volcanic rocks (Condie and others, 1977; Menzies and others, 1979). Although several geochemical diagrams involving major elements believed not to have been severely affected by alteration are used in this study, the final interpretations of the GMF are based on the characteristics of the above mentioned relatively immobile elements.

An evaluation of the mobility of elements in terms of



alteration in the Green Mountain Formation is necessary before proceeding with any geochemical interpretations. Most of the major and trace elements display bimodal frequency distribution curves (Figure 11), and bimodal distributions in various geochemical plots. This bimodality is characteristic of the volcanic suite as a whole. Elements which do not show at least a moderate bimodal distribution include  $K_2O$ ,  $Na_2O$ ,  $TiO_2$ ,  $P_2O_5$ , Sr, Ta, and Rb. Although  $TiO_2$ , Ta, and Sr do not have bimodal frequency distributions, there is little or no overlap of the values determined for the mafic and felsic volcanics.  $K_2O$ ,  $Na_2O$ , Sr,  $P_2O_5$ , and Rb appear to have been significantly effected by alteration. Some of the major elements have flat frequency distributions among rocks in which they are abundant (example  $MgO$  in the mafic rocks). These elements include  $MgO$ ,  $Fe_2O_3$ , and  $CaO$ , and are known to be mobile during alteration processes.

The samples from the Green Mountain Formation are also plotted using the alteration correction method of Beswick and Soucie (1978). An example of a plot used in their method is shown in Figure 12. The method involves the plotting ratios of oxide molecular proportions in the form of  $\log X/Z$  versus  $\log Y/Z$ , where X, Y, and Z are molecular proportions of the major element oxides. A series of plots are used, eventually involving all eight major elements. Although actual corrections were not carried out, an examination of the plots indicate that corrections by their

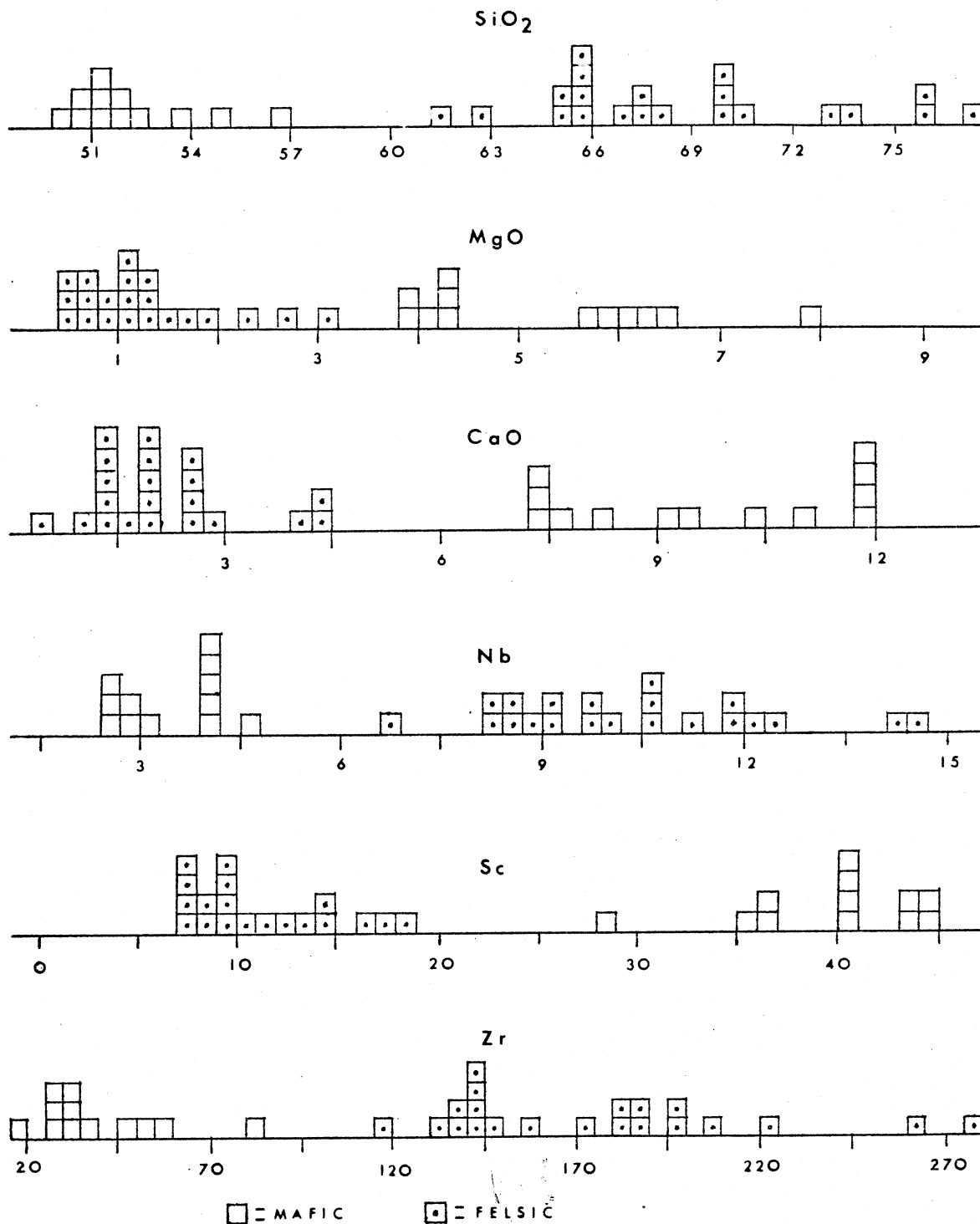


Figure 11. Frequency distribution histograms of major and trace elements of the GMF.

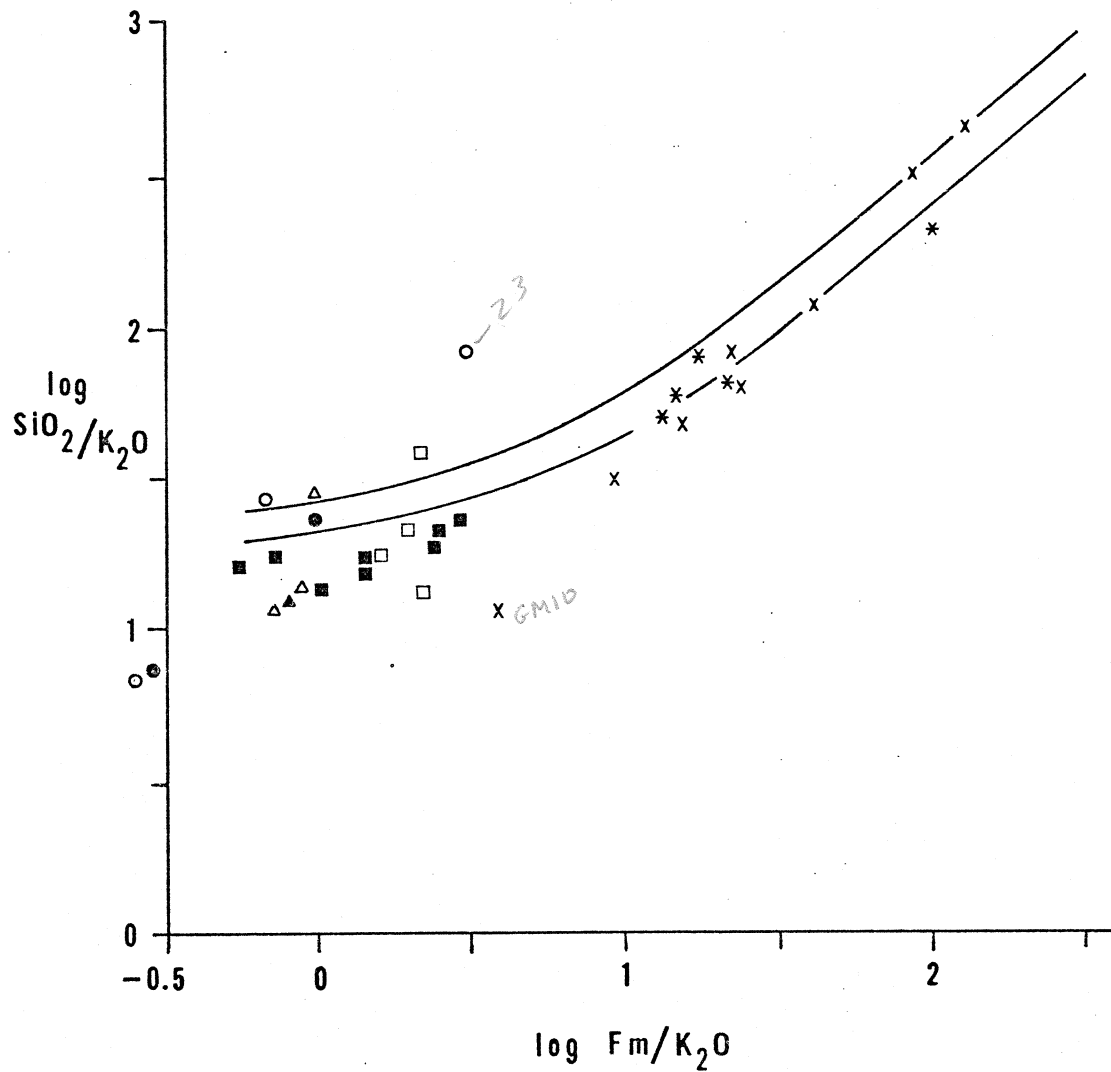


Figure 12. Sample plot of the metasomatism correction method of Beswick and Soucie (1978), using the GMF samples. Symbols on page 56.

method could be made for CaO, MgO, Fe<sub>2</sub>O<sub>3</sub>T, Na<sub>2</sub>O, and K<sub>2</sub>O in some combination. Equally important, is that SiO<sub>2</sub>, MgO, and FeOT require only minor correction in only a few samples, indicating that their concentrations have not been significantly changed. Because MgO and FeOT are treated as one parameter (MgO + FeOT) as in the sample plot of Figure 12, it can not be determined which one needs correction. The Ab-An-Or plot of Figure 13 shows that many of the samples of the GMF are relatively enriched in sodium, and sometimes potassium, in comparison to the field of 'average' volcanics defined by Irvine and Baragar (1971). An examination of the individual analyses of the rocks (Appendix C) shows that both relatively high Na<sub>2</sub>O and/or low CaO values contribute to the overall relative sodium enrichment. Because sodium enrichment affects both mafic and felsic rocks of the GMF, an outside source of this element is likely. Possible sources of sodium may be metasomatism during the intrusion of the granitic rocks surrounding the GMF, or sodium enrichment during submarine eruption and weathering.

To summarize, the characteristics described above indicate that even though some of the elements are effected by alteration, most of the chemical characteristics are approximately representative of the original rocks. The elements which are apparently the most effected by alteration in the Green Mountain Formation are K<sub>2</sub>O, Na<sub>2</sub>O, Rb, and Ba, and to a smaller degree MgO, Fe<sub>2</sub>O<sub>3</sub>T, CaO, Sr,

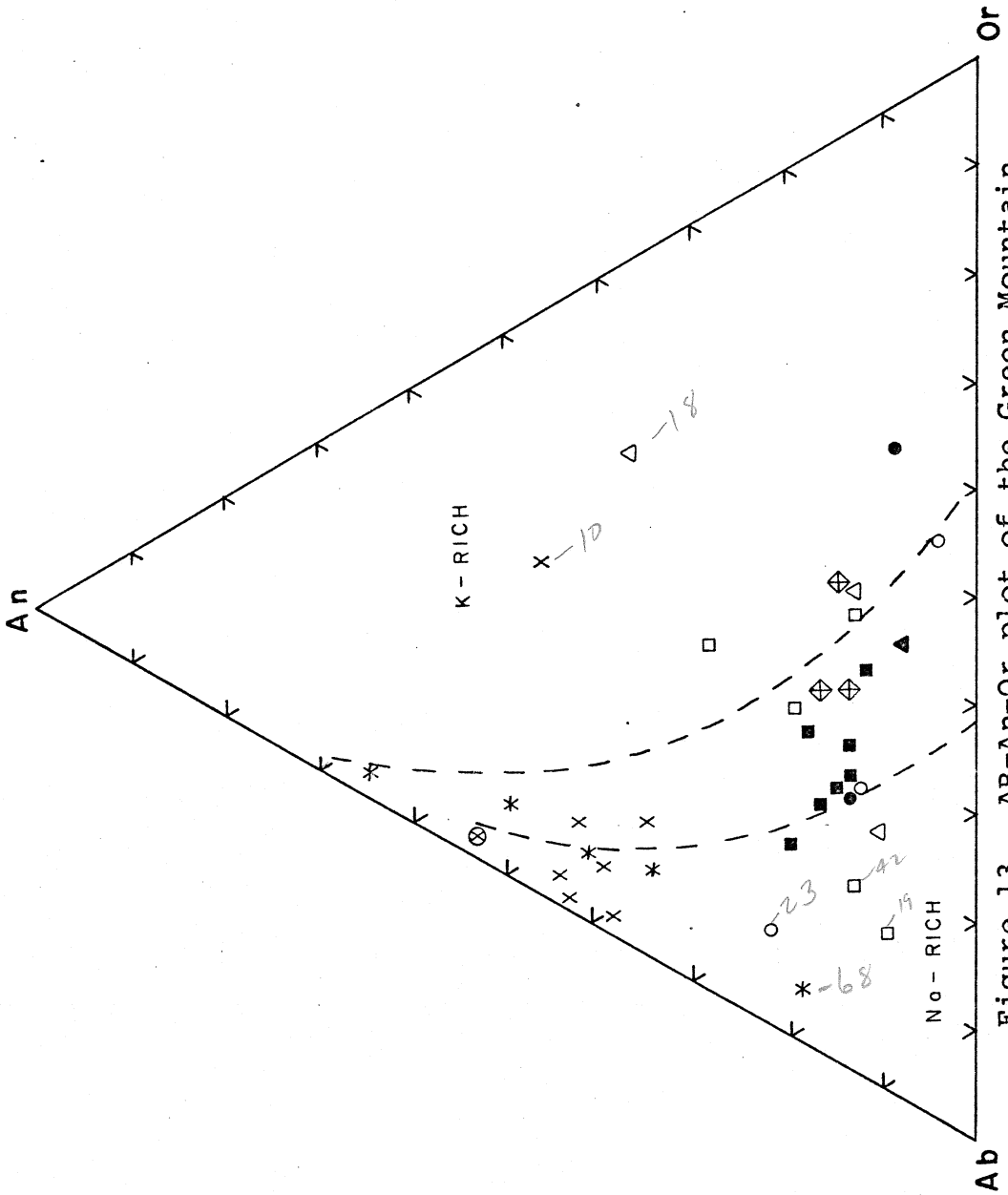


Figure 13. AB-An-Or plot of the Green Mountain Formation (fields after Irvine and Baragar, 1971). Symbols explained on page 56.


MnO, and P<sub>2</sub>O<sub>5</sub>. Although MgO and Fe<sub>2</sub>O<sub>3</sub>T are apparently mobilized, the degree of mobilization appears small enough that they are still useful for geochemical studies.

## CLASSIFICATION

The GMF samples plotted on the geochemical diagrams of Winchester and Floyd (1977) are shown in Figures 14 and 15. These diagrams involve SiO<sub>2</sub>, Nb, Y, Zr, and TiO<sub>2</sub>. The trace elements used in these diagrams are considered to be immobile or nearly immobile during secondary processes. These diagrams show two main characteristics of the GMF: (1) there is a bimodal distribution, and (2) the rocks are subalkaline. Both of these diagrams classify the rocks into the rhyolite, rhyodacite-dacite, and subalkaline basalt groups. A compositional 'gap' occurs in the andesite field.

One classification scheme involving only major elements is also used, namely the Jensen cation plot (Figure 9). This plot also displays a compositional 'gap' in the andesite field, and indicates dominantly calc-alkaline rhyolite, dacite, and basalt. A few samples plot within fields of the tholeiitic series, and overall, most of the samples plot very close to the dividing line between the tholeiitic and calc-alkaline series.

The chemical similarities between the volcanoclastic rocks and the volcanics of the GMF indicate that the analyses of the volcanoclastic rocks are probably representative of the volcanic rocks from which they were derived. Some slight changes in chemical content are apparent, but are not found to be consistent in distinguishing between the volcanoclastics and the volcanics. Possible changes in the felsic volcanoclastics



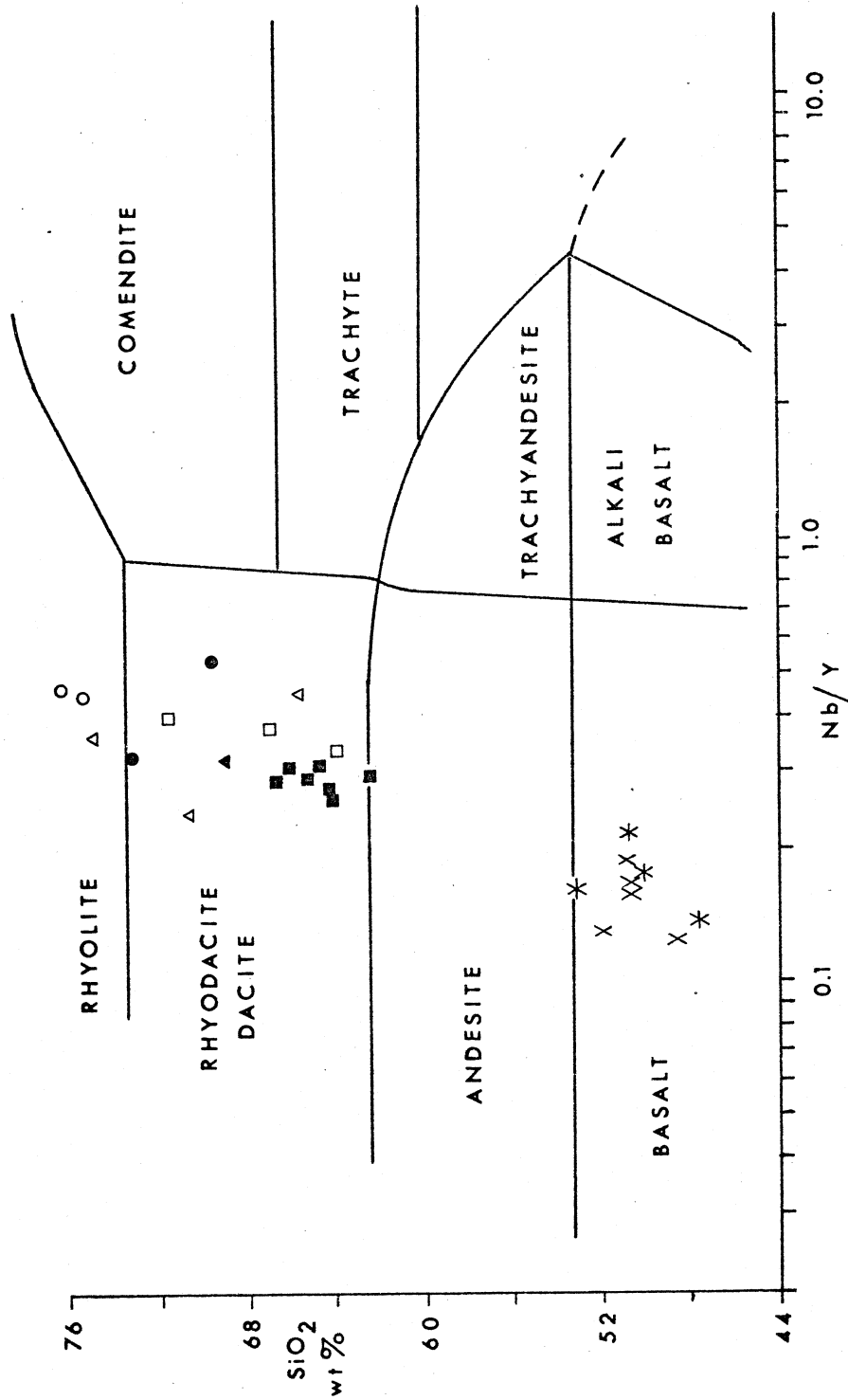


Figure 14. SiO<sub>2</sub> vs Nb/Y classification scheme of Winchester and Floyd (1977), for the GMF. Symbols explained on page 56.



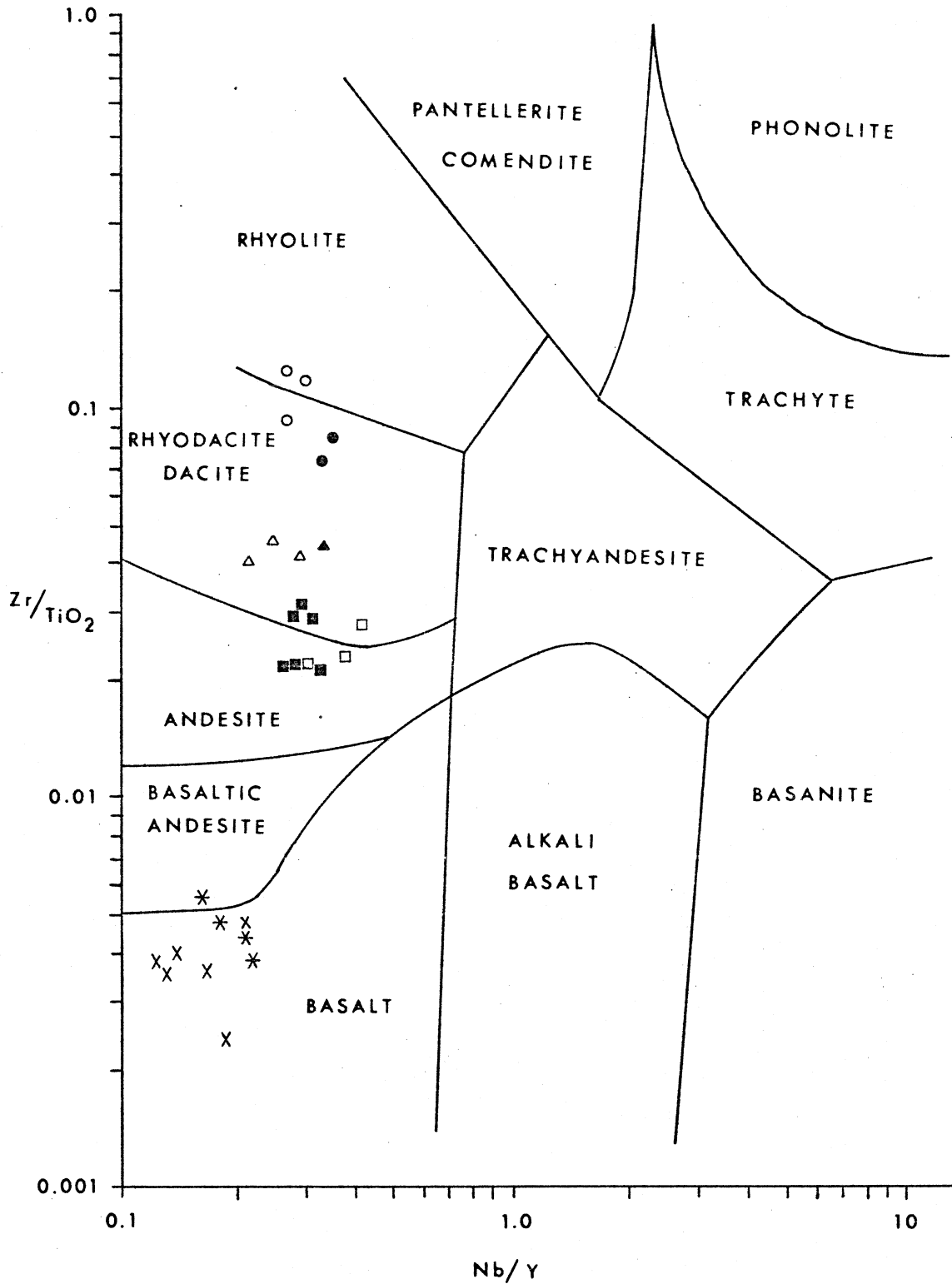


Figure 15. Zr/TiO<sub>2</sub> vs Nb/Y classification scheme of Winchester and Floyd (1977), for the GMF. Symbols explained on page 56.

relative to the felsic volcanics include decreased  $\text{SiO}_2$ ,  $\text{CaO}$ , and  $\text{Na}_2\text{O}$ , and increased  $\text{K}_2\text{O}$ . Trace elements may appear as slightly higher Y, Zr, Hf, REE, and lower Co. The positions of the felsic volcanoclastics on the various geochemical plots fall within the same groups as the volcanics.

The mafic volcanoclastics also are compositionally similar to the mafic volcanics. The upward-fining sequence in the central part of the Fletcher Park section is the best place to make the comparison. The coarser-grained mafic volcanoclastics show only slight differences from the mafic volcanics, and can be summarized as higher  $\text{K}_2\text{O}$ ,  $\text{TiO}_2$ ,  $\text{Fe}_2\text{O}_3\text{T}$ , and Sc, and lower  $\text{CaO}$ , Sr, and Ni. However, changes become significant in the comparison between the coarse and fine-grained mafic volcanoclastics. The fine-grained mafic volcanoclastic samples have significantly higher values of  $\text{SiO}_2$ ,  $\text{TiO}_2$ ,  $\text{K}_2\text{O}$ , and Th, and lower values of  $\text{Al}_2\text{O}_3$ ,  $\text{Fe}_2\text{O}_3\text{T}$ ,  $\text{MgO}$ ,  $\text{CaO}$ , and Cr. Most of these features, except for  $\text{TiO}_2$  and Th, are consistent with mechanical sorting, which has most likely occurred during the deposition of the upward-fining sequence. Unfortunately, the fine-grained volcanoclastic unit is too fine-grained to check any mineralogical changes. The mafic volcanoclastic samples, including the fine-grained units, plot with the mafic volcanics on the various geochemical diagrams, and have similar REE patterns. This similarity suggests the possibility that the mafic units of the upward-fining

sequence may be derived from the same volcanic source. This may also be supported by the gradational contacts observed between the individual units.

The classification results of the GMF are summarized in Table 2, and the average major and trace element concentrations of the major rock types are given in Table 3. The ranges for some major and trace elements exhibit considerable overlap between values of the mafic and felsic end members. The problem becomes even more complex when trying to separate the members of the felsic group. Although actual element concentrations may exceed the proposed limits, the following criterion may be used as a starting point to distinguish the felsic members. A sample is most likely to be a metarhyolite if  $\text{TiO}_2 < 0.35\%$ ,  $\text{Fe}_2\text{O}_3\text{T} < 3.0\%$ ,  $\text{MgO} < 0.8\%$ ,  $\text{MnO} < 0.08\%$ ,  $\text{P}_2\text{O}_5 < 0.07\%$ ,  $\text{Zr} > 180$  ppm,  $\text{Hf} > 4.2$  ppm,  $\text{Nb} > 12$  ppm, and  $\text{La} > 38$  ppm. A sample is most likely to be a metadacite if  $\text{TiO}_2 = 0.45$  to  $0.8\%$ ,  $\text{Fe}_2\text{O}_3\text{T} = 3.5$  to  $7.4\%$ ,  $\text{MgO} = 0.95$  to  $3.0\%$ ,  $\text{MnO} = 0.08$  to  $0.18\%$ ,  $\text{P}_2\text{O}_5 = 0.12$  to  $0.20\%$ ,  $\text{Zr} = 110$  to  $165$  ppm,  $\text{Hf} = 0.2$  to  $2.6$  ppm,  $\text{Nb} = 6.5$  to  $12$  ppm, and  $\text{La} = 30$  to  $35$  ppm. These criterion are only preliminary, and should be used in conjunction with other features such as petrographic observations. A few samples exhibit mixed characteristics in which many major and trace elements have values common to metarhyolites, while others are common to metadacites. This transitional geochemical character may indicate that these samples may be rhyodacitic in composition, or are reworked and/or altered

TABLE 2

SUMMARY OF THE CLASSIFICATION SCHEMES OF THE  
GREEN MOUNTAIN FORMATION

|         | JENSEN<br>CATION<br>PLOT | SiO <sub>2</sub><br>vs<br>Nb/Y | Zr/TiO <sub>2</sub><br>vs<br>Nb/Y | CONCENSUS<br>(including<br>petrography) |
|---------|--------------------------|--------------------------------|-----------------------------------|---|
| GM-002  | R(c)                     | D/Rd                           | R                                 | R                                       |
| GM-009  | B(c)                     | B                              | B                                 | B                                       |
| GM-010A | B(c)                     | B                              | B                                 | B                                       |
| GM-015* | B(t)                     | B                              | B                                 | B                                       |
| GM-016* | A(t)                     | B                              | B                                 | B                                       |
| GM-017  | R(c)                     | D/Rd                           | D/Rd                              | Rd(?)                                   |
| GM-018* | D(c)                     | D/Rd                           | D/Rd                              | Rd(?)                                   |
| GM-019  | D(c)                     | D/Rd                           | D/Rd                              | D                                       |
| GM-023* | R(c)                     | R                              | R                                 | R                                       |
| GM-027  | R(c)                     | R                              | R                                 | R                                       |
| GM-032  | R(c)                     | R                              | D/Rd                              | Rd(?)                                   |
| GM-033  | B(c)                     | B                              | B                                 | B                                       |
| GM-034  | B(c)                     | B                              | B                                 | B                                       |
| GM-036  | D(c)                     | R                              | D/Rd                              | D                                       |
| GM-037  | D(c)                     | D/Rd                           | D/Rd                              | D                                       |
| GM-038  | D(c)                     | D/Rd                           | D/Rd                              | D                                       |
| GM-042  | D(c)                     | D/Rd                           | D/Rd                              | D                                       |
| GM-044  | A(c)                     | A                              | A                                 | D                                       |
| GM-046  | B(c)                     | B                              | B                                 | B                                       |
| GM-047  | B(c)                     | B                              | B                                 | B                                       |
| GM-050  | R(t)                     | D/Rd                           | D/Rd                              | D                                       |
| GM-051* | A(t)                     | B                              | B                                 | B                                       |
| GM-053  | B(c)                     | B                              | B                                 | B                                       |
| GM-056  | B(t)                     | B                              | B                                 | B                                       |
| GM-057  | B(c)                     | B                              | B                                 | B                                       |
| GM-058  | D(c)                     | D/Rd                           | A                                 | D                                       |
| GM-063  | R(t)                     | D/Rd                           | D/Rd                              | D                                       |
| GM-065* | R(c)                     | D/Rd                           | R                                 | R                                       |
| GM-067  | R(c)                     | R                              | D/Rd                              | R                                       |
| GM-068  | B(c)                     | A                              | BA                                | B                                       |
| GM-072  | D(c)                     | D/Rd                           | D/Rd                              | D                                       |
| GM-073  | D(c)                     | D/Rd                           | D/Rd                              | D                                       |
| GM-075  | D(c)                     | D/Rd                           | D/Rd                              | Rd(?)                                   |
| GM-076  | D(c)                     | D/Rd                           | D/Rd                              | D                                       |

A= andesite

B= basalt

BA= basaltic andesite

D= dacite

\* = volcanoclastic

R= rhyolite

Rd= rhyodacite

(c)= calc-alkaline

(t)= tholeiitic

TABLE 3

AVERAGE COMPOSITION OF THE MAJOR ROCK TYPES OF THE  
GREEN MOUNTAIN FORMATION METAVOLCANICS

|                                  | RHYOLITE | RHYODACITE(?) | DACITE | THOLEIITE |
|----------------------------------|----------|---------------|--------|-----------|
| SiO <sub>2</sub>                 | 73.38    | 70.92         | 66.12  | 51.69     |
| TiO <sub>2</sub>                 | 0.25     | 0.42          | 0.62   | 0.85      |
| Al <sub>2</sub> O <sub>3</sub>   | 14.30    | 15.03         | 15.88  | 15.81     |
| Fe <sub>2</sub> O <sub>3</sub> T | 2.24     | 3.45          | 5.33   | 11.14     |
| MgO                              | 0.54     | 0.94          | 1.73   | 5.73      |
| CaO                              | 1.44     | 2.07          | 2.62   | 9.82      |
| Na <sub>2</sub> O                | 3.72     | 3.15          | 4.63   | 3.83      |
| K <sub>2</sub> O                 | 3.96     | 3.94          | 2.88   | 0.48      |
| MnO                              | 0.06     | 0.07          | 0.14   | 0.28      |
| P <sub>2</sub> O <sub>5</sub>    | 0.03     | 0.08          | 0.20   | 0.22      |
| Rb                               | 75       | 75            | 73     | 15        |
| Sr                               | 169      | 249           | 341    | 456       |
| Cs                               | 0.9      | 0.7           | 1.5    | --        |
| Ba                               | 1156     | 1576          | 1186   | 373       |
| Y                                | 40       | 39            | 33     | 19        |
| Zr                               | 220      | 180           | 148    | 40        |
| Hf                               | 5.4      | 4.4           | 3.3    | <2.0      |
| Nb                               | 13       | 10            | 9.2    | 3.4       |
| Ta                               | 0.8      | 0.6           | 0.7    | -- 0.2    |
| Sc                               | 8.5      | 10            | 14     | 40        |
| Cr                               | --       | --            | --     | 88        |
| Ni                               | 3.9      | 2.9           | 5.7    | 21        |
| Co                               | 1.8      | 1.0           | 5.9    | 31        |
| U                                | 3.1      | 2.9           | 2.6    | --        |
| Th                               | 8.5      | 6.2           | 6.5    | 1.5       |
| La                               | 49       | 36            | 34     | 13        |
| Yb                               | 3.6      | 3.0           | 2.5    | 1.6       |

Total Iron as Fe<sub>2</sub>O<sub>3</sub>  
Oxides = weight percent  
Trace Elements = ppm  
-- = not detected

265 K/Rb

17 Nb/Ta 16

35 Y/Tb 4:

(20) Zr/Hf 3  
Hf  
main

rocks.

After examining the geochemical analyses, it is apparent that three (possibly four) distinct rock types are present in the Green Mountain Formation. Therefore, the Green Mountain Formation is comprised of metarhyolite, metadacite, metarhyodacite(?), and metabasalt. Most major and trace elements do not consistently distinguish all of the rock types, but a closer examination of some specific trace elements offers some results. With the number of samples under consideration, the Y/Sc, Hf/Sc, Zr/P<sub>2</sub>O<sub>5</sub> x 10,000, Zr/TiO<sub>2</sub> x 10,000, Nb/Y, and REE characteristics appear to be useful in discriminating the rock types. The ranges and averages of the trace element ratios are given in Table 4, and distinguish between the rhyolite, dacite, and basalt groups.

TABLE 4

TRACE ELEMENT RATIOS TO DISTINGUISH  
THE MAJOR ROCK TYPES OF  
THE GREEN MOUNTAIN FORMATION

|   | RHYOLITE        | DACITE          | THOLEIITE         |
|---|-----------------|-----------------|-------------------|
| Y/Sc  | 4.00 to<br>6.01 | 1.89 to<br>3.07 | 0.33 to<br>0.76   |
| Hf/Sc   | 0.54 to<br>0.76 | 0.14 to<br>0.38 | <0.045            |
| Nb/Y  | 0.26 to<br>0.34 | 0.19 to<br>0.42 | 0.12 to<br>0.22   |
| Zr/P <sub>2</sub> O <sub>5</sub> *                          | 0.62 to<br>2.09 | 0.05 to<br>0.16 | 0.012 to<br>0.025 |
| Zr/TiO <sub>2</sub> *                                       | 0.06 to<br>0.12 | 0.02 to<br>0.03 | 0.002 to<br>0.010 |
| * TiO <sub>2</sub> and P <sub>2</sub> O <sub>5</sub> in ppm | >0.04           | <0.04           |                   |

## RARE EARTH ELEMENTS

The chondrite normalized rare earth patterns of the rocks of the GMF are grouped according to the results of the geochemical classifications. For simplicity, the grouped REE patterns were used to delineate the REE envelopes shown in Figures 16 and 17.

The rhyolitic metavolcanics and volcanoclastics define an REE envelope which is light REE enriched between 120 and 230 times chondrites (La), and has slightly inclined to flat heavy REE between 14.5 and 28 times chondrites (Lu). Europium anomalies range from moderately to strongly negative. The upper limit of the envelope is defined by a volcanoclastic unit from the Fletcher Park area, and indicates that a higher total REE abundance may be characteristic of volcanoclastic sediments in comparison to the parent volcanics.

Chondrite normalized REE patterns of the metadacites also define a consistent envelope. Characteristics of the envelope are light REE enrichment (94 to 110 times chondrites), and inclined heavy REE with values between 8 and 16 times chondrites. Eu anomalies are variable and range from slightly positive to moderately negative. Two of the dacites are exceptions, and have patterns which fall within the basalt envelope described below. Metarhyodacite(?) patterns overlap the rhyolite and dacite envelopes, and are not readily distinguishable. LREE of the metarhyodacites conform with the upper limit of the



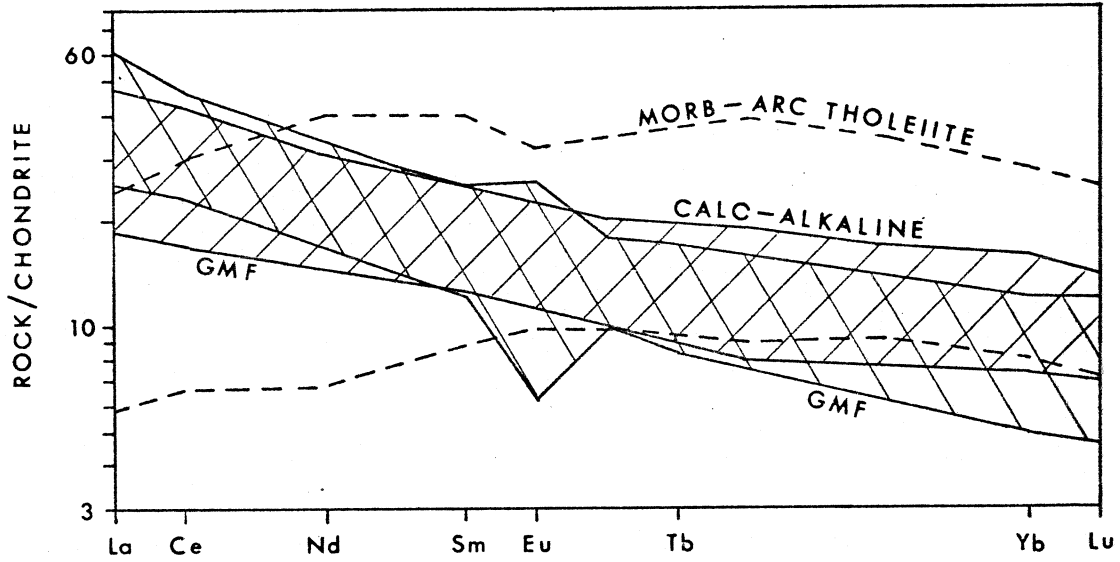


Figure 16. REE envelopes of the mafic rocks of the GMF (MORB-arc tholeiite and calc-alkaline fields after Condie, 1981).

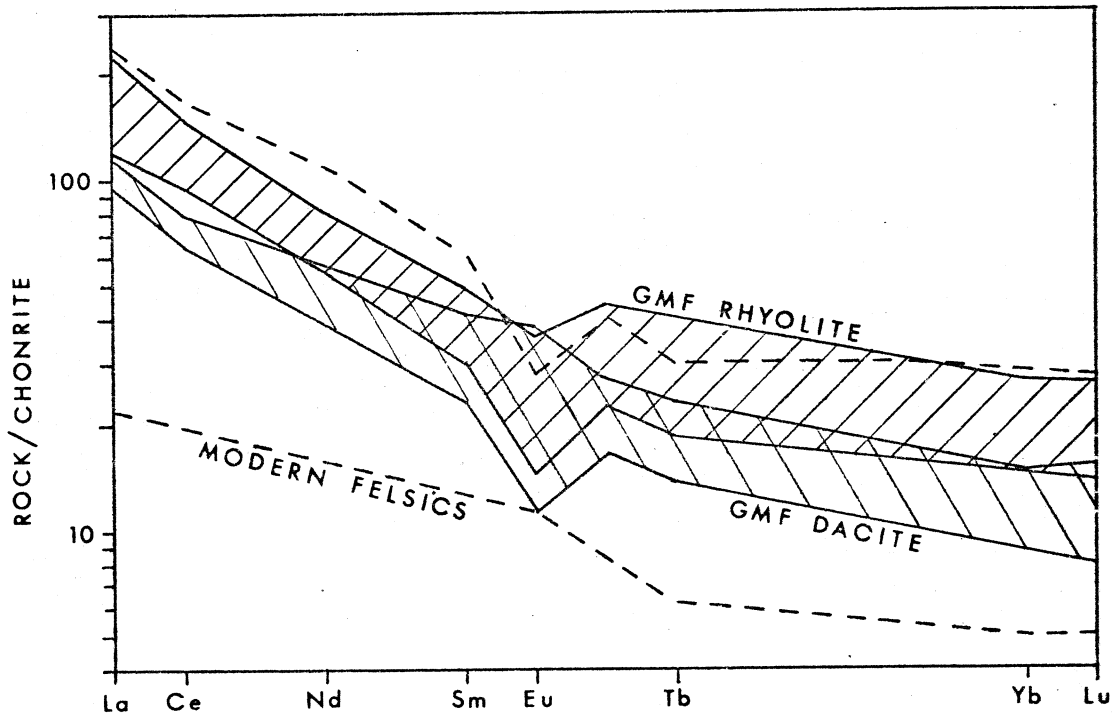


Figure 17. REE envelopes of the felsic rocks of the GMF (calc-alkaline envelope after Condie, 1981).

metadacite envelope, and the HREE overlap both the metarhyolite and metadactite envelopes.

The metabasalt patterns are light REE enriched between 25 and 60 times chondrites (La), and have inclined heavy REE with Lu values between 4.5 and 12 times chondrites. Europium anomalies are variable from moderately positive to moderately negative. The variability of the Eu anomaly is not related to any of the textural varieties of the tholeiitic rocks.

## TECTONIC INDICATORS

This section addresses the interpretation of tectonic environment based on geochemical characteristics. The geochemical comparisons of the GMF are based on observations within Phanerozoic tectonic regimes. The interpretations can only be considered preliminary since the amount of data represented in this study may not be totally representative of the Green Mountain Formation exposed in the Sierra Madre Range.

The supracrustal succession represented by the Green Mountain Formation is compositionally bimodal in character, with metabasalt and metadacite to metarhyolite end members. Rocks of andesitic composition are not observed in the sections studied. The general progression from mafic to dacitic to rhyolitic volcanics may be expected in the evolution of a volcanic sequence. A lack of random interbedding of the various compositional rocks may indicate that a cogenetic sequence is represented, but it is impossible to prove the cogenetic relationship by tracing the rock units to a common volcanic source. A bimodal distribution is usually indicative of an extensional environment (Martin and Piwinsky, 1972). Compositional bimodality has also been observed in some modern island arc volcanic series, namely the island arc tholeiite series, with andesite occurring as a subordinate rock type (Donnelly, 1966; Gill, 1970; Brothers and Searles, 1970; and Donnelly and Rogers, 1980).

Geochemical characteristics which may be displayed on

discrimination diagrams sensitive to modern tectonic environments are used in this study. Especially useful are trace elements such as Ti, Zr, Nb, Hf, Sc, and REE, which are considered to be relatively immobile during secondary processes (See discussion in alteration section). The information from these trace elements can be compared to information from less reliable elements, such as major elements, to see if they indicate similar results.

Because extensive study in past literature has concentrated on the mafic members of volcanic suites, the mafic volcanics of the GMF are examined first for interpretation of tectonic environment. The Zr-Ti-Y plot of Pearce and Cann (1973) indicates that the mafic rocks of the Green Mountain Formation are low-K tholeiites (Figure 18). This diagram is preferred for distinguishing basaltic rocks because it uses relatively immobile trace elements. This is the first plot which indicates the tholeiitic nature of the mafic rocks. The tholeiitic character is also supported by the SiO<sub>2</sub> versus Cr plot of Miyashiro and Shido (1975) shown in Figure 19. Because low-K tholeiites can be found in both continental and oceanic environments, it is necessary to find further distinguishing characteristics. The mafic samples plot dominantly in the island arc tholeiite fields of the TiO<sub>2</sub> vs 100(Mg/Mg + Fe<sup>2+</sup>) and Ti vs Zr plots (Figures 10 and 20). These diagrams appear to eliminate the continental, spreading ridge, and oceanic island environments.

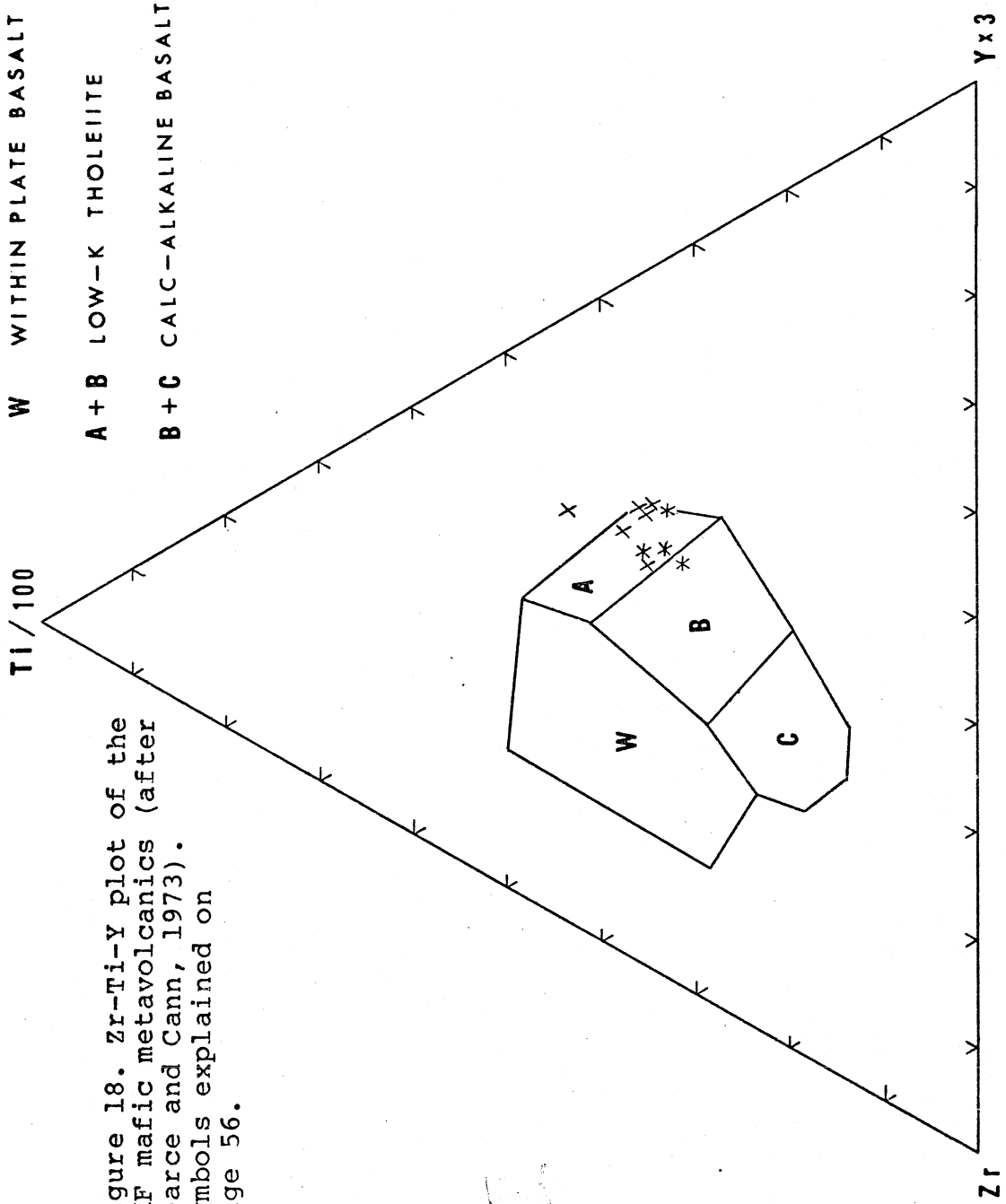


Figure 18. Zr-Ti-Y plot of the GMF mafic metavolcanics (after Pearce and Cann, 1973). Symbols explained on page 56.

Figure 19. SiO<sub>2</sub> vs Cr plot of the GMF mafic metavolcanics (after Miyashiro and Shido, 1975). Symbols explained on page 56.

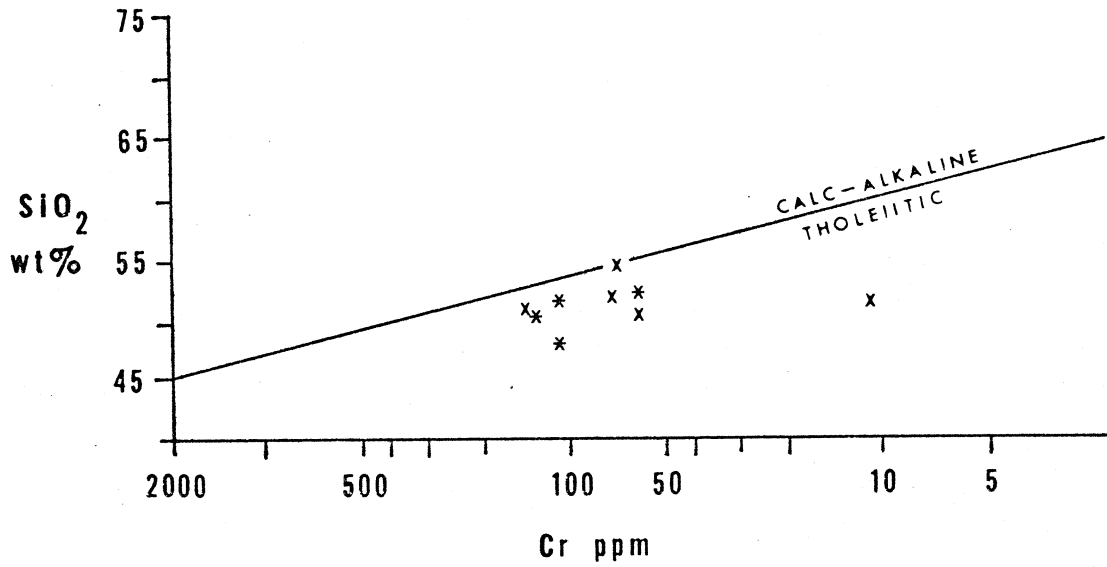
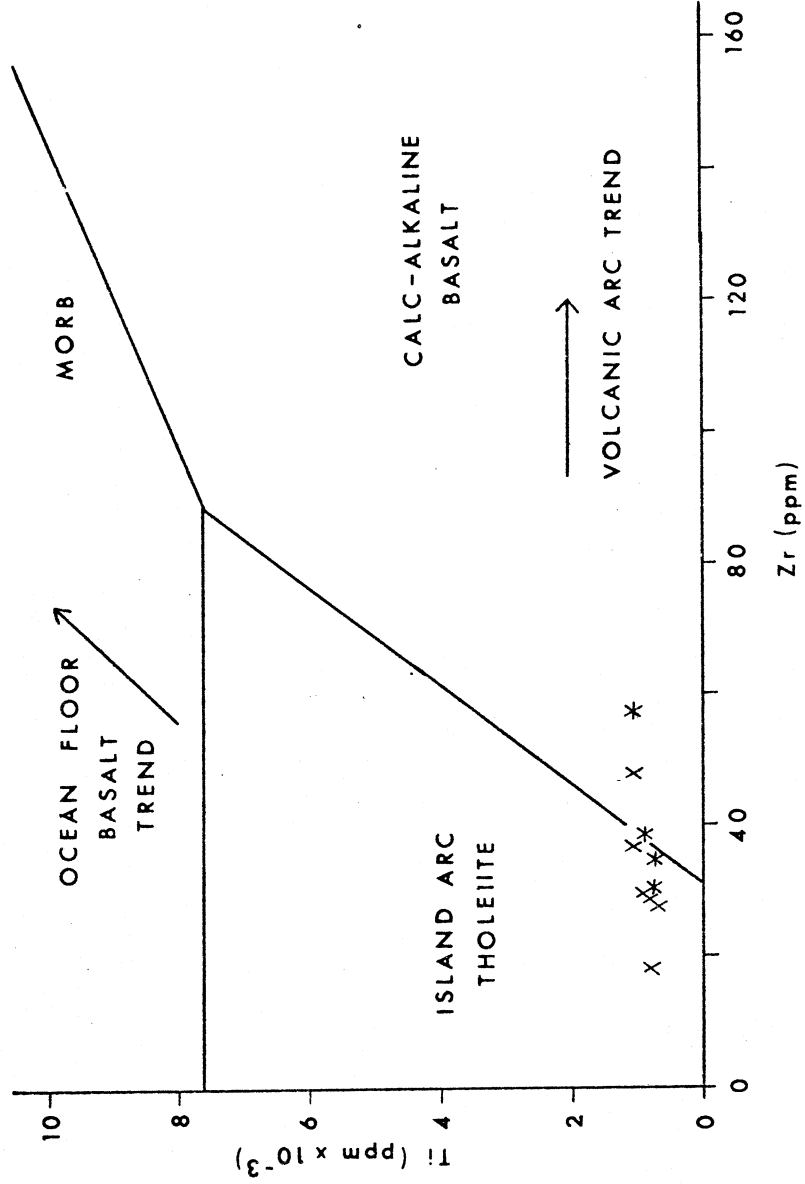


Figure 20. Ti vs Zr plot of the mafic rocks of the GMF (after Garcia, 1978). Symbols explained on page 56.



The geochemical characteristics of the metabasalts of the Green Mountain Formation are compared to mafic volcanics of other tectonic environments (Table 5). Major and trace elements of the metatholeiites are most consistent with the analyses of the island arc tholeiites of Jakes and Gill (1970), and the primitive arc tholeiites of Donnelly and Rogers (1980). Differences observed in the GMF metatholeiites are lower CaO, MgO, and Zr, and higher Na<sub>2</sub>O, Rb, Sr, Ba, Co, Th, and LREE. These differences are consistent with changes which may occur during sea floor alteration and/or epidotization (Hart, 1969; Christensen and others, 1973; Hart and others, 1974; Condie, 1977). The GMF metatholeiites differ from calc-alkaline, high-Al basalt by significantly lower values of Al<sub>2</sub>O<sub>3</sub>, MgO, Y, Zr, and Nb, and higher Fe<sub>2</sub>O<sub>3T</sub>, Sc, and Cr. The GMF metatholeiites differ from rise tholeiite by lower TiO<sub>2</sub>, Y, Zr, Sc, Cr, and Ni. Characteristics which distinguished the GMF metatholeiites from continental tholeiites are lower TiO<sub>2</sub>, Fe<sub>2</sub>O<sub>3T</sub>, Y, Zr, and Ni, and higher Al<sub>2</sub>O<sub>3</sub>.

The samples of the GMF are plotted on the MgO versus FeOT diagram (Figure 21). Points representing the felsic samples plot dominantly within the tholeiitic trend and intermediate between the calc-alkaline and tholeiitic trends. This is the first diagram which suggests possible tholeiitic affinities for the GMF felsic rocks. This plot is in disagreement with the Jensen cation plot (Figure 9) which indicates that the felsic rocks have dominantly



TABLE 5

COMPARISON OF THE THOLEIITE OF THE GREEN MOUNTAIN  
FORMATION TO VARIOUS BASALT TYPES

|                                  | AVERAGE<br>GMF | ISLAND<br>ARC<br>THOLEIITE(1) | PRIMITIVE<br>ARC<br>THOLEIITE(2) | CALC-ALKALINE<br>HIGH-AL<br>BASALT(3) |
|----------------------------------|----------------|-------------------------------|----------------------------------|---------------------------------------|
| SiO <sub>2</sub>                 | 51.97          | 51.57                         | 50.70                            | 50.39                                 |
| TiO <sub>2</sub>                 | 0.87           | 0.80                          | 0.70                             | 1.05                                  |
| Al <sub>2</sub> O <sub>3</sub>   | 15.75          | 15.91                         | 15.60                            | 16.29                                 |
| Fe <sub>2</sub> O <sub>3</sub> T | 11.08          | 10.56                         | 9.40                             | 9.30                                  |
| MgO                              | 5.62           | 6.73                          | 7.50                             | 8.96                                  |
| CaO                              | 9.61           | 11.74                         | 7.70                             | 9.50                                  |
| Na <sub>2</sub> O                | 3.90           | 2.41                          | 3.50                             | 2.98                                  |
| K <sub>2</sub> O                 | 0.54           | 0.44                          | 0.81                             | 1.07                                  |
| MnO                              | 0.28           | 0.17                          | --                               | 0.17                                  |
| P <sub>2</sub> O <sub>5</sub>    | 0.22           | 0.11                          | --                               | 0.21                                  |
| Rb                               | 15             | 5                             | 10                               | 10                                    |
| Sr                               | 456            | 200                           | 176                              | 330                                   |
| Cs                               | --             | 0.05                          | --                               | --                                    |
| Ba                               | 373            | 75                            | 113                              | 115                                   |
| Y                                | 19             | 20                            | 14                               | 25                                    |
| Zr                               | 40             | 60                            | 34                               | 100                                   |
| Hf                               | <2.0           | 1                             | --                               | 2.6                                   |
| Nb                               | 3.4            | --                            | --                               | 5.6                                   |
| Ta                               | <0.5           | --                            | --                               | --                                    |
| Sc                               | 40             | --                            | 38                               | 29                                    |
| Cr                               | 71             | 50                            | 68                               | 40                                    |
| Ni                               | 21             | 25                            | 37                               | 25                                    |
| Co                               | 31             | 20                            | 34                               | --                                    |
| U                                | --             | 0.15                          | 0.15                             | 0.2                                   |
| Th                               | 1.5            | 0.5                           | 0.21                             | 1.1                                   |
| La                               | 13             | 1.1                           | --                               | 9.6                                   |
| Yb                               | 1.6            | 1.4                           | --                               | 2.7                                   |

Symbols described on next page

*P = 0.444 P<sub>205</sub>*

|        | RISE<br>THOLEIITE(4) | OCEAN<br>ISLAND(4) | CONTINENTAL RIFT<br>THOLEIITE(4) |
|--------|----------------------|--------------------|----------------------------------|
| SiO2   | 49.80                | 49.40              | 50.30                            |
| TiO2   | 1.50                 | 2.50               | 2.20                             |
| Al2O3  | 16.00                | 13.90              | 14.30                            |
| Fe2O3T | 10.30                | 12.40              | 13.80                            |
| MgO    | 7.50                 | 8.40               | 5.90                             |
| CaO    | 11.20                | 10.30              | 9.70                             |
| Na2O   | 2.80                 | 2.10               | 2.50                             |
| K2O    | 0.14                 | 0.38               | 0.80                             |
| MnO    | 0.17                 | 0.17               | --                               |
| P2O5   | 0.16                 | 0.16               | --                               |
| Rb     | 1                    | 5                  | 30                               |
| Sr     | 135                  | 350                | 350                              |
| Cs     | 0.02                 | 0.10               | 1                                |
| Ba     | 11                   | 100                | 200                              |
| Y      | 30?                  | 43                 | 30                               |
| Zr     | 100                  | 125                | 200                              |
| Hf     | --                   | --                 | --                               |
| Nb     | <30                  | --                 | --                               |
| Ta     | --                   | --                 | --                               |
| Sc     | 61                   | 61                 | --                               |
| Cr     | 300                  | 250                | 100                              |
| Ni     | 100                  | 150                | 100                              |
| Co     | 32                   | 30                 | 40                               |
| U      | --                   | 0.18               | --                               |
| Th     | 0.2                  | 0.67               | --                               |
| La     | 3.9                  | 7.2                | 33                               |
| Yb     | 4.0                  | 1.7                | 4.4                              |

-----  
 Total iron as Fe2O3 Oxides in weight percent

Trace elements in ppm -- = no data

(1) Jakes and White (1972) (4) Condie (1976)

(2) Donnelly and Rogers (1980)

(3) Jakes and White (1972)

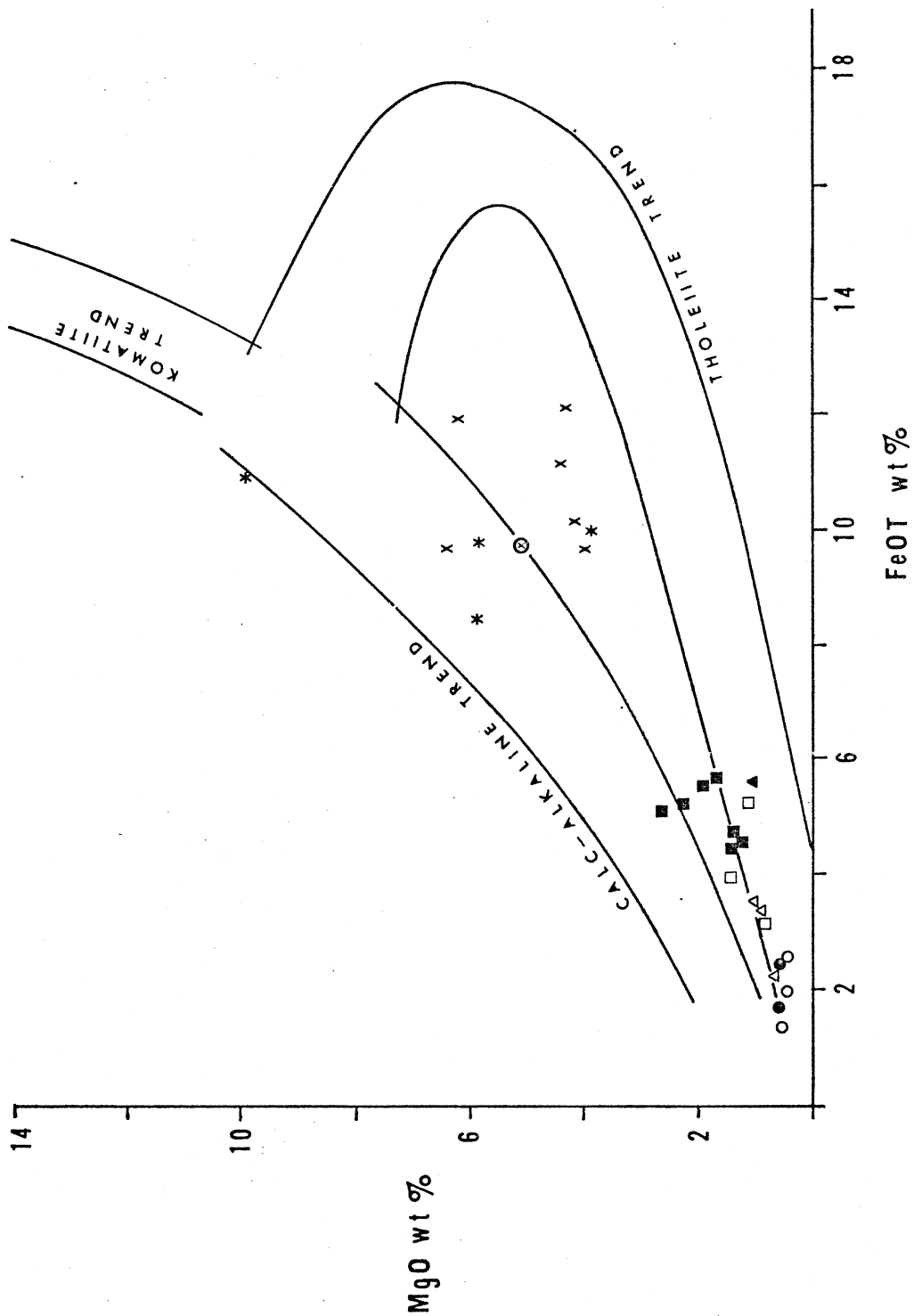


Figure 21. MgO vs FeOT plot of the GMF rocks (fields after Jolly, 1975). Symbols explained on page 56.

calc-alkaline affinities, but plot very close to the boundary between the two series. The plot of MgO versus Fe<sub>2</sub>O<sub>3</sub> + FeO (Figure 22) seems repetitive, but this diagram from Jakes and Gill (1970) also shows two trends of the island arc tholeiite (IAT) series. The GMF samples appear to more closely follow the trend of the IAT series. Two groups of mafic rocks are noticeable on the same diagram. Some of the samples of the higher MgO group are overlain or intruded by samples of the lower MgO group. Although not apparent in the diagram, the individual samples of the low Mg group which have the above relationship are also higher in iron. This possible age relationship is consistent with iron enrichment with time in the mafic members, a characteristic of tholeiitic trends.

The only information on the felsic rocks so far involves major elements. Because major element diagrams are not consistent in their interpretation, the trace elements must be examined. The Th-Hf-Ta diagram of Wood (1980) shows that the felsic rocks plot within the calc-alkaline portion of the convergent plate boundary field (Figure 23). Although Th is known to be mobile during some alteration processes, the close grouping of the points indicates that Th has probably not been significantly affected.

Table 6 shows the average metadacite of the Green Mountain Formation compared to island arc tholeiite series dacite from St. Kitts and the pigeonitic series of Japan (IAT series), and calc-alkaline dacites from island arc and

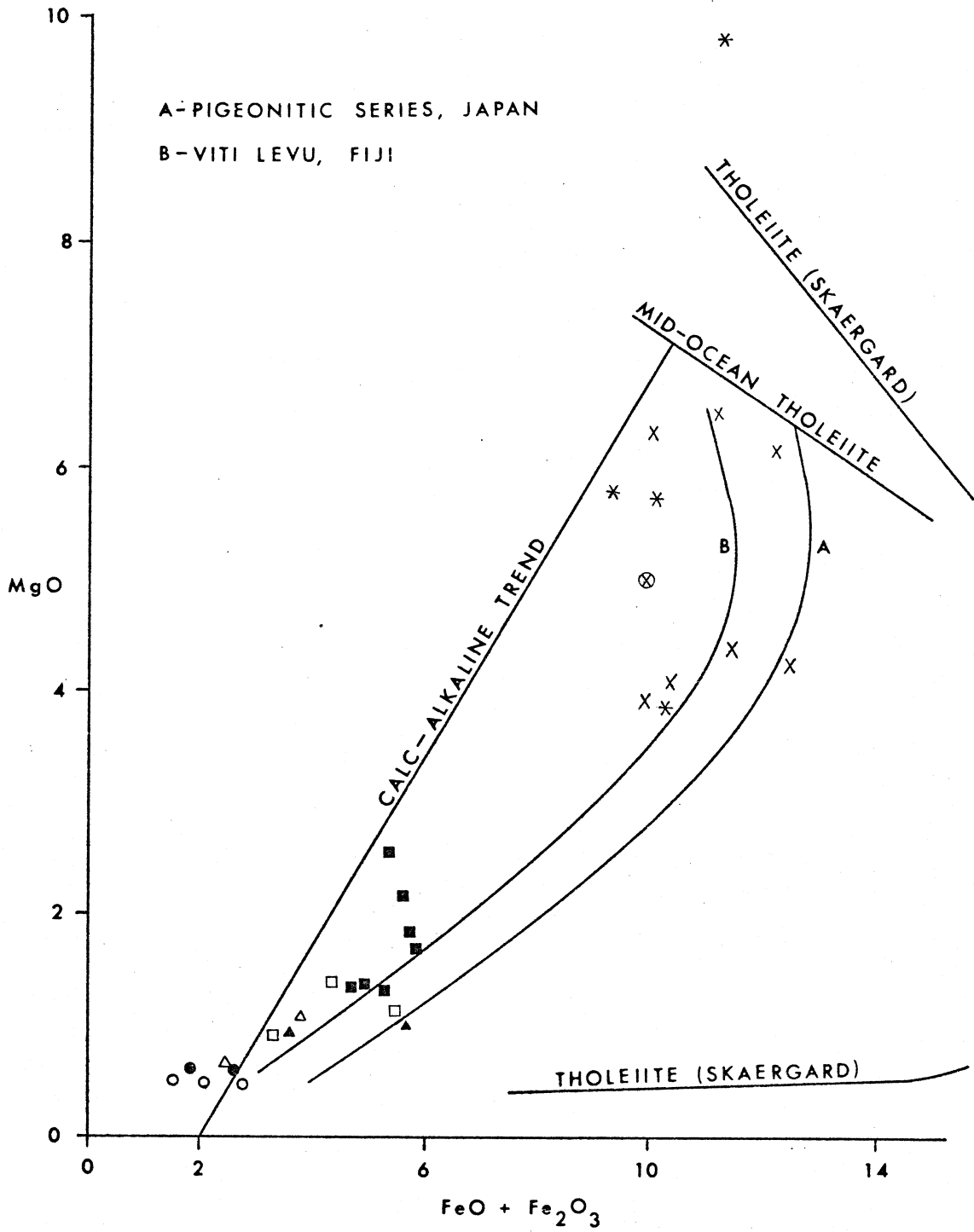


Figure 22. MgO vs FeO + Fe<sub>2</sub>O<sub>3</sub> plot of the GMF rocks (after Jakes and Gill, 1970). Symbols explained on page 56.

*Output*

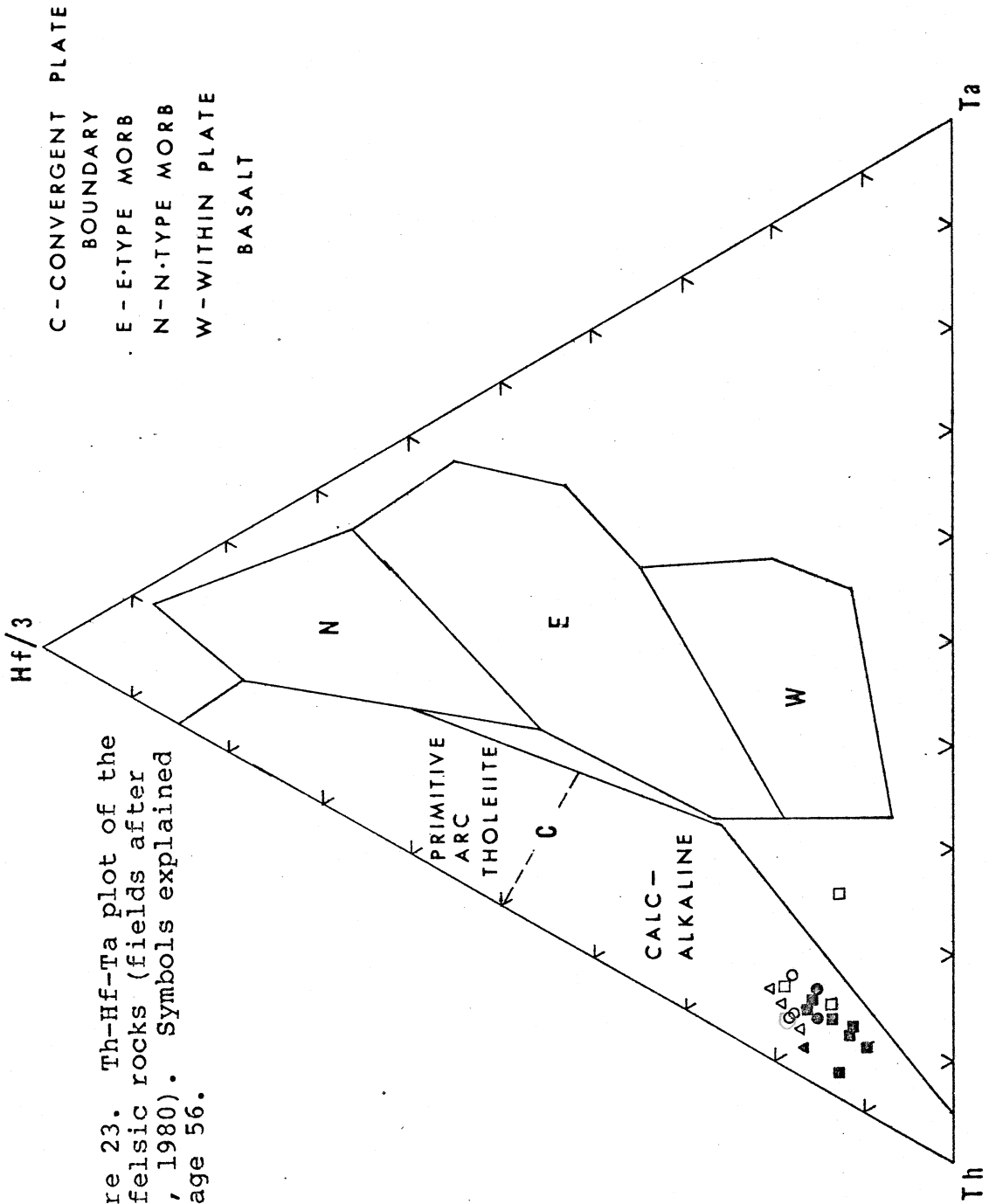


Figure 23. Th-Hf-Ta plot of the GMF felsic rocks (fields after Wood, 1980). Symbols explained on page 56.

TABLE 6

COMPARISON OF THE GMF METADACITES TO DACITES OF  
OTHER TECTONIC ENVIRONMENTS

|                                  | GMF<br>META-<br>DACITE | THOLEIITIC<br>SERIES<br>DACITE | PIGEONITIC<br>SERIES<br>DACITE | CALC-ALK<br>IS. ARC<br>DACITE | CALC-ALK<br>CONTINENTAL<br>MARGIN<br>DACITE |
|----------------------------------|------------------------|--------------------------------|--------------------------------|-------------------------------|---|
| SiO <sub>2</sub>                 | 66.12                  | 67.25                          | 67.45                          | 66.80                         | 67.69                                       |
| TiO <sub>2</sub>                 | 0.62                   | 0.45                           | 0.67                           | 0.23                          | 0.54  |
| Al <sub>2</sub> O <sub>3</sub>   | 15.88                  | 16.04                          | 15.12                          | 18.24                         | 16.21                                       |
| Fe <sub>2</sub> O <sub>3</sub> T | 5.33                   | 5.13                           | 5.42                           | 2.38                          | 3.64  |
| MgO                              | 1.73                   | 1.06                           | 1.16                           | 1.50                          | 1.11  |
| CaO                              | 2.62                   | 5.25                           | 4.47                           | 3.17                          | 3.17  |
| Na <sub>2</sub> O                | 4.63                   | 3.79                           | 4.71                           | 4.97                          | 3.79  |
| K <sub>2</sub> O                 | 2.88                   | 0.80                           | 0.96                           | 1.92                          | 3.75  |
| MnO                              | 0.14                   | 0.14                           | 0.15                           | 0.06                          | 0.07  |
| P <sub>2</sub> O <sub>5</sub>    | 0.20                   | 0.09                           | 0.18                           | 0.09                          | 0.17  |
| Rb                               | 73                     | 13                             | --                             | 45                            | 125   |
| Sr                               | 341                    | 278                            | 320                            | 460                           | 893   |
| Cs                               | 1.5                    | --                             | --                             | --                            | --  |
| Ba                               | 1186                   | 194                            | 350                            | 520                           | 1614  |
| Y                                | 33                     | 29                             | 30                             | 20                            | 18  |
| Zr                               | 148                    | 129                            | 125                            | 100                           | 245   |
| Hf                               | 3.3                    | --                             | --                             | --                            | --  |
| Nb                               | 9.2                    | 2.0                            | --                             | 3.8                           | 24  |
| Ta                               | 0.7                    | --                             | --                             | --                            | --  |
| Sc                               | 14                     | --                             | 14                             | --                            | --  |
| Cr                               | --                     | 11                             | --                             | 13                            | 10  |
| Ni                               | 5.7                    | 4.0                            | --                             | 5.0                           | 22  |
| Co                               | 5.9                    | --                             | 8.0                            | --                            | 21  |
| U                                | 2.6                    | --                             | --                             | 0.6                           | --  |
| Th                               | 6.5                    | --                             | --                             | 1.7                           | --  |
| La                               | 34                     | --                             | 9.9                            | 14                            | 125   |
| Yb                               | 2.5                    | --                             | 5.0                            | 1.4                           | 2.1   |

(1) Brown and others, 1977

(2) Nockolds and Allen, 1956

(La and Yb from Donnelly  
and Rogers, 1980)

(3) Jakes and White, 1972

(4) Ewart, 1979

Total iron as Fe<sub>2</sub>O<sub>3</sub>T

Oxides in weight percent

Trace elements in ppm

-- = no data

TABLE 7

COMPARISON OF THE GMF METARHYOLITES TO RHYOLITES OF  
VARIOUS TECTONIC ENVIRONMENTS

|                                  | GMF<br>META-<br>RHYOLITE | PIGEONITIC<br>SERIES<br>RHYOLITE(1) | VITI LEVU<br>THOLEIITIC<br>SERIES<br>RHYOLITE(2) |
|----------------------------------|--------------------------|-------------------------------------|--|
| SiO <sub>2</sub>                 | 73.38                    | 74.90                               | 71.84  |
| TiO <sub>2</sub>                 | 0.25                     | 0.33                                | 0.50   |
| Al <sub>2</sub> O <sub>3</sub>   | 14.30                    | 12.10                               | 12.87  |
| Fe <sub>2</sub> O <sub>3</sub> T | 2.24                     | 3.51                                | 3.84   |
| MgO                              | 0.54                     | 0.50                                | 0.76   |
| CaO                              | 1.44                     | 2.23                                | 3.60   |
| Na <sub>2</sub> O                | 3.72                     | 4.45                                | 4.68   |
| K <sub>2</sub> O                 | 3.96                     | 1.33                                | 0.89   |
| MnO                              | 0.06                     | 0.11                                | 0.12   |
| P <sub>2</sub> O <sub>5</sub>    | 0.03                     | 0.32                                | 0.12   |
| Rb                               | 75                       | --                                  | 6.8  |
| Sr                               | 169                      | 175                                 | 116  |
| Cs                               | 0.9                      | --                                  | 0.3  |
| Ba                               | 1156                     | 475                                 | 218  |
| Y                                | 40                       | 35                                  | 43   |
| Zr                               | 220                      | 125                                 | 71   |
| Hf                               | 5.4                      | --                                  | 4.5  |
| Nb                               | 12                       | --                                  | --   |
| Ta                               | 0.8                      | --                                  | --   |
| Sc                               | 8.5                      | 10                                  | 16   |
| Cr                               | --                       | --                                  | --   |
| Ni                               | 3.9                      | --                                  | --   |
| Co                               | 1.8                      | --                                  | --   |
| U                                | 3.1                      | --                                  | <0.1   |
| Th                               | 8.5                      | --                                  | <0.2   |
| La                               | 49                       | --                                  | 2.7  |
| Yb                               | 3.6                      | --                                  | 6.0  |

Total iron as Fe<sub>2</sub>O<sub>3</sub>T; Oxides in weight percent  
Trace elements in ppm; -- = no data



|                                  | CONTINENTAL<br>MARGIN<br>RHYOLITE(3) | CALC-ALK<br>ISLAND ARC<br>RHYOLITE(3) | CONTINENTAL<br>RIFT<br>RHYOLITE(3) |
|----------------------------------|--------------------------------------|---------------------------------------|------------------------------------|
| SiO <sub>2</sub>                 | 75.78                                | 75.15                                 | 73.49                              |
| TiO <sub>2</sub>                 | 0.18                                 | 0.25                                  | 0.27                               |
| Al <sub>2</sub> O <sub>3</sub>   | 13.08                                | 13.28                                 | 13.93                              |
| Fe <sub>2</sub> O <sub>3</sub> T | 1.44                                 | 2.00                                  | 2.44                               |
| MgO                              | 0.23                                 | 0.31                                  | 0.35                               |
| CaO                              | 0.68                                 | 1.52                                  | 1.45                               |
| Na <sub>2</sub> O                | 3.68                                 | 4.23                                  | 4.00                               |
| K <sub>2</sub> O                 | 4.86                                 | 3.27                                  | 4.15                               |
| MnO                              | 0.06                                 | 0.06                                  | 0.03                               |
| P <sub>2</sub> O <sub>5</sub>    | 0.04                                 | 0.05                                  | 0.05                               |
| Rb                               | 231                                  | 108                                   | 156                                |
| Sr                               | 118                                  | 103                                   | 121                                |
| Cs                               | --                                   | --                                    | --                                 |
| Ba                               | 409                                  | 782                                   | 849                                |
| Y                                | 29                                   | 25                                    | 30                                 |
| Zr                               | 172                                  | 176                                   | 202                                |
| Hf                               | --                                   | 4.7                                   | --                                 |
| Nb                               | 36                                   | 17                                    | 5.0                                |
| Ta                               | --                                   | --                                    | --                                 |
| Sc                               | --                                   | 10                                    | --                                 |
| Cr                               | 2.0                                  | 4.0                                   | 1.0                                |
| Ni                               | 1.0                                  | 3.0                                   | 3.0                                |
| Co                               | 2.0                                  | 4.0                                   | 6.0                                |
| U                                | --                                   | --                                    | --                                 |
| Th                               | --                                   | --                                    | --                                 |
| La                               | 75                                   | 28                                    | 30                                 |
| Yb                               | 3.0                                  | 3.4                                   | 2.5                                |

Total iron as Fe<sub>2</sub>O<sub>3</sub>T; Oxides in weight percent

Trace elements in ppm; -- = no data

(1) Nockolds and Allen, 1956

(2) Gill, 1970

(3) Ewart, 1979

active continental margin environments. The GMF metadacites are most similar to dacite of the island arc tholeiite series except for higher Rb, Nb, Ba, Th, U, K<sub>2</sub>O, MgO, and REE and lower CaO and Sc. Characteristics which distinguish the GMF metadacites from the dacites of calc-alkaline suites of island arcs are lower Al<sub>2</sub>O<sub>3</sub>, Sr, and P<sub>2</sub>O<sub>5</sub>, and higher Fe<sub>2</sub>O<sub>3T</sub>, TiO<sub>2</sub>, K<sub>2</sub>O, Th, and Y. Although the chemical analyses (including major elements) are more similar to the dacite of the IAT series, the comparisons are not conclusive.

Metarhyolites of the Green Mountain Formation are compared to rhyolites of island arc tholeiite suites, island arc and active continental margin calc-alkaline suites, and continental rift rhyolites (Table 7). Major elements appear to correlate well with continental margin or continental rift rhyolites, but trace elements show similarities to most of the other suites, and are not definitive. Sr, Y, Sc, and Hf values of the GMF metarhyolites are consistent with the island arc tholeiite and pigeonitic series, while Ba, Zr, Ni, and LREE are more similar to calc-alkaline suites. The trace elements of the GMF metadacites are least similar to the continental rift rhyolites.

## RARE EARTH ELEMENTS

The chondrite normalized REE envelope of the GMF metatholeiites are compared to the envelope of MORB and island arc tholeiite, and calc-alkaline basalt (Figure 16). The GMF samples resemble the calc-alkaline envelope, but unlike the calc-alkaline envelope display variable Eu anomalies. As discussed previously, most trace element characteristics of the GMF metatholeiites are consistent with island arc tholeiites. Enrichment of the LREE by secondary processes could alter the patterns, producing patterns similar to calc-alkaline basalts. As discussed in the alteration section, LREE are commonly enriched by sea floor alteration. Physical characteristics discussed in the section of field and petrographic descriptions indeed indicate abundant submarine volcanism.

Chondrite normalized REE patterns of the GMF felsic metavolcanics fall within the range of the modern felsic envelope (Figure 17). Felsic rocks of the island arc tholeiitic series are known to have fairly flat patterns (Jakes and Gill, 1970; Donnelly and Rogers, 1980). The felsic rocks of the GMF have REE which are similar to calc-alkaline felsic volcanics. Although REE enrichment, probable in the GMF mafic volcanics, could also be suspected for the felsic rocks, it is not known if this degree of LREE enrichment of the GMF felsic volcanics can be produced from initially chondritic patterns also typical of IAT series felsic rocks.

## STRUCTURE AND METAMORPHISM

## STRUCTURE

## INTRODUCTION

Rocks of the Green Mountain Formation have undergone at least one period of intense deformation and metamorphism, resulting in isoclinal folding, local transposition of bedding, and faulting. These features are evident throughout the Precambrian terrane, and are well displayed by more detailed mapping in the southern Sierra Madres (Snyder, 1978). This type of structural style is not obvious in the GM and FP areas, but several lines of evidence support the possibility of their presence. The lines of evidence include foliation which parallels the lithologic layering and sheared small scale fold noses in units at the hand specimen scale. An understanding of overall structure is necessary in order to give an accurate description of the sections, and to constrain interpretations of collected data. Detailed mapping was not a primary aim of this study, therefore structural interpretations are of a preliminary nature.

## FLETCHER PARK SECTION

The Fletcher Park section appears to be the least deformed of the two areas (Figure 4). Open folds, present throughout the section, result in the local wavy character of the traceable outcrops, and include a small syncline in the west-central part of the area. Smaller scale open folds are locally observed in individual outcrops, but are minor in occurrence.

Faults also occur in the FP section with two trends of approximately N 40 W and N 35 E. The faults usually display minor displacement, and do not significantly affect the section. One fault in the west-central part of the FP section has resulted in the loss of part of the central mafic unit (Figure 4). Although horizontal displacement appears minor, as seen where the fault crosscuts two dikes, a significant change in bedding attitudes on opposite sides of the fault (not in the immediate vicinity of the fault) is evident. Foliation in the immediate vicinity of the fault is parallel to the fault, and is probably due to shearing during displacement. The apparent loss of part of the upper mafic agglomerate possibly indicates that significant vertical displacement occurred along the fault. An overall rotational motion of the fault is indicated, with the west side displaced northeast and upward relative to the east. Alternatively, the apparent loss of section could be a combination of faulting and folding. A small eastward plunging syncline is apparently cut by the fault. Vertical

displacement of the fault with uplift of the nose of the syncline would also result in a loss of section.

Foliation nearly parallels compositional layering throughout the FP section, although locally foliation is significantly oblique to the bedding. Bedding and foliation are steeply dipping, usually greater than 45 degrees, with trends changing from approximately N 60 W, to between N 50 W and N 30 W, to N 45 E in the western, central, and eastern parts of the section, respectively. The changes in bedding attitudes appear to be a result of rotation along the fault between the west and central parts of the area, and the intrusion of diabase between the central and eastern parts of the area. Foliation, weak in the felsic units and moderate in the mafic units, is defined by micaceous minerals. Isoclinally folded and/or transposed terranes characteristically exhibit foliation which parallels bedding. Since the foliation is parallel to bedding in many parts of the FP section, these structures cannot be eliminated. Because of the lack of major fold noses, repeated section, or mirroring of the section, the succession of units may represent the original bedding sequence of the volcanic-volcaniclastic section.

## GREEN MOUNTAIN SECTION

The Green Mountain section is structurally more complex than Fletcher Park, but is less well known due to lack of detailed mapping.

The important larger scale structure which affects the GM section as a whole is evident in the reconnaissance mapping (Figure 5). Bedding and foliation steeply dip to the south usually between 60 degrees and vertical, and trend generally N 65 W to N 75 W. The GM section contains amphibolites along both the southern and northern boundaries, and felsic schists dominate the central part of the section. The schists of dacitic composition appear to pinch out to the east, while the schists of rhyolitic composition thicken to the east. The two amphibolite sections of GM are separated by less felsic section in the east than in the west. At first inspection it would appear that the overall structure is a plunging isoclinal fold, with the fold nose lying to the east. The area may have started out as an isoclinal fold, but the structure appears to be more complex. The similarity of the two fine to medium-grained amphibolite sections, including a very distinctive thin, pink to orange felsic schist near the northern edge of both amphibolite areas, suggests repetition of the GM section. Felsic schist of rhyolitic composition is only apparent on the south side of the northern fine to medium-grained amphibolite. The presence of a similar rhyolitic schist associated with the southern amphibolite is

not noticed, but may be lost due to the direct contact of the amphibolite with the granitic terrane. A small exposure of dacitic schist occurs in the extreme northern part of the exposure, which is consistent with the dacitic schists overlying the southern amphibolite.

The west to east thinning relationships of the GM units, and contact relationships of compositional layering may best be explained by two possible structural features. These structures are (1) a thrust fault associated with isoclinal folding, or (2) transposition of bedding of a double isoclinally folded terrane. The first option is preferred for two reasons, (1) it is the simplest explanation, and (2) it seems to better accommodate the eastward thinning and thickening relationships of the units. This structure can be explained by a fault occurring along the contact between the rhyolitic and dacitic schists, which is somewhat oblique to the bedding. The rhyolitic schists, where exposed along the fault, are highly fractured and sheared reflecting possible movement along a fault zone. More detailed mapping is necessary to resolve the structural problem of Green Mountain.



## METAMORPHISM

## INTRODUCTION

The Green Mountain Formation has undergone at least one period of dynamothermal metamorphism, with differing metamorphic grades occurring within the two sections studied. The difference in metamorphic grade results in a difference in the degree of preservation due to recrystallization of original features. Retrograde metamorphic effects lend some difficulty in the identification of stable mineral assemblages. These effects include chloritization of biotite and hornblende, sericitization of feldspar, and the occurrence of patchy epidote. ACF plots of the mafic assemblages, and AKF plots of the felsic assemblages are used to correlate mineral content and bulk chemical composition.

## FLETCHER PARK

Rocks of the Fletcher Park section have undergone the lowest grade of metamorphism. Mineral assemblages are indicative of the chlorite and biotite zones of the greenschist facies. The metamorphic mineral assemblages of the mafic rocks, excluding relict minerals, consists of actinolite, epidote, albite, chlorite, +/- muscovite, +/- biotite. Biotite does not occur in all samples, but when present is less abundant than chlorite and is coarser grained. Biotite is most common as parallel growths in pressure shadows of feldspar phenocrysts and lithic fragments. Chlorite replaces biotite as a retrograde product, resulting in two phases of the mineral. Sericite is only abundant in one sample, replacing feldspar and lithic (glass?) fragments. This occurrence is probably a result of potassic alteration subsequent to metamorphism, as evidenced by the very high K<sub>2</sub>O content of the sample. Plagioclase is usually too fine-grained to identify, but is albite when identification is possible in larger grains. Actinolite, epidote, and chlorite are recognized in all mafic samples as part of the characterizing assemblage, and are consistent with the results of the ACF diagram (Figure 24). The exact composition of the chlorite is not known, but optical properties indicate that it is probably an iron-rich type, and an intermediate position on the ACF diagram is chosen.

Mineral assemblages of the felsic units (excluding

Figure 24. ACF plot of the mafic rocks of the Fletcher Park section.

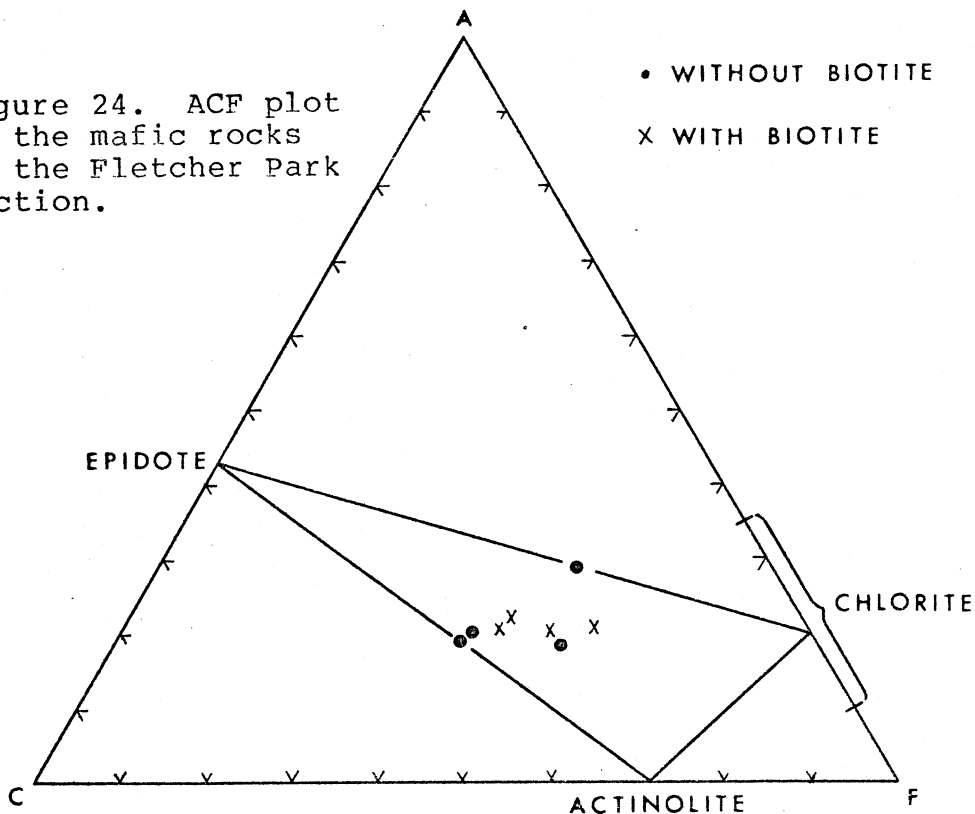
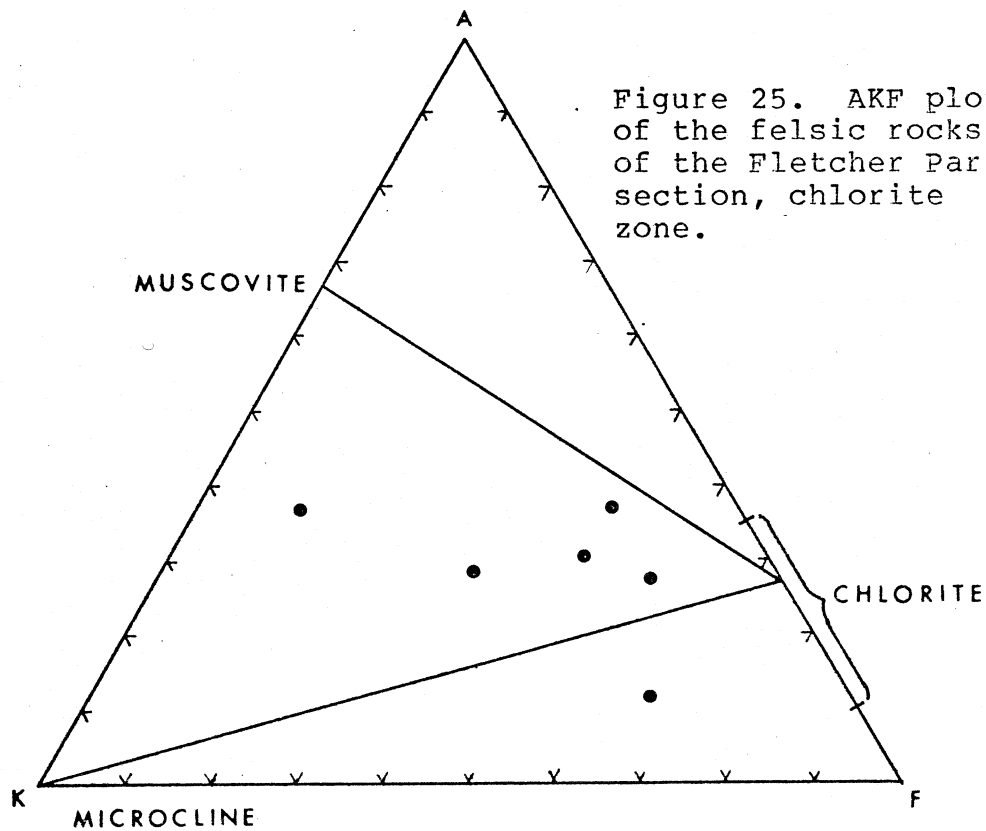


Figure 25. AKF plot of the felsic rocks of the Fletcher Park section, chlorite zone.



relict minerals) consist of two types: (1) quartz, microcline, albite, epidote, muscovite, and chlorite, and (2) quartz, microcline, albite, muscovite, and biotite. These minerals are also indicative of the greenschist facies. Only quartz, microcline, albite, and muscovite are present in all samples, but vary in abundance according to rhyolitic or dacitic composition. Chlorite is present in most samples, often coexisting with biotite. Mineral assemblages of the Fletcher Park felsic units are represented in AKF diagrams (Figures 25 and 26), and are consistent with mineral assemblages observed in thin section. The one sample in Figure 25 which falls outside of the microcline-muscovite-chlorite triangle is apparently altered, evidenced by a very high sodium content. The sodium enrichment greatly decreases the 'A' value of the AKF diagram.

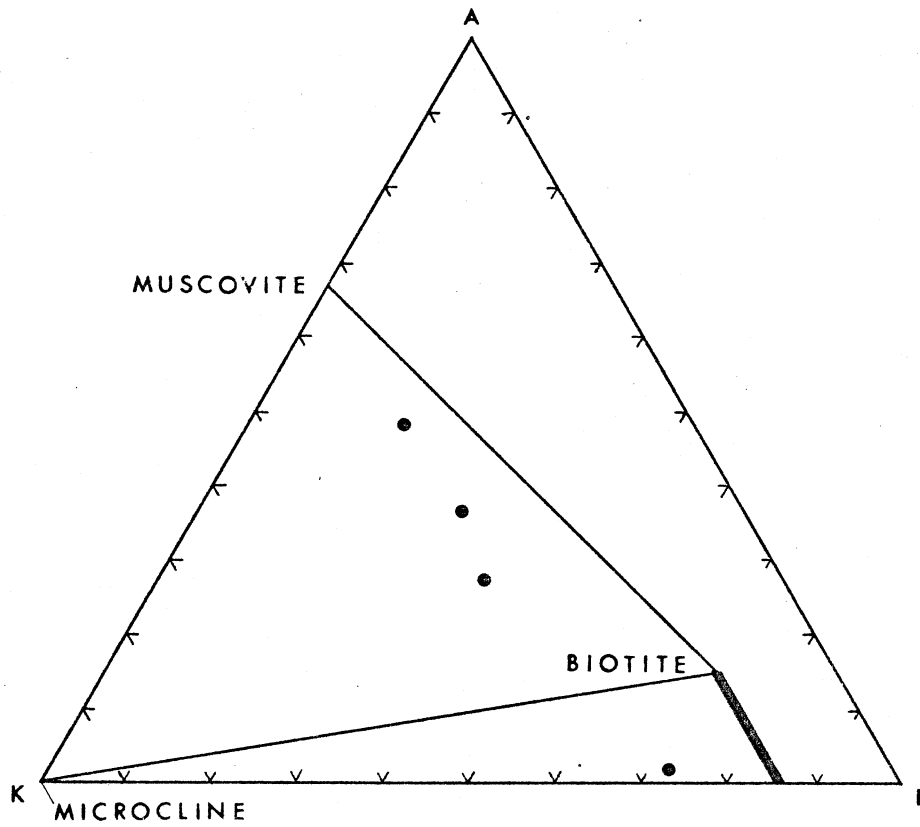
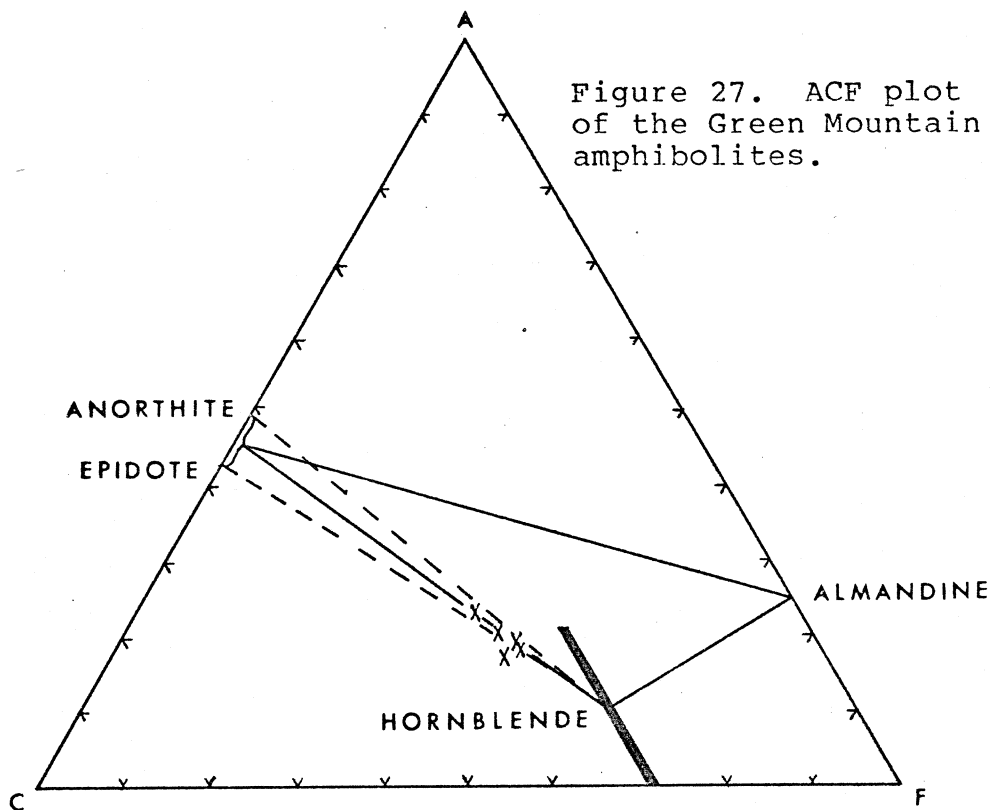


Figure 26. AKF plot of the felsic rocks of the Fletcher Park section, biotite zone.

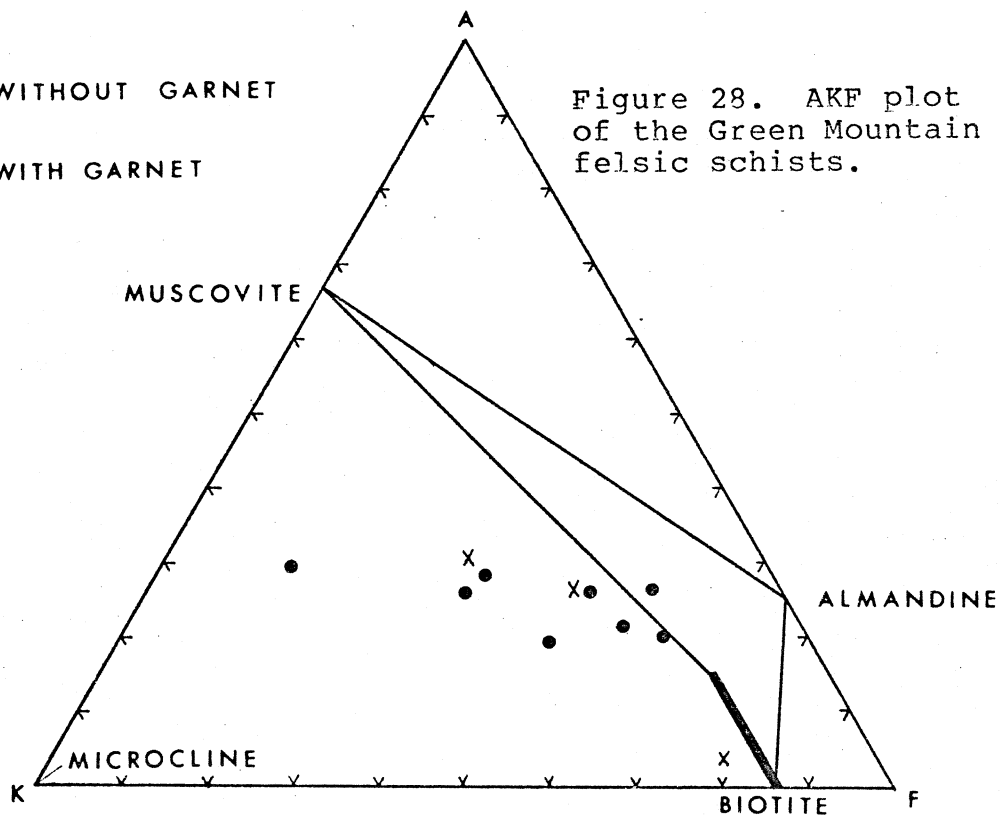
## GREEN MOUNTAIN

Rocks of the Green Mountain section were subjected to a higher degree of metamorphism, resulting in mineral assemblages characteristic of the amphibolite facies. Although some relict minerals are present, such as feldspar phenocrysts, they are minor in occurrence within the dominant metamorphic assemblages. There also appears to be a change in metamorphic grade observable in the GM section, increasing from the central part of the area toward the margins which may be due to the intrusion of the surrounding granitic terrane. The change in grade appears in the field as the presence of garnets in some of the felsic schists, and their origin as armored relicts is discussed below.

The amphibolites of the Green Mountain section contain mineral assemblages of hornblende, oligoclase, epidote, and minor quartz, +/- biotite, +/- sphene, +/- calcite, +/- sericite. The calcite and sericite are most likely either a result of alteration subsequent to metamorphism, or products of retrograde reactions. Oligoclase (andesine in one sample) and hornblende comprise between 75 and 92% of the amphibolites. Epidote generally comprises less than 10%, and shows a general decrease in abundance with increase in the An content of the associated plagioclase. The ACF diagram (Figure 27) shows that the amphibolites plot along the anorthite-hornblende join, indicating a bimineralogic assemblage absent of garnet. A secondary triangle, drawn to separate the anorthite and epidote members, still



- WITHOUT GARNET
- x WITH GARNET



accommodates the amphibolite samples. This allows the addition of epidote as part of the assemblage. The one sample which falls outside the triangle is anomalous and can be explained by sodium enrichment.

The felsic schists of the GM section contain two mineral assemblages: (1) oligoclase, microcline, quartz, biotite, and muscovite, and (2) oligoclase, microcline, quartz, biotite, muscovite, and garnet. The relative abundances of oligoclase, microcline, and quartz are dependent on the rhyolitic or dacitic composition of the felsic schists, and along with biotite comprise greater than 85% of the samples. Garnet occurs locally, and is absent in the central part of the Green Mountain section. The epidote abundance and anorthite content of the plagioclase show the same inverse relationship as the amphibolites. The mineral assemblages of the GM felsic schists agree with the amphibolites in placing metamorphic grade in the amphibolite facies. The AKF diagram (Figure 28) shows all but one point plotting within the microcline-muscovite-biotite triangle. The plot is consistent with the observed mineral assemblages, except for the three samples which contain garnet. These three samples should plot in the muscovite-biotite-almandine triangle. This indicates that a disequilibrium assemblage exists. Petrographic observations show that coarse-grained muscovite surrounds the garnet, and probably shielded the garnet from complete reaction to form an equilibrium assemblage. In view of this observation, the



stable mineral assemblage is actually microcline, muscovite, and biotite, and the apparent increase in grade may be a relict feature of a higher grade of metamorphism. The last stage of dynamothermal metamorphism, recognized in both sections, is evidenced by bent twin lamellae in plagioclase, strain fractures, and mortar textures associated with relict phenocrysts and porphyroblasts.

## DISCUSSION OF TECTONIC ENVIRONMENT

One of the purposes of this project is also to determine a possible tectonic environment(s) in which the Green Mountain Formation was formed. The interpretations are based on rock types present in the section, geochemical characteristics of the suite, and their relationship to other rock types on a regional scale.

The presence of dominantly pyroclastic rocks, debris flows, and volcanoclastic sediments in the Green Mountain Formation is not necessarily indicative of a particular tectonic environment. The coarse-grained character of many of the pyroclastic and volcanoclastic deposits indicates that deposition was probably on and/or near the flanks of a volcanic center, or in depositional basins adjacent to a volcanic source. Sedimentary structures such as cross-bedding, graded bedding, and possible cut-and-fill structures indicate that deposition was at least in part and probably dominantly in a subaqueous environment. The lack of mature sediments indicate that extensive reworking of the volcanics was minimal, and deposition from a continental source did not occur directly with the metavolcanics. The lack of deep sea sediments such as bedded chert and carbonaceous muds may suggest that deposition was probably not within the deeper parts of a basin.

Geochemical characteristics are most consistent with the GMF suite representing a convergent plate boundary assemblage, namely an island arc environment. The mafic

rocks represent low-K tholeiites most similar to the island arc tholeiite series. The fact that the felsic volcanics are not consistently distinguishable as belonging to either the IAT or calc-alkaline series is not critical. What is important is the consistent indication of a convergent plate margin environment for the formation both mafic and felsic members of the GMF. A convergent plate boundary, with the formation of an island arc environment, has been previously proposed for the Green Mountain Formation, and the characteristics of the GMF determined in this study are consistent with this type of interpretation. The Proterozoic terrane which contains the Green Mountain Formation is in fault contact with the Archean craton to the north and its associated Proterozoic sediments. These features are most easily explained by a northward migrating island arc due to a southward dipping subduction zone as suggested by Hills and Houston (1979) (Figure 29). This model involves the closing of a marginal basin and collision of an oceanic arc system along the Wyoming Shear Zone. The mature sediments of the Proterozoic supracrustal rocks north of the shear zone, consisting of quartzite, shale, carbonate, and minor volcanics, are consistent with deposition within a marginal basin along the edge of the Archean craton. The GMF metavolcanics and volcanoclastic rocks necessitate ensimatic deposition, probably along the margin of the arc proper and the arc-trench gap or back-arc basin. Interfingering relationships are not observed

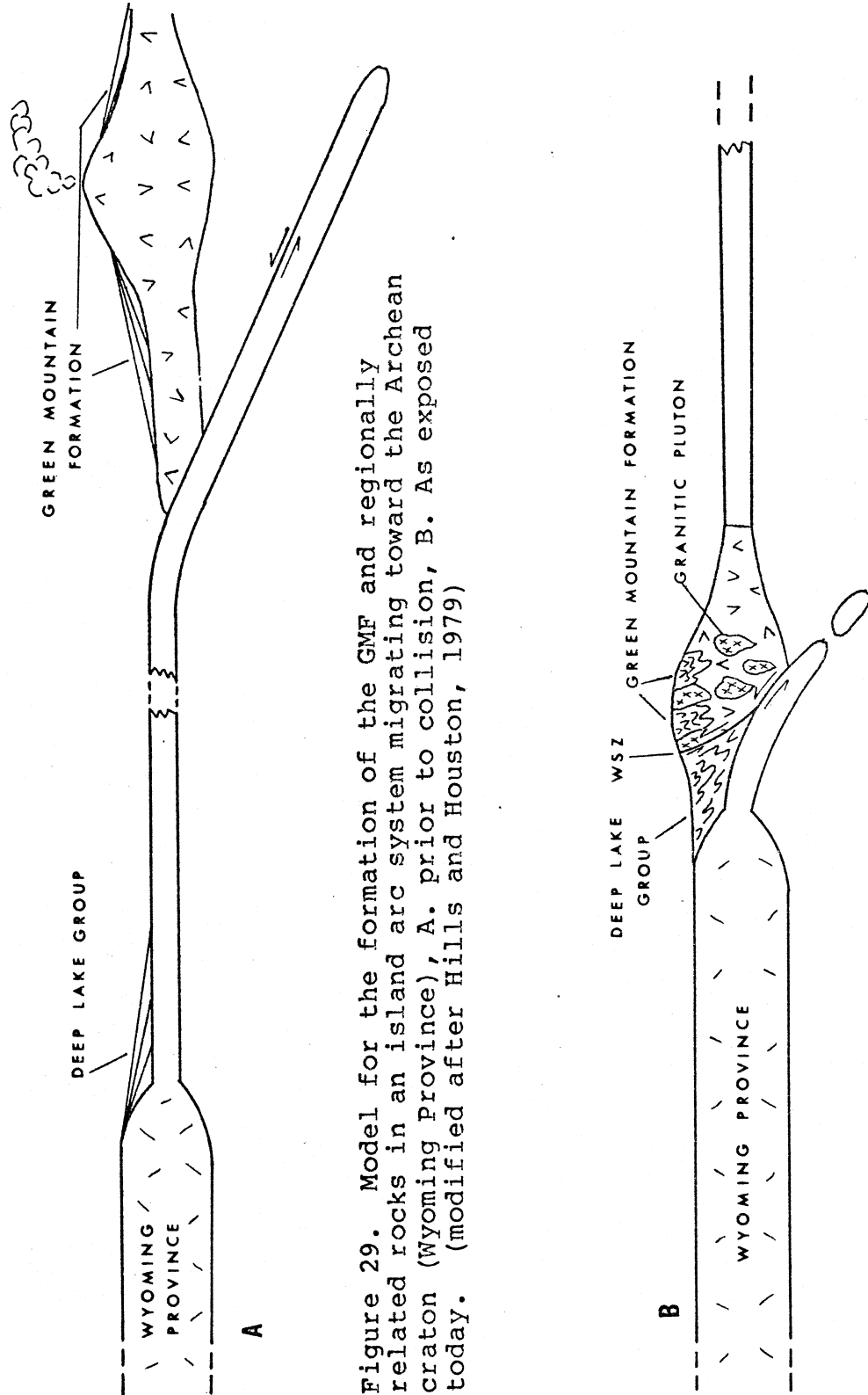


Figure 29. Model for the formation of the GMF and regionally related rocks in an island arc system migrating toward the Archean craton (Wyoming Province), A. prior to collision, B. As exposed today. (modified after Hills and Houston, 1979)

between the Proterozoic rocks north and south of the shear zone. Either this part of the tectonic environment is not preserved, or the marginal basin was a separate depositional site from the arc-trench gap or back-arc basin. The absence of andesites and graywackes argues against a calc-alkaline suite typical of mature arc systems, although the felsic rocks of the GMF have some geochemical characteristics of calc-alkaline volcanics. The presence of mafic rocks of the island arc tholeiite series, along with the absence of andesites favors an immature arc system interpretation for the GMF. If the felsic volcanics are indeed calc-alkaline, the GMF may represent evolution from arc tholeiite series volcanism to calc-alkaline volcanism with time.

Alternatively, the interbedding of rocks of the two petrogenetic series may be due to mixing of laterally different volcanic sequences. This relationship is observed in many modern island arcs where tholeiitic series volcanism changes to calc-alkaline volcanism as distance from the trench increases (Miyashiro, 1974). Other features which are common to island arc systems such as the presence of tectonic melange and paired metamorphic belts including the high pressure metamorphic series are not recognized in the GMF. Paired metamorphic belts are observed in modern island arcs due to underthrusting of the oceanic plate beneath the arc. Miyashiro (1972) suggests that the high pressure series may not develop where underthrusting is not rapid enough to produce the unusually low geothermal gradient

required. The absence of the high pressure series is observed in many metamorphic belts of the Atlantic region where spreading rates are indeed much slower. Whether or not the paired metamorphic belts are preserved during subsequent metamorphism is questionable.

To summarize, the Green Mountain Formation appears to represent immature island arc volcanism of the island arc tholeiite series or mixed tholeiitic and calc-alkaline series rocks. The GMF may represent part of an island arc system which migrated toward the Archean craton along a southward dipping subduction zone. The Proterozoic metavolcanic succession of the GMF was brought together with the Archean continent and associated marginal basin sediments by thrusting and/or lateral shearing along the Wyoming Shear Zone.

## SUMMARY AND CONCLUSIONS

The Green Mountain Formation is located south of the Archean-Proterozoic boundary recognized in the Sierra Madre Range as the Wyoming Shear Zone. The succession is comprised of interbedded metavolcanic and volcanoclastic rocks intruded by an extensive granitic terrane.

The Fletcher Park sequence appears to be made up of two volcanic cycles (Figure 30), each consisting of a general stratigraphic sequence of metabasalt overlain by metadacite and/or metarhyolite, terminating with a layer of cherty exhalite. Rocks of basaltic composition are represented by matrix-supported agglomerates which resemble mudflow or pyroclastic deposits, with interbedded lapilli tuff or thin, brecciated flows and volcanoclastic sediments. Upward-fining mafic volcanoclastic sequences show gradations from pebbly volcanic sandstone to volcanic siltstone. Local intrusions of basaltic sills and dikes are present in some parts of the section. Metadacites are represented by fine-grained volcanic ash occurring within the metabasalt agglomerates and overlying the upper agglomerates. Metadacite ash-flow tuffs occur within the upper felsic volcanic sequence. Minor units include lapilli tuff and a metadacite lava flow(?). Metarhyolites occur as volcanic breccias and ash-flow tuff overlying the lower mafic section, and as fine-grained tuff, ash-flow tuff, and volcanoclastic sediments in the eastern part of the FP section. The volcanoclastic deposits of rhyolitic and

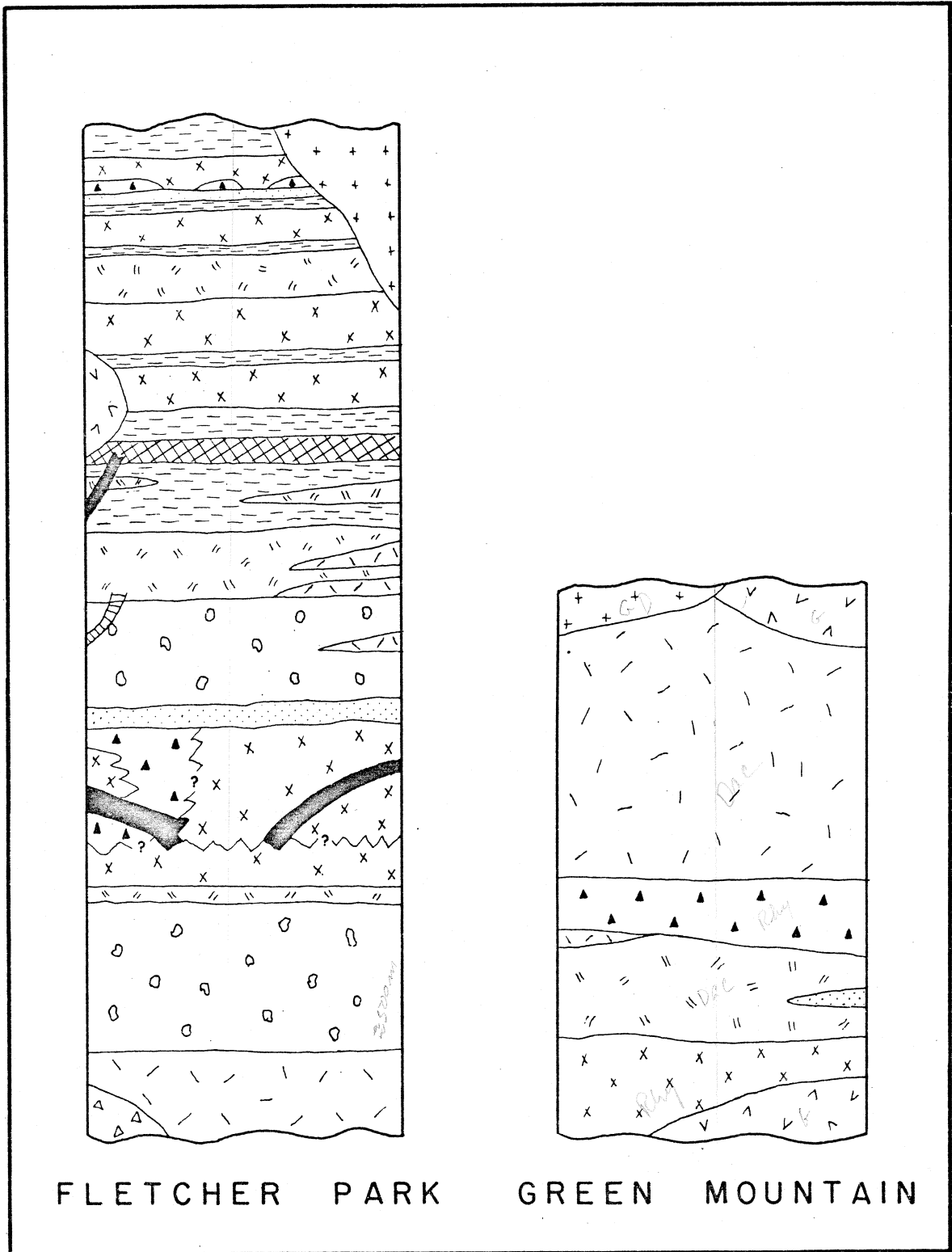


Figure 30. Diagrammatic stratigraphy of the Fletcher Park and Green Mountain sections. Explanation on corresponding geologic maps Figures 4 and 5. Vertical scale exaggerated.



dacitic composition locally contain cross-bedding and graded bedding which consistently indicate a stratigraphic younging direction to the east. Cherty exhalite units, which are locally ferruginous, appear to mark the top of the volcanic cycles. These chert beds partially penetrate the underlying felsic volcanic units and locally contain intermixed milky white carbonate. Lastly, the section is intruded by a medium-grained diabase, which displays discordant contacts with the section and contains xenoliths of the adjacent lithologies.

The primary features of the volcanoclastic sediments of both mafic and felsic composition indicate that a large part of the FP section represents submarine deposition. The uniform, well-sorted grain size of the volcanoclastics are consistent with deposits formed during subaqueous eruptions (Fiske and Matsuda, 1964). Because ash-flows can be preserved during their emplacement into oceanic environments, and phreatic explosions are often produced during this process, the volcanoclastics of the Green Mountain Formation may have had a similar origin. The close association of the ash-flow tuffs with the volcanoclastic sediments supports this idea. The upward-fining, graded mafic volcanoclastic sequences may have been produced by turbidity currents, although some of the sedimentary structures characteristic of turbidity currents are not observed. These features include ripple marks and cross-bedding.

The Green Mountain section is comprised of associated amphibolites, amphibolite breccias, feldspar-quartz-mica schists, and felsic breccia (Figure 30). Except for possible relict phenocrysts and rock fragments, the higher grade of metamorphism has obscured most of the original features.

Amphibolites either have fine to medium-grained textures, or are very coarse-grained. Banding is a widespread feature, probably a result of deformation and/or metamorphism. All amphibolites are conformable with compositional layering, and contain hornblende and plagioclase as the main minerals. Most of the layers are uniform in appearance, but many have a fragmental appearance with clasts ranging up to several centimeters. Most of the fine- to medium-grained amphibolites probably represent mafic flows, sills, or pyroclastic deposits, but no diagnostic relict textures are observed. Thin-layered fragmental amphibolite may either represent similar lithologies to the lapilli tuff or brecciated flows of the Fletcher Park section, or may be zones of transposition. Massive appearing fragmental amphibolites are also present, and are similar in appearance to the matrix-supported mafic agglomerates of the Fletcher Park section. Coarse grained amphibolites, which are minor in occurrence, are concordant with adjacent units and laterally discontinuous. These coarse-grained amphibolites probably represent diabase sills.

The felsic schists are rhyolitic to dacitic in composition, and are represented by microcline-quartz-oligoclase schists and oligoclase-microcline-quartz schists, respectively. Granoblastic textures are typical of the schists. Porphyroblasts of oligoclase are a common feature, possibly representing relict phenocrysts. A few of the dacitic schists have feldspar-quartz patches which may represent small lithic fragments. The rhyolitic and dacitic schists may represent units similar to the felsic volcanics of the Fletcher Park section, including ash flow tuff, fine-grained tuff, and volcanoclastic sediments. Felsic breccia occurs as a minor rock type in the Green Mountain section, with angular to subrounded clasts representing a variety of lithologies.

The overall similarities of the GM section to the FP section are apparent, but direct correlation is impossible. Both sections contain porphyritic and non-porphyritic felsic rocks, either of which may be rhyolitic or dacitic in composition. Individual units of the Green Mountain section could represent ash-flow tuffs, fine-grained tuffs, and volcanoclastic sediments similar to the felsic metavolcanics of the Fletcher Park section. Felsic breccias and mafic matrix-supported agglomerates are also observed in both sections. The Green Mountain section contains amphibolite breccia in which clast size range up to about 3cm, and may represent units similar to the mafic lapilli tuff or brecciated flows observed the Fletcher Park section. An

equivalent to the exhalite units of the Fletcher Park section were not observed at Green Mountain.

The Green Mountain section contains the same compositional rock types as the Fletcher Park section. The composition of the rock types mainly include metabasalt, metadacite, and metarhyolite. Reconstruction of the GM section, by removal of the main northwest trending fault, results in a north to south compositional succession of metarhyolite, overlain by metabasalt (amphibolite), ending with metadacite. In the Fletcher Park section, where stratigraphic indicators are abundant, the general stratigraphic sequence is metatholeiite, metarhyolite, and exhalite, followed by a second sequence of metatholeiite, metadacite, metarhyolite, and exhalite (Figure 30). The Green Mountain succession does show similarities to Fletcher Park. The rhyolitic schists of Green Mountain may similarly mark the end of a volcanic cycle, and the amphibolite followed by dacitic schist may represent part of a new volcanic cycle. The comparison of the relative positions of the amphibolite and felsic schists of Green Mountain to the better known stratigraphy of Fletcher Park indicates that the Green Mountain section probably has a stratigraphic up direction to the north.

The Fletcher Park and Green Mountain sections are metamorphosed to greenschist and amphibolite facies, respectively, with a general increase in regional metamorphic grade occurring southward and eastward from the

Fletcher Park area. Major deformation has produced isoclinally folded terranes with associated thrust faults and/or transposition of bedding in areas of the Green Mountain Formation. These features are not always obvious in the FP and GM study areas of this project, but can not be eliminated.

Geochemically, the metavolcanics and volcaniclastics of the Green Mountain Formation are classified as subalkaline metabasalt (low-K tholeiite), metadacite, and metarhyolite, and include the possibility of a transitional felsic member of rhyodacitic composition. Evaluation of the samples in terms of alteration shows that most of the elements do not appear to be severely mobilized. It is believed that the chemical analyses, for the most part, are relatively representative of the original concentrations. In terms of the major elements, Na<sub>2</sub>O and K<sub>2</sub>O are the most severely effected, while CaO, MgO, and Fe<sub>2</sub>O<sub>3</sub>T appear to only show moderate to minor mobilization. In terms of most major and trace elements, the volcaniclastic sediments are not significantly different in chemical composition from their volcanic protoliths. Some chemical differences are observed, most of which are consistent with changes expected by mechanical sorting and/or chemical alteration during submarine eruption and deposition.

Geochemical diagrams using the trace and major elements of the Green Mountain Formation do not always show consistent results in terms of tectonic interpretation. The

only consistent indications of the major and trace elements of both the felsic and mafic GMF rocks are their formation at a convergent plate boundary. The Th-Hf-Ta, Zr-Ti-Y, Ti vs Zr, and  $TiO_2$  vs  $100(Mg/Mg + Fe^{2+})$  indicate a convergent plate boundary and/or island arc environment. Trace and major element plots show mixed results for the volcanic rocks of the GMF in distinguishing between calc-alkaline and island arc tholeiite trends. Most trace element diagrams for the mafic rocks indicate that they are low-K tholeiites of the island arc tholeiite series. A comparison of average analyses of basalts of various tectonic environments to the GMF tholeiites are also most consistent with the IAT series. Higher LREE and other LIL elements are more similar to calc-alkaline basalts, but are also common indications of sea floor alteration. Iron enrichment is indicated for the GMF mafic rocks in the  $MgO$  vs  $Fe_2O_3 + FeO$  diagram, which is also consistent with a tholeiitic trend.

There is a lack of trace element diagrams to distinguish felsic rocks of different tectonic environments. Interpretations rely on REE, the Th-Hf-Ta plot, and comparison to average analyses of equivalent rock types of the various tectonic environments. LREE and the Th-Hf-Ta diagram indicate that the felsic rocks have calc-alkaline affinities. A comparison of the GMF dacites to average analyses of equivalent rocks of several tectonic environments appear to show the most similarities to dacites of the IAT series, but some significant similarities to

calc-alkaline dacites such as REE are inconsistent. The rhyolites do not show enough similarities to any of the tectonic environments to be conclusive.

Overall characteristics of the Green Mountain Formation appear to indicate that the succession represents immature island volcanism of the island arc tholeiitic or mixed calc-alkaline and tholeiitic series rocks. The volcanic plus volcanoclastic succession was probably accreted onto the Archean Wyoming Province along the Wyoming Shear Zone, probably due to northward migration of an island arc system along a southward dipping subduction zone.

Several problems exist which may be resolvable by future studies. The first problem is whether or not the two sections evaluated in this study are truly representative of the total GMF of the Sierra Madres. The areas of this study only comprise about one fifth of the exposed GMF. The second problem is whether or not the mafic and felsic rocks of the GMF represent a cogenetic suite of rocks. The apparent orderly progression from tholeiite to dacite to rhyolite may argue in favor of a cogenetic suite, but only detailed trace element geochemical modelling may resolve the problem. The third problem is the applicability of discrimination diagrams based on modern rocks to determine chemical trends and tectonic environments of Precambrian rocks. This problem may only be resolved by the continued study of Precambrian rocks in general to see if similar trends consistently develop.

In view of these types of problems, the interpretations presented in this paper cannot be considered conclusive. Since the rocks studied in this project probably represent the best preserved exposures of the GMF, and some geochemical consistencies and trends are discernable, the information presented provides a good basis for further comparison and study.



(125)

APPENDIX A  
PHOTOGRAPHIC PLATES

PLATE 1

Cross-bedding in felsic volcanoclastic sediments  
(lens cap = 6cm).

(126)

PLATE 2

Porphyritic texture in rhyolite ash-flow tuff  
(lens cap = 6cm).

(127)

PLATE 3

Pumice and other lithic clasts in ash-flow tuff  
(lens cap = 6cm).

(128)

PLATE 4

Felsic breccia with angular clasts (lens cap = 6cm).

---

(129)

PLATE 5

Mafic matrix-supported agglomerate  
(hammer head = 15cm).

(130)

PLATE 6

Channel-shaped accumulation of mafic volcanic  
conglomerate (lens cap = 6cm).

---

## APPENDIX B

BRIEF PETROLOGIC DESCRIPTIONS OF  
THE GREEN MOUNTAIN FORMATION

## FLETCHER PARK SECTION

## METARHYOLITES

GM001\*: Medium green, fine-grained, porphyritic rock. Phenocrysts are composed of subhedral perthitic albite twinned An8 and microcline (2%, <3mm), highly sericitized. The matrix is composed of modally indistinguishable microcline, quartz, sericite, and chlorite (<0.05mm) with approximately 15% anhedral granoblastic quartz (0.1mm) often in bands(?) to 0.5mm.

GM002: Pale gray to pink, very fine-grained, porphyritic rock. Sample contains broken subhedral perthitic phenocrysts of An20 and quartz to 2mm (5%), and pumice fragments to 2mm (10%), in a mostly cryptocrystalline groundmass. The groundmass is composed of modally indistinguishable quartz, albite, and sericite. Minor epidote, chlorite, and hematite are present. The rock has a relict porphyritic texture and is weakly foliated.

GM006\*: Medium gray, fine-grained, porphyritic rock. Phenocrysts are broken and composed of perthitic albite twinned An20 and tartan twinned microcline (5%, <2mm), and equant quartz (1%, <2mm). The matrix is composed of cryptocrystalline potassium feldspar, quartz, and sericite. Accessory minerals include epidote and calcite. Relict banding defined by slightly coarser grained minerals.

GM023: White to pale green, fine-grained, porphyritic rock. Phenocrysts are composed of rounded, highly sericitized An12 (<2mm, 5%). The matrix is composed of discontinuous, wavy laminations of alternating cryptocrystalline and granoblastic (<0.1mm) albite, quartz, and K-feldspar. Minor epidote and chlorite are present.

GM027: Pale green, fine-grained, porphyritic rock. The sample is composed of broken phenocrysts of antiperthitic(?) microcline and An10 to 4mm (10-15%), and quartz phenocrysts to 1mm (<1%), in a cryptocrystalline groundmass. Some grains are identified as albite, quartz, and K-feldspar. Minor minerals include biotite, chlorite, and epidote. The matrix is weakly foliated.

## METARHYODACITES(?)

GM017: Pale green to gray, fine-grained, fragmental rock. The sample is composed of broken phenocrysts of An10 (3%), pumice and other stretched ovate to angular rock fragments (20%) to 5mm. The fine-grained groundmass contains granoblastic albite, microcline, and quartz; platy biotite and chlorite to 0.05mm (10%), and subhedral epidote to 1mm (7%). Also present are minor sericite and hematite. The matrix is well foliated.

GM018: Medium green, fine-grained, moderately foliated rock. The sample contains modally indistinguishable granoblastic albite, K-feldspar, and quartz, and subhedral epidote (15%), chlorite (10%), and sericite (10%). The average grain size is less than 0.1mm. Minor An14 grains to 0.2mm (2%) may be phenocryst fragments.

GM032: Medium green to gray, fine-grained, porphyritic rock. The sample is comprised of broken subhedral phenocrysts of perthitic An30 to 4mm (15-20%) in a granoblastic groundmass averaging 0.1mm. The groundmass is composed of albite, microcline, and quartz. Epidote (5%) occurs as minute rounded grains and grain aggregates. Biotite and sericite plates to 0.2mm comprise 7 and 4%, respectively, with minor chlorite. The groundmass is weakly foliated and has a relict pyroclastic texture.

## METADACITES

GM019: Medium gray to green, medium to coarse-grained, porphyritic rock. The phenocrysts are subhedral with little sign of breakage, and are composed of An30 (to 2mm; 15%). The groundmass is granoblastic and comprised of albite, microcline, and quartz ranging up to 0.2mm, biotite (10%), and pumice fragments (2%) ranging up to 4mm. Minor minerals include sericite, epidote, and chlorite which define a moderate foliation.

GM042: dark greenish gray, fine-grained, microporphyritic rock. The sample contains rock fragments of cryptocrystalline character which are highly sericitized and chloritized, and range up to 2mm. Saussuritized phenocrysts of An32 (10%) and microlitic An26 (20%), are contained within a fine granoblastic matrix of albite, quartz, and K-feldspar(?). Foliation is moderate and defined by flakes of chlorite ranging up to 0.1mm (15%). Minor subhedral epidote to 0.1mm and hematite are present. The sample is strongly sericitized.

GM044: Dark gray, fine-grained, poorly foliated rock. The sample is too fine-grained to distinguish mineral modes, but is comprised of albite, K-feldspar, and quartz of less than



0.1mm, except for some coarser grains ranging up to 0.3mm. Biotite flakes to 0.2mm (10%), chlorite (15%), and sericite define a poor foliation. Minor epidote and opaque minerals are present. Rock fragments comprise about 4%, and include pumice, shards(?), and microporphyrific volcanics.

GM050: Dark gray, aphanitic, poorly foliated rock. The sample contains broken phenocrysts of An26 (5%) to 3mm, in a cryptocrystalline matrix averaging less than 0.1mm. The matrix appears to be comprised of albite, K-feldspar(?), and quartz, and flakes of biotite and chlorite (10%). Also present are minor epidote grains and patches (4%), and sericite (10%).

#### METATHOLEIITE

GM007\*: Dark green, very fine-grained rock. The mineral content is comprised of saussuritized anhedral albite twinned An34 ranging up to 0.2mm (50%), platy chlorite to 0.2mm (25%), and granoblastic albite (10%?), magnetite and hematite (7%), sericite (2%), quartz (2%), and K-feldspar (1%), and epidote (3%).

GM009: Light to dark green, blotchy, moderately foliated rock. The sample is comprised of approximately 40% rock fragments ranging up to 1cm. The fragments are very fine-grained to cryptocrystalline, composed of modally indistinguishable feldspar, actinolite, chlorite, and epidote. Some of the fragments contain microphenocrysts of An26. The groundmass is comprised of actinolite (30%), chlorite (10%), epidote (15%), and An20 microphenocrysts to 0.5mm (30%), and albite (15%?). The average grain size is less than 0.3mm. A relict intergranular texture is suggested.

GM010A: Pale to medium green, medium-grained, clastic appearing rock. The mineral content is comprised of subhedral pseudomorphs of actinolite after pyroxene (15%), chlorite to 0.5mm (10%), epidote (15%) as minute grains and patches ranging up to 0.1mm, and about 20% unidentifiable feldspar. Sericite is an abundant alteration product (%). Minor quartz, hematite, and lithic fragments are also present.

GM015: Dark green, medium-grained, clastic appearing rock. The sample is composed of equigranular actinolite (25%), epidote (20%), and albite (30%) ranging up to 0.5mm. Biotite (4%) and chlorite (20%) flakes ranging up to 0.1mm define the moderate foliation. Minor quartz, hematite, magnetite, and lithic fragments are also present. Overall, the grains have a rounded to subangular character resulting in a clastic texture.

GM016: Medium green, aphanitic rock. The sample is composed of cryptocrystalline actinolite, chlorite, epidote, and feldspar. Modes unfeasible.

GM046: Dark green, aphanitic, poorly foliated rock. The sample represents the matrix of the mafic agglomerate. The rock is composed of subhedral actinolite to 0.5mm (20%), biotite (10%) and chlorite (15%) flakes to 0.5mm define a moderate foliation, subhedral epidote to 0.1mm (20%), and anhedral albite (30%) to 0.2mm. Minor minerals include quartz and hematite.

GM047: Medium green, fine-grained porphyritic rock. The sample represents a clast from a mafic agglomerate. The clast is a microcrystalline mixture of actinolite, chlorite, epidote, and albite. Porphyritic actinolite, epidote, and chlorite pseudomorphs after pyroxene to 3mm comprise 10%, and An30 phenocrysts to 5mm comprise 15%. Modal estimates of the groundmass is unfeasible. Minor minerals include quartz and hematite.

GM051: Medium green, fine-grained, weakly foliated rock. The rock is composed of fine grained anhedral granoblastic actinolite (15%), albite (30%), and epidote (25%), and flakey biotite (10%) and chlorite (10%), and minor quartz. The average grain size is approximately 0.2mm. The rock is moderately foliated and has a relict clastic texture.

GM053: Light to dark green, blotchy appearing, moderately foliated rock. A rock fragment greater than 1/2 of the thin section is microporphyritic (An30; to 0.5mm, 30%), associated with epidote-actinolite pseudomorphs after pyroxene (15%) to 2mm, and granoblastic albite. Foliation is defined by chlorite flakes to 0.3mm. A relict intergranular texture is evident. The matrix around the fragment has the same character as the fragment, except the microphenocrysts have a subparallel orientation.

## GREEN MOUNTAIN

MICROCLINE-OLIGOCLASE-QUARTZ SCHISTS  
(METARHYOLITE AND METARHYODACITE)

GM035\*: Light brown to pale greenish brown, fine-grained, sandy appearing rock. The sample is composed of granoblastic quartz (35%), tartan twinned microcline (35%), and untwinned oligoclase (An 17, 15%). The average grain size is approximately 0.1mm. Foliation is defined by biotite laths (20%) to 0.3mm. Minor epidote and muscovite (poikilitic to 1mm) each about 2% are also present.

GM065: Pale brown, fine-grained, well foliated rock. The sample is composed of granoblastic tartan twinned microcline (40%), albite twinned and untwinned oligoclase (An12, 17%), and quartz (20%). The average grain size is about 0.2mm. Foliation is defined by 0.2mm plates of biotite (15%). Minor minerals include epidote and 0.1mm plates of secondary muscovite (poikilitic), and zircon.

GM067: Light gray, fine-grained, well foliated rock. The sample is composed of granoblastic tartan twinned microcline (25%), oligoclase An21 (25%), and quartz (35%), averaging 0.2mm. Muscovite (5%) occurs as poikilitic laths to 2mm. Porphyroblasts of anhedral An26 to 2mm (3%) may be relict phenocrysts. Minor idioblastic garnet (<1%) is surrounded by the coarser-grained muscovite. Minor calcite and zircon are present.

GM075: Medium gray, medium-grained, moderately foliated rock. The sample is composed of granoblastic tartan twinned microcline (25%), oligoclase An17 (25%), and quartz (30%), averaging 0.2mm. Foliation is defined by biotite (11%) to 0.3mm. An29 porphyroblasts to 2mm (5%) may represent relict phenocrysts. Minor poikilitic muscovite to 0.3mm, calcite, and zircon are also present.

OLIGOCLASE-MICROCLINE-QUARTZ SCHISTS  
(METADACITES)

GM036: Medium gray, medium-grained, porphyroblastic rock. The sample is composed of granoblastic An22 (45%) which is usually untwinned, tartan twinned microcline (15%), and quartz (30%), averaging 0.2mm. Foliation is defined by biotite flakes to 0.2mm (20%). Porphyroblasts of perthitic An38 (5%) may represent relict phenocrysts. Minor minerals include chlorite, epidote, and poikilitic muscovite.

GM037: Dark gray, medium-grained, porphyroblastic rock. Same as GM036 except porphyroblasts are An28 (3%), no epidote, and idioblastic garnet to 2mm (<1%).

GM038: Same as GM037 except plagioclase is An26 and porphyroblasts are of An20 and no garnet.

GM058: Medium gray, medium-grained, non-porphyroblastic rock. The sample is composed of granoblastic oligoclase An26 (50%), quartz (25%), and tartan twinned microcline (10%) averaging 0.3mm. Foliation is defined by biotite flakes to 1mm (15%). Minor epidote (5%), sericite and subhedral garnet to 0.3mm, and magnetite are also present. The granoblastic is zoned with the core more sodic than the rim.

GM063: Fine-grained, medium gray rock with black streaks. The sample has a granoblastic texture averaging 0.3mm. The minerals are oligoclase An18 (40%), tartan twinned microcline (16%), and quartz (25%). Biotite (15%) defines the foliation as 0.3mm plates. Minor epidote/clinozoisite, muscovite, and calcite are also present. Porphyroblastic An17 to 1mm comprises 5% of the rock, and is perthitic.

GM072 and GM073: medium-grained, dark green, porphyritic rocks. The samples have a granoblastic texture averaging 0.3mm. The minerals are oligoclase An20 (30%), tartan twinned microcline (24%), and quartz (25%). Foliation is defined by biotite (7%) and chlorite (9%) as flakes to 0.2mm. Porphyroblastic perthitic An15 (15%) ranges up to 2mm. Minor minerals include epidote, muscovite, magnetite, hematite, and zircon.

GM076: medium-grained, medium dark gray-white-black blotchy rock. The sample is composed of granoblastic oligoclase An18 (32%), microcline (20%), and quartz (20%) ranging up to 0.2mm. Foliation is defined by biotite (20%) and chlorite (5%) as flakes up to 0.3mm. Porphyroblastic perthitic An15 (5%) may represent relict phenocrysts. Minor muscovite/sericite, apatite(?), and epidote.

#### AMPHIBOLITES (METATHOLEIITES)

GM033: Dark green, medium-grained, well foliated rock. Nematoblastic hornblende (50%) to 5mm defines foliation and lineation. Granoblastic oligoclase An17 comprises (30%) and is sometimes zoned. Also present are subhedral epidote to 1mm (10%), and minor quartz, calcite, and apatite.

GM034: Medium green, fine to medium-grained, well foliated rock. Same as GM033 except hornblende comprises (65%) and the plagioclase is An58 (25%). Epidote is less than 1%.

GM055\*: Dark green, fine-grained, fragmental appearing rock. Minerals comprising the sample include nematoblastic hornblende to 1mm (60%), also in relict rock fragments to 1.5cm, albite twinned and untwinned An24 (35%). Epidote and

clinozoisite occur as irregular grains to 0.2mm (2%). Minor biotite and sericite are also present.

GM056: Same as GM033 except 70% hornblende and 25% untwinned and albite twinned An58. Epidote is less than 1%.

GM057: Same as GM034 except 45% hornblende, 35% untwinned An21, 20% epidote, and 4% biotite.

GM068: Medium gray, fine-grained, moderately foliated rock. The sample is composed of nematoblastic hornblende to 2mm (30%), 50% granoblastic An17, 5% epidote/clinozoisite, and 5% microcline (tartan twinned). Minor minerals include quartz and sericite.

GM070\*: Dark green, porphyroblastic, medium-grained rock. The sample is composed of 5mm idioblastic hornblende (55%) which is moderately foliated and lineated. The plagioclase comprises 35% as An30, with 5% associated epidote. No relict textures.

\* not analyzed

## APPENDIX C

## GEOCHEMICAL ANALYSES AND CIPW NORMS

## RHYDLITES (INCLUDING VOLCANICLASTICS)

| ELEMENT                          | GM002 | GM023* | GM027 | GM065* | GM067 |
|----------------------------------|-------|--------|-------|--------|-------|
| SiO <sub>2</sub>                 | 64.88 | 75.43  | 76.52 | 69.58  | 72.44 |
| TiO <sub>2</sub>                 | 0.23  | 0.18   | 0.21  | 0.31   | 0.29  |
| Al <sub>2</sub> O <sub>3</sub>   | 19.11 | 12.58  | 12.51 | 15.64  | 14.29 |
| Fe <sub>2</sub> O <sub>3</sub> T | 2.10  | 2.83   | 1.46  | 1.84   | 2.64  |
| MgO                              | 0.47  | 0.45   | 0.53  | 0.60   | 0.60  |
| CaO                              | 0.48  | 2.41   | 1.41  | 1.30   | 1.69  |
| Na <sub>2</sub> O                | 4.01  | 4.55   | 3.93  | 2.66   | 4.44  |
| K <sub>2</sub> O                 | 7.48  | 0.74   | 2.26  | 7.27   | 2.47  |
| MnO                              | 0.04  | 0.05   | 0.03  | 0.41   | 0.08  |
| P <sub>2</sub> O <sub>5</sub>    | 0.01  | 0.01   | 0.01  | 0.03   | 0.03  |
| L.O.I.                           | 1.04  | 0.85   | 0.62  | 0.52   | 0.41  |
| Total                            | 99.85 | 100.08 | 99.49 | 100.16 | 99.38 |
| Rb                               | 130   | 14     | 40    | 117    | 59    |
| Sr                               | 123   | 217    | 171   | 186    | 187   |
| Cs                               | --    | --     | --    | 1.3    | 0.9   |
| Ba                               | 1756  | 395    | 1175  | 1753   | 1007  |
| Y                                | 55    | 40     | 46    | 41     | 33    |
| Zr                               | 279   | 209    | 196   | 265    | 186   |
| Hf                               | 6.6   | 5.4    | 4.5   | 6.5    | 4.8   |
| Nb                               | 15    | 12     | 12    | 14     | 11    |
| Ta                               | 0.8   | 0.5    | 0.8   | 1.0    | 1.0   |
| Sc                               | 9.1   | 10     | 8.3   | 8.5    | 7.6   |
| Cr                               | --    | --     | --    | --     | --    |
| Ni                               | 4.2   | 1.2    | 4.5   | 4.7    | 4.3   |
| Co                               | 1.9   | 1.5    | 1.4   | 1.1    | 2.8   |
| U                                | 3.5   | 2.5    | 3.1   | 3.7    | 3.9   |
| Th                               | 10    | 7.8    | 6.3   | 11     | 8.2   |
| La                               | 48    | 73     | 49    | 54     | 35    |
| Ce                               | 93    | 130    | 91    | 118    | 80    |
| Sm                               | 8.9   | 8.5    | 8.1   | 7.1    | 5.6   |
| Eu                               | 2.4   | 1.2    | 1.6   | 1.0    | 1.0   |
| Tb                               | 1.8   | 1.0    | 1.1   | 1.2    | 0.9   |
| Yb                               | 5.2   | 2.8    | 3.5   | 4.5    | 3.2   |
| Lu                               | 0.9   | 0.5    | 0.6   | 0.7    | 0.5   |

Explanation on last page

## RHYODACITES(?) (INCLUDING VOLCANICLASTICS)

| ELEMENT                          | GM017 | GM018* | GM032 | GM075 |
|----------------------------------|-------|--------|-------|-------|
| SiO <sub>2</sub>                 | 65.79 | 69.50  | 75.57 | 69.01 |
| TiO <sub>2</sub>                 | 0.52  | 0.41   | 0.34  | 0.38  |
| Al <sub>2</sub> O <sub>3</sub>   | 17.33 | 14.29  | 12.44 | 15.26 |
| Fe <sub>2</sub> O <sub>3</sub> T | 3.61  | 3.63   | 2.42  | 3.94  |
| MgO                              | 1.03  | 0.95   | 0.63  | 1.09  |
| CaO                              | 1.83  | 4.08   | 1.22  | 1.04  |
| Na <sub>2</sub> O                | 3.24  | 1.19   | 4.37  | 3.65  |
| K <sub>2</sub> O                 | 4.82  | 4.18   | 2.14  | 4.40  |
| MnO                              | 0.08  | 0.07   | 0.07  | 0.07  |
| P <sub>2</sub> O <sub>5</sub>    | 0.11  | 0.12   | 0.04  | 0.06  |
| L.D.I.                           | 1.52  | 1.26   | 0.27  | 0.40  |
| Total                            | 99.88 | 99.67  | 99.51 | 99.30 |
| Rb                               | 109   | 91     | 24    | 75    |
| Sr                               | 231   | 451    | 134   | 178   |
| Cs                               | 0.7   | --     | --    | --    |
| Ba                               | 1410  | 986    | 1532  | 1786  |
| Y                                | 43    | 43     | 39    | 30    |
| Zr                               | 224   | 185    | 140   | 172   |
| Hf                               | 5.6   | --     | 3.6   | 3.9   |
| Nb                               | 12    | 10     | 8.4   | 10    |
| Ta                               | 0.7   | --     | 0.5   | 0.7   |
| Sc                               | 13    | --     | 9.3   | 7.9   |
| Cr                               | --    | --     | --    | --    |
| Ni                               | 3.4   | 2.5    | 1.9   | 3.6   |
| Co                               | 4.7   | --     | 0.8   | 1.1   |
| U                                | 3.7   | 3.5    | 2.3   | 2.8   |
| Th                               | 7.6   | 6.0    | 4.4   | 6.6   |
| La                               | 39    | 34     | 36    | 33    |
| Ce                               | 70    | --     | 69    | 67    |
| Sm                               | 6.6   | 7.5    | 6.5   | 6.6   |
| Eu                               | 2.2   | 2.3    | 2.5   | 1.1   |
| Tb                               | 1.0   | 1.2    | 0.9   | 0.8   |
| Yb                               | 3.8   | 2.5    | 2.5   | 2.6   |
| Lu                               | 0.6   | 0.5    | 0.4   | 0.5   |

## DACITES (INCLUDING VOLCANICLASTICS)

| ELEMENTS                         | AF     | GM    | GM    | GM    | F     | F      |
|----------------------------------|--------|-------|-------|-------|-------|--------|
|                                  | GM019  | GM036 | GM037 | GM038 | GM042 | GM044* |
| SiO <sub>2</sub>                 | 71.77  | 77.20 | 64.65 | 64.66 | 64.80 | 60.48  |
| TiO <sub>2</sub>                 | 0.51   | 0.25  | 0.65  | 0.61  | 0.56  | 0.73   |
| Al <sub>2</sub> O <sub>3</sub>   | 12.72  | 10.86 | 17.20 | 15.97 | 16.83 | 16.19  |
| Fe <sub>2</sub> O <sub>3</sub> T | 3.30   | 2.42  | 4.92  | 5.80  | 4.38  | 7.11   |
| MgO                              | 0.95   | 1.06  | 1.36  | 2.21  | 1.47  | 2.98   |
| CaO                              | 1.94   | 1.30  | 2.01  | 2.56  | 2.27  | 4.17   |
| Na <sub>2</sub> O                | 5.52   | 2.49  | 4.91  | 4.84  | 6.33  | 2.96   |
| K <sub>2</sub> O                 | 1.45   | 3.33  | 3.24  | 2.49  | 2.22  | 3.56   |
| MnO                              | 0.08   | 0.08  | 0.13  | 0.14  | 0.08  | 0.14   |
| P <sub>2</sub> O <sub>5</sub>    | 0.09   | 0.06  | 0.13  | 0.22  | 0.17  | 0.25   |
| L.O.I.                           | 1.68   | 0.20  | 0.19  | 0.44  | 0.48  | 0.88   |
| Total                            | 100.01 | 99.25 | 99.39 | 99.94 | 99.59 | 99.45  |
| Rb                               | 26     | 89    | 75    | 36    | 53    | 71     |
| Sr                               | 176    | 132   | 305   | 366   | 275   | 644    |
| Cs                               | 0.4    | 0.8   | --    | 0.7   | 0.7   | 1.9    |
| Ba                               | 526    | 849   | 1266  | 1055  | 708   | 1940   |
| Y                                | 26     | 27    | 43    | 32    | 28    | 36     |
| Zr                               | 142    | 186   | 195   | 131   | 157   | 116    |
| Hf                               | 3.0    | 4.6   | 5.3   | 2.1   | 3.4   | 3.2    |
| Nb                               | 11     | 11    | 12    | 8.5   | 9.0   | 6.7    |
| Ta                               | 0.4    | 0.8   | 0.9   | 0.5   | 0.8   | 0.5    |
| Sc                               | 10     | 7.2   | 14    | 15    | 13    | 19     |
| Cr                               | --     | --    | --    | --    | --    | --     |
| Ni                               | 1.3    | 4.4   | 1.1   | 2.5   | 6.6   | 9.2    |
| Co                               | 3.1    | 2.2   | 3.2   | 11    | 2.9   | 8.0    |
| U                                | 2.0    | 2.6   | 3.3   | 2.3   | 2.5   | 2.5    |
| Th                               | 4.9    | 7.5   | 8.5   | 6.1   | 6.8   | 4.2    |
| La                               | 18     | 38    | 37    | 36    | 18    | 31     |
| Ce                               | 27     | 62    | 66    | 60    | 32    | 59     |
| Sm                               | 3.2    | 4.2   | 6.7   | 5.7   | 4.0   | 6.2    |
| Eu                               | 0.9    | 0.8   | 2.7   | 1.9   | 1.3   | 1.8    |
| Tb                               | 0.5    | 0.7   | 1.1   | 0.7   | 0.7   | 1.0    |
| Yb                               | 2.0    | 2.1   | 2.3   | 1.8   | 2.0   | 2.8    |
| Lu                               | 0.3    | 0.3   | 0.3   | 0.3   | 0.3   | 0.4    |



## DACITES (CONTINUED)

| ELEMENTS                         | $\varphi$ | <i>GM</i> | <i>GM</i> | <i>GM</i> | <i>GM</i> | <i>GM</i> |
|----------------------------------|-----------|-----------|-----------|-----------|-----------|-----------|
|                                  | GM050     | GM058     | GM063     | GM072     | GM073     | GM076     |
| SiO <sub>2</sub>                 | 66.93     | 61.85     | 65.25     | 66.39     | 66.57     | 65.15     |
| TiO <sub>2</sub>                 | 0.81      | 0.63      | 0.68      | 0.46      | 0.45      | 0.61      |
| Al <sub>2</sub> O <sub>3</sub>   | 14.56     | 16.79     | 15.63     | 15.59     | 15.45     | 15.69     |
| Fe <sub>2</sub> O <sub>3</sub> T | 5.76      | 6.11      | 6.25      | 5.14      | 4.92      | 3.94      |
| MgO                              | 1.11      | 1.81      | 1.66      | 1.35      | 1.29      | 2.58      |
| CaO                              | 2.69      | 4.18      | 2.07      | 2.56      | 1.85      | 2.17      |
| Na <sub>2</sub> O                | 3.60      | 5.51      | 4.15      | 4.12      | 4.00      | 4.41      |
| K <sub>2</sub> O                 | 3.12      | 2.13      | 3.23      | 3.11      | 4.09      | 2.67      |
| MnO                              | 0.21      | 0.18      | 0.12      | 0.13      | 0.16      | 0.14      |
| P <sub>2</sub> O <sub>5</sub>    | 0.22      | 0.26      | 0.25      | 0.18      | 0.17      | 0.22      |
| L.O.I.                           | 0.71      | 0.49      | 0.10      | 0.18      | 0.11      | 0.44      |
| Total                            | 99.72     | 99.94     | 99.39     | 99.21     | 99.06     | 99.69     |
| Rb                               | 54        | 177       | 91        | 87        | 93        | 37        |
| Sr                               | 367       | 349       | 290       | 357       | 302       | 322       |
| Cs                               | 0.7       | --        | 1.0       | 3.7       | 3.9       | 0.7       |
| Ba                               | 1351      | 262       | 997       | 1305      | 1672      | 1035      |
| Y                                | 43        | 30        | 31        | 32        | 28        | 30        |
| Zr                               | 182       | 141       | 147       | 142       | 139       | 136       |
| Hf                               | 2.9       | --        | 3.4       | 3.2       | 3.3       | 3.3       |
| Nb                               | 10        | 8.9       | 8.2       | 10        | 8.3       | 9.1       |
| Ta                               | 1.5       | --        | 0.6       | 0.8       | 0.6       | 0.6       |
| Sc                               | 16        | --        | 14        | 11        | 10        | 7.9       |
| Cr                               | 11        | --        | --        | --        | --        | --        |
| Ni                               | 2.6       | 4.6       | 4.9       | 3.8       | 3.6       | 2.3       |
| Co                               | 3.5       | --        | 8.7       | 6.7       | 5.6       | --        |
| U                                | 2.4       | 3.6       | 3.7       | 3.3       | 2.6       | 1.8       |
| Th                               | 5.4       | 6.0       | 7.9       | 7.6       | 5.6       | --        |
| La                               | 37        | 35        | 32        | 33        | 31        | 33        |
| Ce                               | 66        | --        | 57        | 64        | 69        | 71        |
| Sm                               | 7.4       | 6.7       | 5.7       | 6.4       | 5.8       | 6.5       |
| Eu                               | 1.8       | 1.3       | 1.3       | 1.3       | 1.0       | 1.6       |
| Tb                               | 1.1       | 1.2       | 1.0       | 1.0       | 0.9       | 1.0       |
| Yb                               | 4.0       | 2.5       | 2.8       | 2.4       | 2.0       | 2.5       |
| Lu                               | 0.7       | 0.5       | 0.5       | 0.3       | 0.3       | 0.5       |

## THOLEIITES (INCLUDING VOLCANICLASTICS)

| ELEMENTS                         | GM009  | GM010 <sup>at A</sup> | GM015* | GM016* | GM033  | GM034 |
|----------------------------------|--------|-----------------------|--------|--------|--------|-------|
| SiO <sub>2</sub>                 | 51.88  | 48.90                 | 48.69  | 54.41  | 53.18  | 50.85 |
| TiO <sub>2</sub>                 | 0.84   | 0.70                  | 0.97   | 1.06   | 1.03   | 0.78  |
| Al <sub>2</sub> O <sub>3</sub>   | 15.80  | 18.01                 | 15.89  | 14.97  | 15.82  | 15.80 |
| Fe <sub>2</sub> O <sub>3</sub> T | 10.61  | 8.51                  | 12.75  | 11.31  | 10.99  | 10.73 |
| MgO                              | 3.86   | 7.52                  | 5.94   | 4.33   | 3.82   | 5.69  |
| CaO                              | 11.56  | 6.97                  | 8.77   | 7.26   | 9.40   | 10.91 |
| Na <sub>2</sub> O                | 4.29   | 1.86                  | 3.71   | 4.54   | 4.30   | 3.71  |
| K <sub>2</sub> O                 | 0.13   | 3.46                  | 0.35   | 0.52   | 0.83   | 0.60  |
| MnO                              | 0.39   | 0.25                  | 0.34   | 0.24   | 0.19   | 0.20  |
| P <sub>2</sub> O <sub>5</sub>    | 0.23   | 0.18                  | 0.25   | 0.28   | 0.26   | 0.21  |
| L.D.I.                           | 1.16   | 2.98                  | 2.11   | 1.30   | 0.42   | 0.41  |
| Total                            | 100.75 | 99.34                 | 99.77  | 100.22 | 100.24 | 99.89 |

|    |     |      |     |     |     |     |
|----|-----|------|-----|-----|-----|-----|
| Rb | 1.1 | 79   | 4.2 | --  | 10  | 8.0 |
| Sr | 524 | 242  | 342 | --  | 511 | 562 |
| Cs | --  | --   | --  | --  | --  | --  |
| Ba | --  | 2042 | 230 | 357 | 661 | 272 |

|    |     |     |     |    |     |     |
|----|-----|-----|-----|----|-----|-----|
| Y  | 20  | 18  | 23  | -- | 25  | 19  |
| Zr | 30  | 28  | 37  | -- | 57  | 30  |
| Hf | --  | --  | 2.0 | -- | 1.9 | --  |
| Nb | 2.6 | 2.5 | 2.8 | -- | 4.0 | 4.1 |
| Ta | --  | --  | --  | -- | --  | --  |

|    |    |     |    |    |    |     |
|----|----|-----|----|----|----|-----|
| Sc | 37 | 44  | 44 | 40 | 53 | 44  |
| Cr | 57 | 147 | 59 | 17 | 69 | 119 |
| Ni | 24 | 23  | 14 | -- | 20 | 27  |
| Co | 30 | 15  | 33 | 31 | 36 | 37  |

|    |     |     |     |     |     |     |
|----|-----|-----|-----|-----|-----|-----|
| U  | --  | 0.4 | 0.8 | 0.9 | 1.2 | 0.6 |
| Th | 1.1 | 0.9 | 1.3 | 1.9 | 1.9 | 1.3 |

|    |     |     |     |     |     |     |
|----|-----|-----|-----|-----|-----|-----|
| La | 10  | 11  | 13  | 11  | 19  | 10  |
| Ce | 24  | 25  | 24  | 11  | 38  | 24  |
| Sm | 3.2 | 2.5 | 3.4 | 3.8 | 4.5 | 3.1 |
| Eu | 0.6 | 1.4 | 1.0 | 0.8 | 1.9 | 1.2 |
| Tb | 0.4 | 0.4 | 0.7 | 0.7 | 0.6 | 0.4 |
| Yb | 1.6 | 1.4 | 1.2 | 1.9 | 1.4 | 1.6 |
| Lu | 0.2 | 0.2 | 0.2 | 0.3 | 0.2 | 0.3 |

|            |     |     |     |     |     |      |
|------------|-----|-----|-----|-----|-----|------|
| $L_N/Sm_N$ | 1.7 | 2.4 | 2.1 | 1.6 | 2.3 | 1.77 |
|------------|-----|-----|-----|-----|-----|------|

|        |   |   |   |     |     |     |
|--------|---|---|---|-----|-----|-----|
| $Yb_N$ | 8 | 7 | 6 | 9.5 | 9.5 | 6.5 |
|--------|---|---|---|-----|-----|-----|

|  |      |      |       |      |      |      |
|--|------|------|-------|------|------|------|
| { Mg No.                                       | 43   | 65   | 49    | 44   | 42   | 52   |
| { FeO (=0.865Fe <sub>2</sub> O <sub>3</sub> T) | 9.18 | 7.36 | 11.03 | 9.78 | 9.51 | 9.28 |

|  |      |      |      |      |      |      |
|--|------|------|------|------|------|------|
| { Mg No.                                     | 50   | 70   | 56   | 51   | 49   | 59   |
| { FeO = 0.65Fe <sub>2</sub> O <sub>3</sub> T | 6.90 | 5.53 | 8.29 | 7.35 | 7.14 | 6.98 |
| { FeO molar x 100                            | 9.6  | 7.9  | 11.5 | 10.2 | 9.9  | 9.7  |

|                 |      |      |      |      |      |      |
|-----------------|------|------|------|------|------|------|
| MgO molar x 100 | 9.57 | 18.6 | 14.7 | 10.7 | 9.47 | 14.1 |
|-----------------|------|------|------|------|------|------|

$$Mg\ No. = \frac{MgO}{MgO + 0.49Fe_2O_3}$$

## THOLEIITES (CONTINUED)

| ELEMENTS  | GM046      | <sup>A</sup> GM047 | GM051*      | GM053      | GM056       | GM057      |
|---|------------|--------------------|-------------|------------|-------------|------------|
| SiO <sub>2</sub>  | 50.98      | 49.88              | 50.72       | 50.79      | 47.60       | 50.24      |
| TiO <sub>2</sub>  | 0.74       | 0.76               | 1.03        | 0.80       | 0.88        | 0.72       |
| Al <sub>2</sub> O <sub>3</sub>                                      | 15.99      | 17.77              | 16.34       | 15.79      | 15.46       | 17.70      |
| Fe <sub>2</sub> O <sub>3</sub> T                                    | 9.78       | 10.90              | 12.28       | 10.97      | 12.16       | 9.33       |
| MgO   | 6.28       | 6.34               | 4.21        | 3.98       | 9.76        | 5.79       |
| CaO   | 10.10      | 7.26               | 8.29        | 11.58      | 11.82       | 11.60      |
| Na <sub>2</sub> O   | 3.44       | 4.58               | 4.10        | 3.78       | 2.01        | 3.33       |
| K <sub>2</sub> O  | 0.86       | 0.60               | 1.30        | 0.09       | 0.18        | 0.66       |
| MnO   | 0.30       | 0.30               | 0.29        | 0.42       | 0.26        | 0.26       |
| P <sub>2</sub> O <sub>5</sub>                                       | 0.11       | 0.18               | 0.29        | 0.23       | 0.20        | 0.18       |
| L.O.I.  | 1.36       | 0.38               | 0.97        | 1.11       | 0.10        | 0.33       |
| Total   | 99.94      | 98.95              | 99.82       | 99.54      | 100.43      | 100.14     |
| Rb  | 20         | 13                 | 29          | 0.9        | 2.2         | 10         |
| Sr  | 457        | 440                | 601         | 500        | 186         | 654        |
| Cs  | --         | --                 | --          | --         | --          | --         |
| Ba  | 337        | 247                | 741         | 337        | --          | 197        |
| Y   | 13         | 17                 | 22          | 17         | 19          | 17         |
| Zr  | 18         | 81                 | 48          | 29         | 39          | 35         |
| Hf  | --         | --                 | --          | --         | --          | --         |
| Nb  | 2.4        | 3.8                | 4.5         | 2.8        | 3.9         | 3.0        |
| Ta  | --         | 0.2                | --          | --         | --          | 0.5        |
| Sc  | 40         | 40                 | 29          | 37         | 43          | 40         |
| Cr  | 68         | 71                 | 12          | 58         | 105         | 130        |
| Ni  | 27         | 28                 | 7.5         | 19         | 30          | 28         |
| Co  | 25         | 35                 | 25          | 32         | 43          | 35         |
| La/Ta   |            | 42                 |             |            |             | 34         |
| U   | --         | 0.8                | --          | 1.8        | --          | --         |
| Th  | 0.7        | 1.2                | 2.4         | 1.3        | 0.9         | 1.6        |
| La  | 11         | 8.3                | 18          | 13         | 11          | 17         |
| Ce  | 23         | 20                 | 40          | 29         | 25          | 31         |
| Sm  | 2.1        | 3.1                | 4.3         | 3.0        | 3.4         | 3.3        |
| Eu  | 0.6        | 0.5                | 1.1         | 0.4        | 0.5         | 0.6        |
| Tb  | 0.4        | 0.6                | 0.7         | 0.5        | 0.6         | 0.6        |
| Yb  | 1.2        | 1.4                | 2.1         | 1.1        | 1.5         | 1.5        |
| Lu  | 0.2        | 0.2                | 0.4         | 0.2        | 0.2         | 0.2        |
| La/Sm <sub>N</sub>  | 2.9        | 2.7                | 2.3         | 2.4        | 1.8         | 2.8        |
| Yb <sub>N</sub>   | 6          | 7                  | 10.5        | 6.5        | 9.5         | 7.5        |
| { FeO<br>(FeO = 0.865 Fe <sub>2</sub> O <sub>3</sub> T)<br>(mg No.) | 8.46<br>57 | 9.43<br>54         | 10.62<br>41 | 9.49<br>43 | 10.52<br>62 | 8.07<br>56 |
| { FeO = 0.65 Fe <sub>2</sub> O <sub>3</sub> T<br>(mg No.)           | 6.36<br>64 | 7.09<br>61         | 8.32<br>47  | 7.13<br>50 | 7.90<br>69  | 6.07<br>63 |
| { FeO molar x 100   | 8.85       | 9.86               | 11.6        | 9.92       | 11.0        | 8.50       |
| MgO molar x 100   | 15.6       | 15.7               | 10.4        | 9.87       | 24.2        | 14.4       |

n=12  
 $\bar{x} = 26$   
 $\bar{x} = 3.3$   
 $\bar{x} = 0.55$

| ELEMENT                          | THOLEIITE | GRANITIC ROCKS |       |                   |       | DIABASE |
|----------------------------------|-----------|----------------|-------|-------------------|-------|---------|
|                                  | GM068     | I              | GM054 | GM078             | GM079 | I CN-2  |
| SiO <sub>2</sub>                 | 56.62     |                | 71.75 | 63.97             | 72.44 | 50.74   |
| TiO <sub>2</sub>                 | 0.85      |                | 0.33  | 0.49              | 0.30  | 0.65    |
| Al <sub>2</sub> O <sub>3</sub>   | 15.68     |                | 15.79 | 15.17             | 13.87 | 17.50   |
| Fe <sub>2</sub> O <sub>3</sub> T | 7.74      |                | 2.99  | 6.49              | 2.68  | 10.40   |
| MgO                              | 4.33      |                | 3.98  | 1.65              | 0.69  | 5.10    |
| CaO                              | 7.45      |                | 2.05  | 2.57              | 1.70  | 8.77    |
| Na <sub>2</sub> O                | 6.32      |                | 3.68  | 3.45              | 3.57  | 2.52    |
| K <sub>2</sub> O                 | 0.56      |                | 3.59  | 5.29              | 3.53  | 0.97    |
| MnO                              | 0.16      |                | 0.06  | 0.08              | 0.03  | 0.23    |
| P <sub>2</sub> O <sub>5</sub>    | 0.21      |                | 0.07  | 0.20              | 0.05  | 0.22    |
| L.D.I.                           | 0.10      |                | 0.19  | 0.22              | 0.53  | 2.58    |
| Total                            | 100.02    |                | 99.60 | 99.58             | 99.39 | 99.85   |
| Rb                               | 5.5       |                | 62    | 146               | 52    | --      |
| Sr                               | 450       |                | 239   | 387               | 226   | --      |
| Cs                               | --        |                | --    | 1.2               | --    | --      |
| Ba                               | 355       |                | 1141  | 1267              | 1077  | --      |
| Y                                | 21        |                | 29    | 30                | 21    | --      |
| Zr                               | 52        |                | 163   | 73 <sup>120</sup> | 161   | --      |
| Hf                               | --        |                | 5.0   | 1.7               | 4.1   | --      |
| Nb                               | 4.0       |                | 11    | 8.2               | 10    | --      |
| Ta                               | --        |                | 1.1   | 0.6               | 0.8   | --      |
| Sc                               | 35        |                | 7.6   | 14                | 6.6   | --      |
| Cr                               | 9.0       |                | --    | 11                | --    | --      |
| Ni                               | 10        |                | 4.6   | 7.3               | 3.5   | --      |
| Co                               | 21        |                | 2.9   | 31                | 3.0   | --      |
| U                                | --        |                | 2.3   | 5.4               | 3.5   | --      |
| Th                               | 2.7       |                | 9.3   | 5.0               | 9.7   | --      |
| La                               | 13        |                | 21    | 33                | 41    | --      |
| Ce                               | 34        |                | 45    | 52                | 74    | --      |
| Sm                               | 4.1       |                | 4.5   | 4.9               | 5.9   | --      |
| Eu                               | 0.6       |                | 0.8   | 1.2               | 1.0   | --      |
| Tb                               | 0.6       |                | 1.0   | 0.6               | 1.0   | --      |
| Yb                               | 2.4       |                | 3.5   | 1.1               | 3.1   | --      |
| Lu                               | 0.4       |                | 0.5   | 0.1               | 0.5   | --      |

Total iron as Fe<sub>2</sub>O<sub>3</sub>T  
 Major elements in weight percent  
 Trace elements in ppm

-- = no data

\* = volcanoclastic

*Wafmn* 1.75  
*YbN* 12  
*FeO* 6.70  
*mg No* 53

| MINERAL | R     | T     | CIPW NORMS |       |       | RD    | RD    |
|---------|-------|-------|------------|-------|-------|-------|-------|
|         | GM002 | GM009 | GM010      | GM015 | GM016 | GM017 | GM018 |
| Q       | 11    | --    | --         | --    | 2.3   | 24    | 37    |
| C       | 3.6   | --    | --         | --    | --    | 3.8   | 0.7   |
| Or      | 45    | 0.8   | 21         | 2.1   | 3.1   | 29    | 25    |
| Ab      | 34    | 37    | 16         | 32    | 39    | 28    | 10    |
| An      | 2.3   | 24    | 32         | 27    | 19    | 8.5   | 20    |
| Mt      | 0.6   | 3.4   | 3.3        | 3.7   | 3.8   | 3.0   | 2.8   |
| Il      | 0.4   | 1.6   | 1.4        | 1.9   | 2.0   | 1.0   | 0.8   |
| Hm      | 1.4   | --    | --         | --    | --    | --    | --    |
| Ru      | --    | --    | --         | --    | --    | --    | --    |
| Di      | --    | 27    | 2.4        | 14    | 13    | --    | --    |
| Hy      | 1.2   | 1.7   | 13         | 7.1   | 17    | 3.2   | 3.2   |
| Ol      | --    | 4.2   | 10         | 12    | --    | --    | --    |
| Ap      | 0.1   | 0.6   | 0.5        | 0.7   | 0.7   | 0.3   | 0.3   |
| Total   | 99.6  | 100.3 | 99.6       | 100.5 | 99.9  | 100.8 | 99.8  |

| MINERAL | R     | R     | RD    | T     | T     | GM036 |       |
|---------|-------|-------|-------|-------|-------|-------|-------|
|         | GM019 | GM023 | GM027 | GM032 | GM033 |       | GM034 |
| Q       | 30    | 41    | 42    | 39    | 0.2   | --    | 46    |
| C       | --    | --    | 1.0   | 0.8   | --    | --    | 1.0   |
| Or      | 8.7   | 4.4   | 14    | 13    | 5.0   | 3.6   | 20    |
| Ab      | 47    | 39    | 33    | 37    | 37    | 32    | 21    |
| An      | 5.8   | 12    | 7.0   | 5.8   | 22    | 25    | 6.1   |
| Mt      | 3.0   | 2.5   | --    | 1.3   | 3.7   | 3.3   | 1.5   |
| Ru      | --    | --    | 0.2   | --    | --    | --    | --    |
| Di      | 2.6   | 0.1   | --    | --    | 20    | 30    | --    |
| Hy      | 1.2   | 1.4   | 1.3   | 1.6   | 10    | 1.7   | 2.7   |
| Ol      | --    | --    | --    | --    | --    | 9.2   | --    |
| Ap      | 0.2   | 0.02  | 0.03  | 0.1   | 0.7   | 0.5   | 0.2   |
| Total   | 99.5  | 100.7 | 100.1 | 100.2 | 100.6 | 99.8  | 99.7  |

## CIPW NORMS

| MINERAL |       |       |       |       | T     | T     | GM050 |
|---------|-------|-------|-------|-------|-------|-------|-------|
|         | GM037 | GM038 | GM042 | GM044 | GM046 | GM047 |       |
| Ne      | --    | --    | --    | --    | --    | 1.1   | --    |
| Q       | 17    | 17    | 13    | 14    | --    | --    | 26    |
| C       | 2.3   | 1.2   | 0.3   | 0.5   | --    | --    | 0.9   |
| Or      | 19    | 15    | 13    | 21    | 5.1   | 3.6   | 19    |
| Ab      | 42    | 41    | 54    | 26    | 30    | 37    | 31    |
| An      | 9.2   | 11    | 10    | 19    | 26    | 27    | 12    |
| Mt      | 3.1   | 3.1   | 4.6   | 3.0   | 3.3   | 3.3   | 3.3   |
| Il      | 0.5   | 1.3   | 1.1   | 1.4   | 1.4   | 1.5   | 1.6   |
| Hm      | 0.7   | --    | --    | --    | --    | --    | --    |
| Ru      | --    | --    | --    | --    | --    | --    | --    |
| Di      | --    | --    | --    | --    | 20    | 7.3   | --    |
| Hy      | 5.4   | 9.2   | 5.1   | 14    | 6.2   | --    | 5.7   |
| Ol      | --    | --    | --    | --    | 8.4   | 19    | --    |
| Ap      | 0.3   | 0.6   | 0.4   | 0.6   | 0.3   | 0.5   | 0.6   |
| Total   | 99.6  | 99.3  | 99.9  | 99.8  | 100.7 | 100.3 | 100.2 |

| MINERAL | T     | T     |       |       |       | GM063 | R     |
|---------|-------|-------|-------|-------|-------|-------|-------|
|         | GM051 | GM053 | GM054 | GM056 | GM057 |       | GM065 |
| Q       | --    | --    | 32    | --    | --    | 21    | 23    |
| C       | --    | --    | 0.7   | --    | --    | 2.2   | 1.1   |
| Or      | 7.8   | 0.5   | 21    | 1.1   | 4.0   | 19    | 43    |
| Ab      | 35    | 33    | 31    | 17    | 28    | 36    | 23    |
| An      | 23    | 26    | 9.8   | 33    | 32    | 8.7   | 6.2   |
| Mt      | 3.7   | 3.4   | 2.7   | 3.5   | 3.2   | 3.2   | 0.4   |
| Il      | 2.0   | 1.6   | 0.6   | 1.7   | 1.4   | 1.3   | 0.6   |
| Hm      | --    | --    | --    | --    | --    | --    | --    |
| Ru      | --    | --    | --    | --    | --    | --    | --    |
| Di      | 14    | 26    | --    | 20    | 21    | --    | --    |
| Hy      | 1.0   | 7.6   | 1.9   | 11    | 1.1   | 8.2   | 1.5   |
| Ol      | 13    | 1.5   | --    | 13    | 9.2   | --    | --    |
| Ap      | 0.7   | 0.6   | 0.2   | 0.5   | 0.5   | 0.6   | 0.1   |
| Total   | 100.2 | 99.2  | 99.9  | 100.8 | 100.4 | 100.2 | 100.5 |

| MINERAL | CIPW NORMS |             |       |       |             |       |       |
|---------|------------|-------------|-------|-------|-------------|-------|-------|
|         | R<br>GM067 | Th<br>GM068 | GM072 | GM073 | RD<br>GM075 | GM076 | GM078 |
| Q       | 33         | --          | 22    | 21    | 27          | 20    | 14    |
| C       | 1.3        | --          | 1.2   | 1.4   | 2.8         | 2.1   | --    |
| Or      | 15         | 3.3         | 19    | 25    | 26          | 16    | 32    |
| Ab      | 38         | 54          | 35    | 34    | 31          | 38    | 30    |
| An      | 8.3        | 13          | 12    | 8.2   | 4.8         | 9.4   | 10    |
| Mt      | 1.9        | 3.4         | 2.9   | 2.9   | 2.6         | 3.1   | 2.9   |
| Il      | 0.6        | 1.6         | 0.9   | 0.9   | 0.7         | 1.2   | 1.0   |
| Hm      | 0.5        | --          | --    | --    | --          | --    | --    |
| Ru      | --         | --          | --    | --    | --          | --    | --    |
| Di      | --         | 19          | --    | --    | --          | --    | 1.0   |
| Hy      | 1.5        | 0.9         | 6.6   | 6.1   | 4.1         | 9.8   | 8.8   |
| Ol      | --         | 4.9         | --    | --    | --          | --    | --    |
| Ap      | 0.1        | 0.5         | 0.5   | 0.4   | 0.2         | 0.6   | 0.5   |

|       | GM079 |
|-------|-------|
| Q     | 34    |
| C     | 1.2   |
| Or    | 21    |
| Ab    | 31    |
| An    | 8.2   |
| Mt    | 1.8   |
| Il    | 0.6   |
| Hm    | 0.6   |
| Ru    | --    |
| Di    | --    |
| Hy    | 1.7   |
| Ol    | --    |
| Ap    | 0.1   |
| Total | 100.2 |

| SYMBOLS          |
|------------------|
| Q = Quartz       |
| C = Corundum     |
| Or = Orthoclase  |
| Ab = Albite      |
| An = Anorthite   |
| Mt = Magnetite   |
| Il = Ilmenite    |
| Hm = Hematite    |
| Ru = Rutile      |
| Di = Diopside    |
| Hy = Hypersthene |
| Ol = Olivine     |
| Ap = Apatite     |
| Ne = Nepheline   |

## APPENDIX D

## SAMPLE COLLECTION AND PREPARATION

More than 100 samples were collected from the Fletcher Park and Green Mountain sections. The samples were collected in triplicate for use as hand sample, thin section, and geochemical analysis. Samples were collected to represent the variety of compositional and textural rock types, as well as their relative abundances. In the laboratory, 49 samples were selected for thin section study, and 40 samples for geochemical analysis. The sample locations are shown in Figures 31 and 32.

The geochemical samples were broken down to less than 4cm pieces by hammer. Jaw crushers were then used to crush the 4cm pieces down to chips less than 5mm. The fine powder and altered or weathered fragments were discarded from the above crushing steps. The 5mm fragments were next processed through a high speed rotary grinder which crushed the sample to less than 2mm. This size fraction was split for further processing for x-ray fluorescence and neutron activation samples. For neutron activation study, the 2mm fraction was ground in a mechanical agate mortar and pestle for 5 minutes, and approximately 0.5 grams of the powder was placed in a small polyurethane vial. The vials containing the samples were then sent to the Sandia National Laboratory nuclear reactor for irradiation. For x-ray fluorescence, the 2mm fraction was ground for 5 minutes in a Retch Microjet-5 high speed grinder, producing a 10 $\mu$  range



powder. The powder was used to make two different types of target samples for analysis. Fusion discs were made for major element analysis. This procedure involves the melting of a mixture of 0.5 grams of powdered sample, 2.68 grams of Spectroflux 105, and a few beads of ammonium nitrate (oxidizing agent to allow analysis of sodium) in a platinum crucible. When completely molten, the sample mixture was pressed into flat glass discs and allowed to cool. Pressed powder pellets were made for trace element analysis. In this procedure, a mixture of 4 grams of sample powder and 1 gram of microcrystalline cellulose was pressed into pellets with a microcrystalline cellulose backing. The pellets were compressed using a hydraulic press at 20 tons of pressure.

GM-019 •  
• GM-023  
GM-022 •  
GM-025 • • GM-024  
• GM-026  
GM-029 • GM-032  
• GM-027

• GM-019  
• GM-021  
GM-020  
• GM-018  
• GM-017  
• GM-014, 015, 016  
GM-011, 012, 013

GM-010 •  
• GM-009  
• GM-008  
• GM-052  
• GM-051  
• GM-053  
GM-004 • • GM-003  
GM-002 • • GM-001  
GM-005, 006, 007

• GM-050

GM-048 • GM-049  
• GM-046, 047

• GM-045

• GM-044  
• GM-043  
• GM-042

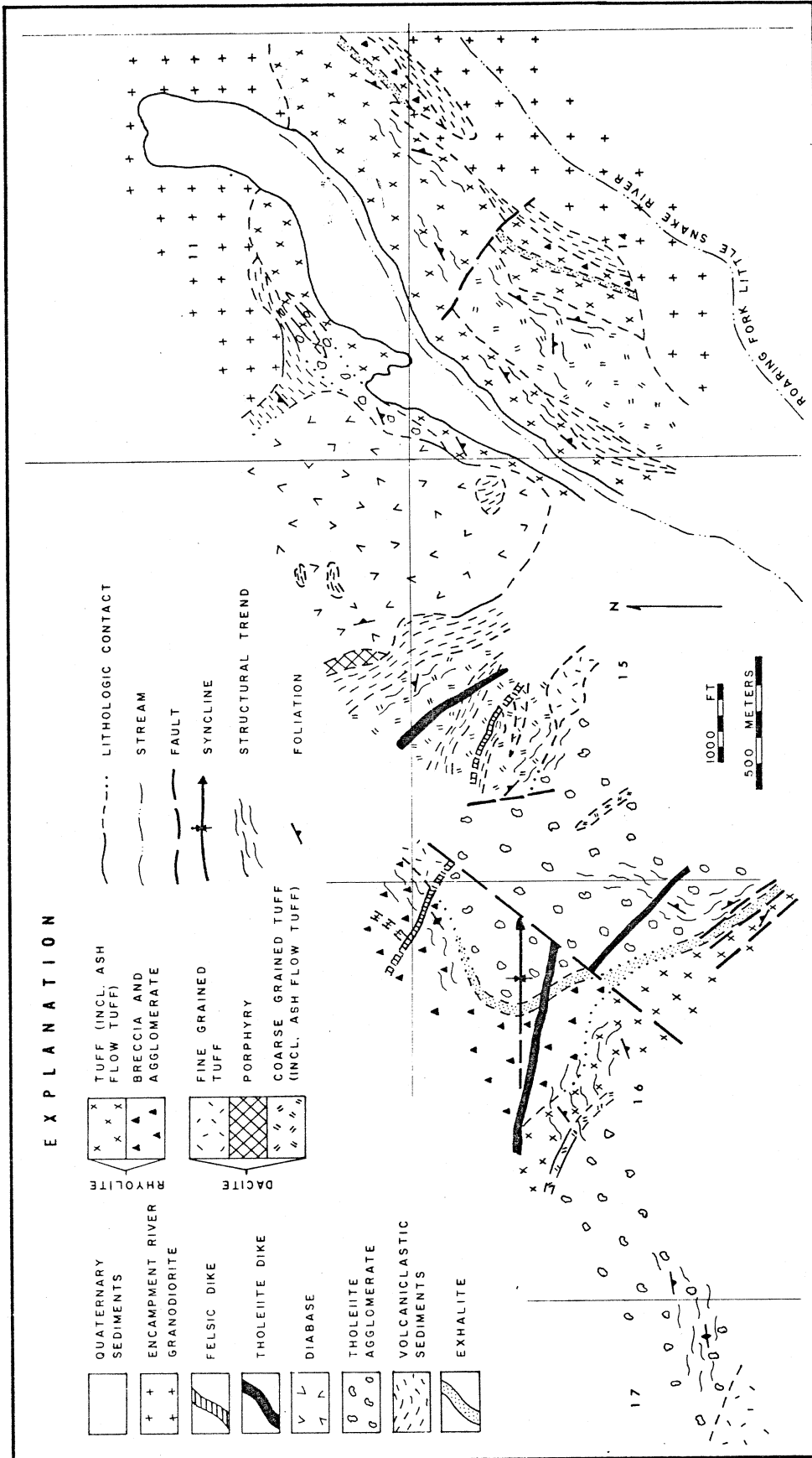


Figure 31. Sample locations of the Fletcher Park section (overlay).

• GM-078

• GM-057  
• GM-058

• GM-059

• GM-060  
• GM-061  
• GM-063  
• GM-063  
• GM-032X  
• GM-033  
• GM-034  
• GM-035  
• GM-036

• GM-065

• GM-064

• GM-066

• GM-073

• GM-068  
• GM-069

• GM-072

• GM-067

• GM-077  
• GM-076  
• GM-038

• GM-037

• GM-075

• GM-056  
• GM-074  
• GM-055

• GM-071  
• GM-070

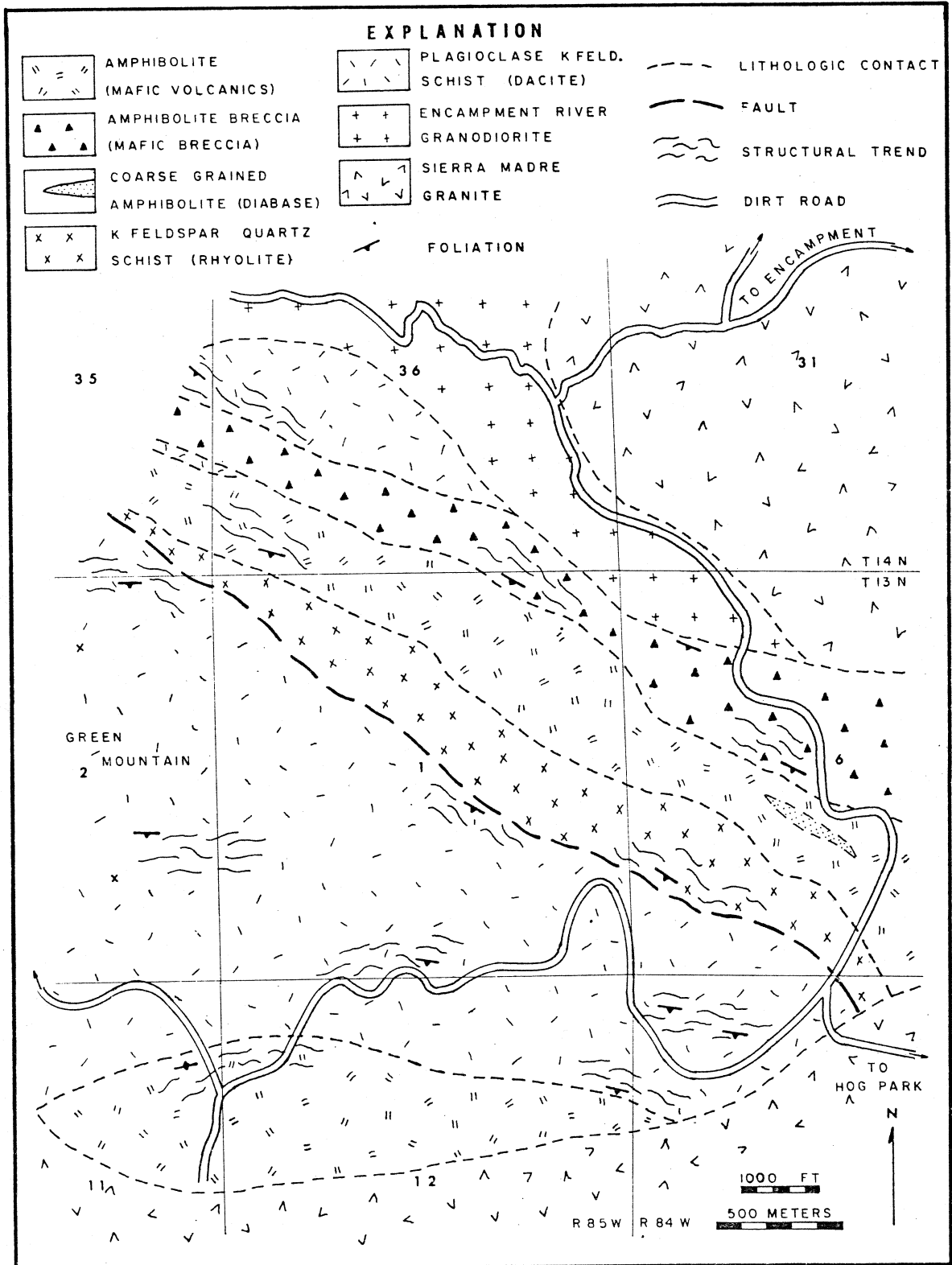


Figure 32. Sample locations of the Green Mountain section (overlay).

## APPENDIX E

## INSTRUMENTAL NEUTRON ACTIVATION ANALYSIS

Approximately 0.5 grams of powder from each of the collected samples were irradiated at the Sandia National Laboratory reactor in Albuquerque, New Mexico. The irradiated samples were analyzed for Na and seventeen trace elements on a Nuclear Data 6600 4,096 channel gamma-ray spectrometer with a high resolution Li-drifted germanium detector. The methods used are described by Gordon et al (1968). Table 8 summarizes the instrumental parameters.

U.S.G.S. rock standards AGV-1 and G-2 and two intralab standards LOSP and BLCR were used to calculate element concentrations for the unknown rock samples (Table 9). The ND 6600 system is connected to a computing system which calculates the unknown concentrations by comparing the peak area of an element in the unknown sample with the same peak in the standards. The computer also corrects for errors associated with dead time, radioactive decay between the sample and standard counting times, and the weight difference between the sample and the standard. Depending on the half-life of the radionuclide and interfering elements, the cooling period prior to counting was 4, 7, and 28 days after irradiation, and counting time was 5000, 8000, and 12,000 seconds. Analytical errors for this method are estimated +/- 5% for major elements and +/- 10% for trace elements.

TABLE 8

## NEUTRON ACTIVATION INSTRUMENTAL PARAMETERS

| RADIONUCLIDE | PEAK<br>ENERGY(KeV) | COOLING<br>TIME(DAYS) | COUNTING<br>TIME(SECS) |
|--------------|---------------------|-----------------------|------------------------|
| Sm-153       | 103.2               | 4                     | 5000                   |
| Np-239 (U)   | 277.6               | 4                     | 5000                   |
| La-140       | 487.0               | 4                     | 5000                   |
| Na-24        | 1368.4              | 4                     | 5000                   |
| Lu-177       | 208.8               | 7                     | 8000                   |
| Np-239 (U)   | 277.6               | 7                     | 8000                   |
| Yb-175       | 282.6               | 7                     | 8000                   |
| Tb-160       | 298.6               | 7                     | 8000                   |
| Yb-175       | 396.1               | 7                     | 8000                   |
| Eu-154       | 121.8               | 28                    | 12000                  |
| Ce-140       | 145.5               | 28                    | 12000                  |
| Yb-169       | 177.2               | 28                    | 12000                  |
| Eu-152       | 216.0               | 28                    | 12000                  |
| Ta-182       | 222.1               | 28                    | 12000                  |
| Tb-160       | 298.6               | 28                    | 12000                  |
| Pa-233 (Th)  | 311.8               | 28                    | 12000                  |
| Cr-51        | 320.1               | 28                    | 12000                  |
| Hf-181       | 482.2               | 28                    | 12000                  |
| Ba-131       | 496.3               | 28                    | 12000                  |
| Eu-152       | 779.1               | 28                    | 12000                  |
| Cs-134       | 795.8               | 28                    | 12000                  |
| Tb-160       | 879.3               | 28                    | 12000                  |
| Sc-46        | 889.3               | 28                    | 12000                  |
| Tb-160       | 1178.1              | 28                    | 12000                  |
| Co-60        | 1332.5              | 28                    | 12000                  |
| Eu-152       | 1408.1              | 28                    | 12000                  |

TABLE 9

ELEMENT CONCENTRATIONS FOR INTRALAB ROCK STANDARDS  
USED IN NEUTRON ACTIVATION ANALYSIS

| ELEMENT                          | LOSP  | BLCR  |
|----------------------------------|-------|-------|
| SiO <sub>2</sub>                 | 75.90 | 53.50 |
| TiO <sub>2</sub>                 | 0.20  | 0.89  |
| Al <sub>2</sub> O <sub>3</sub>   | 12.30 | 18.10 |
| Fe <sub>2</sub> O <sub>3</sub> T | 1.81  | 7.62  |
| MgO                              | 0.07  | 4.85  |
| CaO                              | 0.93  | 8.39  |
| Na <sub>2</sub> O                | 3.49  | 3.57  |
| K <sub>2</sub> O                 | 4.83  | 1.32  |
| Sc                               | 5.7   | 32    |
| Cr                               | 2.7   | 130   |
| Co                               | 0.6   | 30    |
| Cs                               | 2.0   | 2.5   |
| Ba                               | 960   | 370   |
| Hf                               | 11    | 4.3   |
| Ta                               | 1.9   | 0.5   |
| Th                               | 2.4   | 4.0   |
| U                                | 4.2   | 1.5   |
| La                               | 70    | 12    |
| Ce                               | 160   | 28    |
| Sm                               | 17    | 4.0   |
| Eu                               | 2.4   | 1.3   |
| Tb                               | 3.1   | 0.8   |
| Yb                               | 11    | 3.5   |
| Lu                               | 1.8   | 0.6   |

Oxides in weight percent  
Trace elements in ppm



## APPENDIX F

## X-RAY FLUORESCENCE TECHNIQUE

Major and minor elements Si, Fe, Al, Mg, Ca, Na, K, Ti, P, and Mn, and the trace elements Sr, Rb, Ni, Zr, Y, and Nb were analyzed by X-ray Fluorescence techniques. Specific procedures which were followed are described by Norrish and Chappell (1967) and Norrish and Hutton (1969). The general technique of XRF quantitative analysis involves the comparison of the x-ray intensity of a specific element of an unknown with standards of known concentrations using the linear calibration method. Calibration curves were constructed using many standards by plotting concentration versus  $(I K_{\alpha}(\text{unknown})/I K_{\alpha}(\text{FSL})) \times (\mu(\text{FSL})/\mu(\text{unknown}))$  for major elements and concentration versus  $(I K_{\alpha}(\text{unknown})/I K_{\alpha}(\text{FSL})) \times (I RhK_c(\text{FSL})/I RhK_c(\text{unknown}))$  for the trace elements. In the above equations,  $I$  = intensity of the peak,  $\mu$  = mass absorption, and FSL = drift pellet. The major and minor elements were analyzed using lithium borate glass disks, and trace elements were analyzed using pressed powder pellets. Both sample preparation techniques used in this study are described in Appendix D.

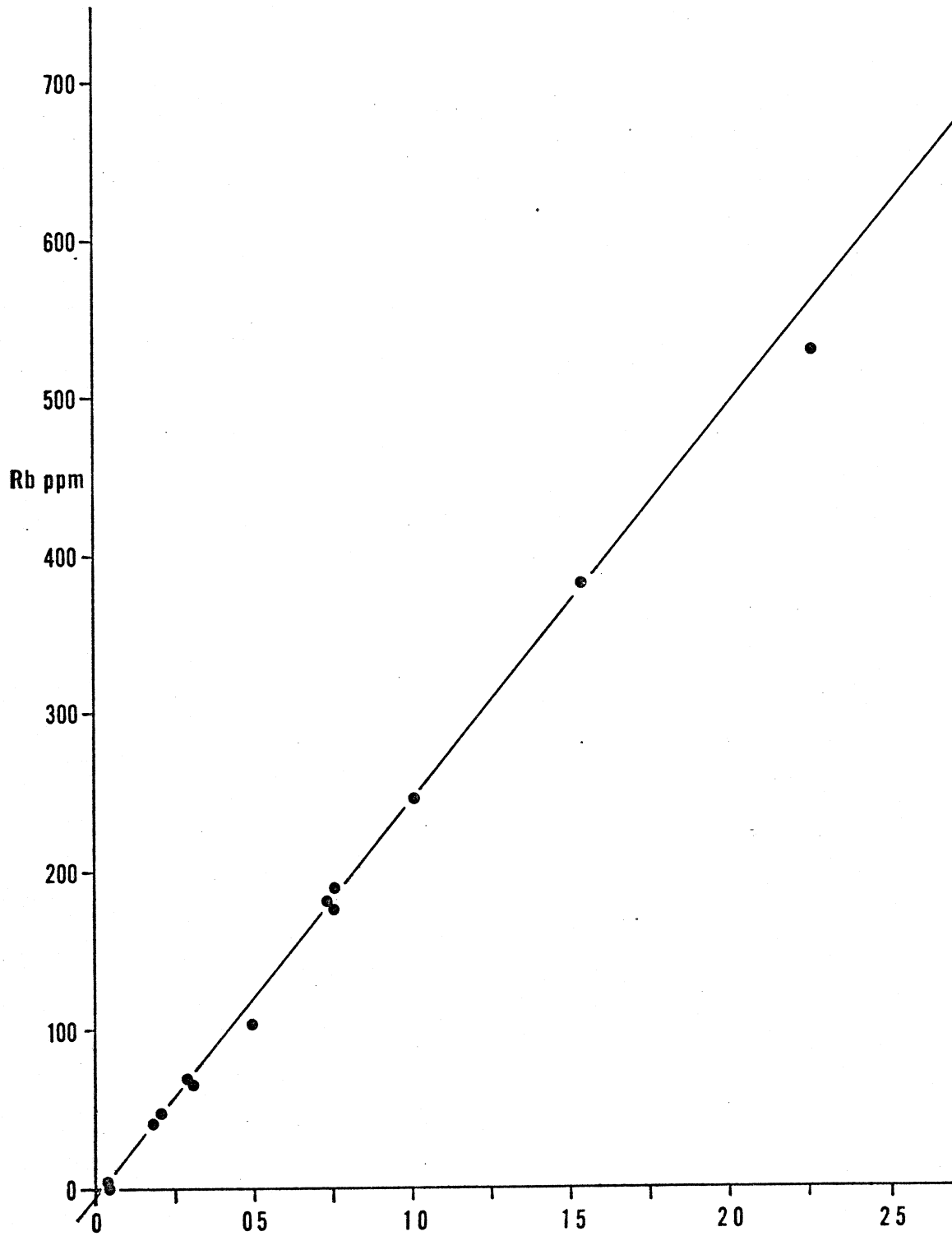
The XRF system used for the analyses was a Rigaku 3064 X-ray Fluorescence Spectrometer equipped with a Rhodium x-ray tube source with an end mounted window. A flow proportional counter (P-10 gas filled) was used for the major elements, and a scintillation counter for the trace

elements. The system is operated by the New Mexico Bureau of Mines and Mineral Resources located on the NMIMT campus in Socorro, New Mexico. Instrumental parameters are summarized in table 10. The standards used for the construction of the calibration curves were USGS standards GSP-1, AGV-1, BHVO, BCR-1, PCC-1, G-2, and QLO-1; NIM (S. Africa) standards NIM-S, NIM-D, and NIM-N; CRPG (France) standards GH and GA; ANRT (France) standards AN-G, BE-N, MA-N; and GSJ (Japan) standards JG-1 and JB-1. The calibration curve displayed in Figure 33 is an example of typical calibration results for the trace elements. Data reduction for the major elements was done by the use of a computer program which received counting results directly from the spectrometer system. Concentrations for the major elements were calculated by a program using the correction coefficient matrix of Norrish and Chappell (1967). Analytical error is <1% for the major elements, <5% for Rb, Sr, and Nb, and <10% for Zr, Y, and Ni.

TABLE 10

| ELEMENT | PEAK       | Kv / Ma | CRYSTAL  | COLLIMATOR |
|---------|------------|---------|----------|------------|
| Si      | K $\alpha$ | 45 / 55 | RX4      | FINE       |
| Al      | K $\alpha$ | "       | PET      | COARSE     |
| Fe      | K $\alpha$ | "       | LiF(200) | FINE       |
| Mg      | K $\alpha$ | "       | TAP      | COARSE     |
| Ca      | K $\alpha$ | "       | LiF(200) | COARSE     |
| Na      | K $\alpha$ | "       | TAP      | FINE       |
| K       | K $\alpha$ | "       | LiF(200) | COARSE     |
| Ti      | K $\alpha$ | "       | LiF(200) | COARSE     |
| Mn      | K $\alpha$ | "       | LiF(200) | COARSE     |
| P       | K $\alpha$ | "       | LiF(200) | COARSE     |
| Rb      | K $\alpha$ | 40 / 60 | LiF(220) | COARSE     |
| Sr      | K $\alpha$ | "       | LiF(200) | COARSE     |
| Zr      | K $\alpha$ | "       | LiF(200) | COARSE     |
| Y       | K $\alpha$ | "       | LiF(200) | COARSE     |
| Ni      | K $\alpha$ | "       | LiF(200) | COARSE     |
| Nb      | K $\alpha$ | "       | LiF(200) | FINE       |

Figure 33. Sample calibration curve for trace element analysis by X-ray fluorescence.



$$\frac{I_{RbK_{\alpha}}(\text{unknown})}{I_{RbK_{\alpha}}(\text{FSL})} \times \frac{I_{RhK_C}(\text{FSL})}{I_{RhK_C}(\text{unknown})}$$

## BIBLIOGRAPHY

- Anderson, C.A., and Blacet, P.M., 1972, Precambrian geology of the Northern Bradshaw Mountains, Yavapai County, Arizona: U.S.G.S. Bulletin 1336, 82p.
- Beswick, A.E., and Soucie, G., 1978, A correction procedure for metasomatism in an Archean greenstone belt: *Precambrian Research*, v.6, p. 235-248.
- Boardman, S.J., 1976, Geology of the Precambrian metamorphic rocks of the Salida area, Chaffee County, Colorado: *The Mountain Geologist*, v.13, p.89-100.
- Brothers, R.N., and Searle, E.J., 1970, The geology of Raoul Island, Kermadec Group, Southwest Pacific: *Bull. Volcanologique*, v. 34-2, p. 7-37.
- Brown, G.M., Holland, J.G., Sigurdsson, H., Tomblin, J.F., and Arculus, R.J., 1977, Geochemistry of the Lesser Antilles Volcanic Island Arc: v. 41. p. 785-801.
- Carmichael, I.S., Turner, F.J., and Verhoogen, J., 1974, *Igneous Petrology*: McGraw-Hill, New York, 739 p.
- Condie, K.C., 1976, *Plate Tectonics and Crustal Evolution*, Pergamon Press, Inc., New York, 288 p.
- Condie, K.C., 1980, The Tijeras greenstone: Evidence for depleted upper mantle beneath New Mexico during the Proterozoic: *Journal of Geology*, v. 88, p. 603-609.
- Condie, K.C., 1981, *Archean Greenstone Belts*: Elsevier, Amsterdam, 434 p.
- Condie, K.C., 1982, Early and middle Proterozoic supracrustal successions and their tectonic settings: *American Journal of Science*, v. 282, p. 341-357.
- Condie, K.C., 1982, Plate tectonics model for Proterozoic continental accretion in the southwestern United States: *Geology*, v. 10, p. 37-42.
- Condie, K.C., and Budding, A.J., 1979, Geology and geochemistry of Precambrian rocks, Central and South-Central New Mexico: New Mexico Bureau of Mines and Mineral Resources, Memoir 35, 58 p.
- Condie, K.C., and Nuter, J.A., 1981, Geochemistry of the Dubois greenstone succession: An early Proterozoic bimodal volcanic association in West-Central Colorado: *Precambrian Research*, v. 15, p. 131-155.

- Condie, K.C., Viljoen, M.J., Kable, E.J.D., 1977, Effects of alteration of element distributions in Archean tholeiites from the Barberton Greenstone Belt, South Africa: Contributions to Mineralogy and Petrology, v. 64, p. 75-89.
- Divis, A.F., 1976, Geology and geochemistry of the Sierra Madre Range, Wyoming: Quarterly of the Colorado School of Mines, v. 71, no. 3, 127 p.
- Donnelly, T.W., 1966, Geology of St. Thomas and St. John, U.S. Virgin Islands. In: Caribbean Geological Investigations (Hess, H.H., ed.): Geological Society of America Memoir 98, p. 85-176.
- Donnelly, T.W., and Rogers, J.J.W., 1980, Igneous series in island arcs: The northwest Caribbean compared to worldwide island arc assemblages: Bulletin Volcanologique, v. 43-2, p. 347-380.
- Ebbett, B.E., 1958, Geological map of the Encampment district, Wyoming: Miscellaneous Map, MP-1113.
- Ewart, A., 1979, A review of the mineralogy and chemistry of Tertiary and Recent dacitic, latitic, and rhyolitic, and related sialic volcanic rocks, In: Barker, F., ed., Trondhjemites, dacites, and related rocks: Elsevier, Amsterdam, p. 13-121.
- Ewart, A., and LeMaitre, R.W., 1980, Some regional compositional differences within Tertiary-Recent orogenic magmas: Chemical Geology, v. 30, p. 257-283.
- Floyd, P.A., 1977, Rare earth element mobility and geochemical characterization of splitic rocks: Nature, v. 269, p. 134-137.
- Floyd, P.A., and Winchester, J.A., 1975, Magma type and tectonic setting discrimination using immobile elements: Earth and Planetary Science Letters, v.27, p. 211-218.
- Garcia, M.O., 1978, Criteria for the recognition of ancient volcanic arcs: Earth Science Reviews, v. 14, p. 147-165.
- Gill, J.B., 1970, Geochemistry of Viti Levu, Fiji, and its evolution as an island arc: Contributions to Mineralogy and Petrology, v.27, p. 179-203.
- Gill, R.C.O., 1979, Comparative petrogenesis of Archean and modern low-K tholeiites: A critical review of some geochemical aspects: Physics and Chemistry of the Earth, v.11, p. 431-447.

- Glicksen, A.Y., 1972, Primitive ocean crust and island nuclei of sodic granite: Geological Society of America Bulletin, v. 83, p. 3323-3344.
- Graff, P., 1979, A review of the stratigraphy and uranium potential of early Proterozoic metasediments in the Sierra Madre, Wyoming. In: Contributions to Geology, Univ. of Wyoming, v. 17, no. 2, p. 149-158.
- Hart, S.R., 1969, K, Rb, Cs contents and K/Rb, K/Cs ratios of fresh and altered submarine basalts: Earth and Planetary Science Letters, v. 6, p. 295-303.
- Hart, S.R., Erlank, A.J., and Kable, E.J.D., 1974, Sea floor basalt alteration: Some chemical and Sr isotope effects: Contributions to Mineralogy and Petrology, v. 44, p. 219-240.
- Hajash, A., 1975, Hydrothermal processes along mid-ocean ridges: An experimental investigation: Contributions to Mineralogy and Petrology, v. 53, p. 205-226.
- Hills, F.A., and Gast, P.W., Houston, R.S., and Swainback, I., 1968, Precambrian geochronology of the Medicine Bow Mountains of southeastern Wyoming: Geological Society of America Bulletin, v. 79, p. 1757-1784.
- Hills, F.A., and Houston, R.S., 1979, Early Proterozoic tectonics of the central Rocky Mountains, North America. In: Contributions to Geology, Univ. of Wyoming, v. 17, no. 2, p. 89-110.
- Houston, R.S., and McCallum, M.E., 1961, Mullen Creek-Nash Fork shear zone, Medicine Bow Mountains, of southeastern Wyoming [abstract]: Geological Society of America, Special Paper 68, 91p.
- Humphris, S.E., and Thompson, G., 1978, Trace element mobility during hydrothermal alteration of oceanic basalts: Geochimica et Cosmochimica Acta, v. 42, p. 127-136.
- Humphris, S.E., and Thompson, G., 1978, Hydrothermal alteration of oceanic basalts by seawater: Geochimica et Cosmochimica Acta, v. 42, p. 107-125.

- Hynes, A., 1980, Carbonatization and mobility of Ti, Y, and Zr in the Ascot Formation metabasalts, S.E. Quebec: Contributions to Mineralogy and Petrology, v. 75, p. 79-87.
- Irvine, T.N., and Baragar, W.R.A., 1971, A guide to the chemical classification of the common volcanic rocks: Canadian Journal of Earth Science, v. 8, p. 523-548.
- Jakes, P., and Gill, J., 1970, Rare earth elements and the island arc tholeiite series: Earth and Planetary Science Letters, v. 9, p. 17-28.
- Jakes, P., and White, A.J.R., 1971, Composition of island arcs and continental growth: Earth and Planetary Science Letters, v. 12, p. 224-230.
- Jakes, P., and White, A.J.R., 1972, Major and trace element abundances in volcanic rocks of orogenic areas, Geological Society of America Bulletin, v. 83, p. 29-40.
- Jensen, L.S., 1976, A new cation plot for classifying subalkalic volcanic rocks: Ontario Division of Mines, Miscellaneous Paper 66, 22 p.
- Jolly, W.T., 1975, Subdivision of the Archean lavas of the Abitibi area, Canada, from Fe-Mg-Ni-Cr relations: Earth and Planetary Science Letters, v. 27, p. 200-210.
- Karlstrom, K.E., and Houston, R.S., 1979, Stratigraphy of the Phantom Lake metamorphic suite and Deep Lake Group, and a review of the Precambrian tectonic history of the Medicine Bow Mountains, In: Contributions to Geology, Univ. of Wyoming, v. 17, no. 2, p. 111-134.
- Lackey, L.L., 1965, Petrography of metavolcanic and igneous rocks of Precambrian age in the Huston Park area, Sierra Madre, Wyoming: Unpub. Masters thesis, Univ. of Wyoming, Laramie, 78 p.
- Lanthier, R., 1979, Stratigraphy and structure of the lowermost part of the Precambrian Libby Creek Group, central Medicine Bow Mountains, Wyoming, In: Contributions to Geology, Univ. of Wyoming, v. 17, no. 2, p. 135-148.
- Ludden, J.N., and Thompson, G., 1978, Behavior of rare earth elements during submarine weathering of tholeiitic basalts: Nature, v. 274, p. 147-149.



- Ludden, J.N., and Thompson, G., 1979, An evaluation of the behavior of the rare earth elements during the weathering of sea-floor basalts: *Earth and Planetary Science Letters*, v. 43, p. 85-92.
- MacGeehan, P.J., and MacLean, W.H., 1980, An Archean sub-sea floor geothermal system, 'calc-alkaline' trends, and massive sulfide genesis: *Nature*, v. 286, p. 767-771.
- Martin, R.F., and Piwinski, A.J., 1972, Magmatism and tectonic setting: *Journal of Geophysical Research*, v. 77, p. 4966-4975.
- McCallum, M.E., 1964, Cataclastic migmatites of the Medicine Bow mountains, Wyoming. In: *Contributions to Geology*, Univ. of Wyoming, v. 3, p. 78-88.
- Menzies, M., Seyfried, W. Jr., and Blanchard, D., 1979, Experimental evidence of rare earth element mobility in greenstones: *Nature*, v. 282, p. 398-399.
- Merry, R.D., 1963, Precambrian geology, shear zones and associated mineral deposits of the Hog Park area, Wyoming: Unpub. Masters thesis, Univ. of Wyoming, 73 p.
- Miyashiro, A., 1972, Metamorphism and related magmatism in plate tectonics: *American Journal of Science*, v. 272, p. 629-656.
- Miyashiro, A., 1973, Volcanic rock series in island arcs and active continental margins: *American Journal of Science*, v. 274, p. 321-355.
- Miyashiro, A., and Shido, F., 1975, Tholeiitic and calc-alkaline series in relation to the behaviors of titanium, vanadium, chromium, and nickel: *American Journal of Science*, v. 275, p. 265-277.
- Nockolds, S.R., and Allen, R., 1956, The geochemistry of some igneous rock series-III: *Geochimica et Cosmochimica Acta*, v.79, p. 37-77.
- Norrish, K., and Chappel, B.W., 1967, Determinative methods of mineralogy: J. Zussman, ed., Academic Press; Chapter 4.
- Norrish, K., and Hutton, J.J., 1969, An accurate X-ray spectrographic method for the analysis of a wide range of geologic samples: *Geochimica et Cosmochimica Acta*, v.33, p. 431-453.

- O'Connor, J.T., 1965, A classification of quartz-rich igneous rocks based on feldspar ratios: United States Geological Survey, Professional Paper 525-B, p. B79-B84.
- Parsons, W.H., 1969, Criteria for the recognition of volcanic breccias: Review: Geological Society of America Memoir 115, p. 263-302.
- Pearce, J.A., and Cann, J.R., 1973, Tectonic setting of basic volcanic rocks determined using trace element analyses: Earth and Planetary Science Letters, v. 19, p. 290-300.
- Robertson, J.M., 1981, Bimodal volcanism in the Early Proterozoic Pecos greenstone belt, southern Sangre de Cristo mountains, New Mexico: Geological Society of America, Abstracts with programs, v. 13, p. 103.
- Spencer, A.C., 1904, The copper deposits of the Encampment district, Wyoming: United States Geological Survey, Professional Paper 25, 107p.
- Snyder, G.L., 1979, Geological map of the northernmost Park Range and southernmost Sierra Madre, Jackson and Routt Counties, Colorado: United States Geological Survey, Miscellaneous Investigations Map I-1113.
- Staudigel, H., Hart, S.R., and Richardson, S.H., 1981, Alteration of the oceanic crust: Processes and timing: Earth and Planetary Science Letters, v. 52, p. 311-327.
- Van Schmus, W.R., and Bickford, M.E., 1981, Proterozoic chronology and evolution of the midcontinent region, North America, In: A. Kroner (ed.), Precambrian Plate Tectonics: Elsevier, Amsterdam, 781p.
- Winchester, J.A., and Floyd, P.A., 1976, Geochemical magma type discrimination: Application to altered and metamorphosed basic igneous rocks: Earth and Planetary Science Letters, v. 28, p. 459-469.
- Winchester, J.A., and Floyd, P.A., 1977, Geochemical discrimination of different magma series and their differentiation products using immobile elements: Chemical Geology, v. 20, p. 325-343.
- Wood, D.A., 1980, The application of a Th-Hf-Ta diagram to problems of tectonomagmatic classification and to establishing the nature of crustal contamination of basaltic lavas of the British Tertiary volcanic province: Earth and Planetary Science Letters, v. 50, p. 11-30.